5-10-2017

INTERVENTION TO EXTRASYNAPTIC GABAA RECEPTORS FOR SYMPTOM RELIEF IN MOUSE MODELS OF RETT SYNDROME

Weiwei Zhong

INTERVENTION TO EXTRASYNAPTIC $GABA_A$ RECEPTORS FOR SYMPTOM RELIEF IN MOUSE MODELS OF RETT SYNDROME

by

WEIWEI ZHONG

Under the Direction of Chun Jiang, PhD

ABSTRACT

Rett Syndrome (RTT) is a neurodevelopmental disorder affecting 1 out of 10,000 females worldwide. Mutations of the X-linked *MECP2* gene encoding methyl CpG binding protein 2 (MeCP2) accounts for >90% of RTT cases. People with RTT and mice with *Mecp2* disruption show autonomic dysfunction, especially life-threatening breathing disorders, which involves defects in brainstem neurons for breathing controls, including neurons in the locus coeruleus (LC). Accumulating evidence obtained from *Mecp2*$^{-/Y}$ mice suggests that imbalanced excitation/inhibition or the impaired synaptic communications in central neurons plays a major role. LC neurons in *Mecp2*$^{-/Y}$ mice are hyperexcited, attributable to the deficiency in GABA synaptic inhibition. Several previous studies indicate that augmenting synaptic GABA receptors

(GABARs) leads to a relief of RTT-like symptoms in mice. The extrasynaptic GABARs located outside synaptic cleft, which have the capability to produce sustained inhibition, and may be a potential therapeutic target for the rebalance of excitation/inhibition in RTT. In contrast to the rich information of the synaptic GABARs in RTT research, however, whether *Mecp2* gene disruption affects the extrasynaptic GABARs remains unclear. In this study, we show evidence that the extrasynaptic GABAR mediated tonic inhibition of LC neurons was enhanced in *Mecp2*$^{-/Y}$ mice, which seems attributable to the augmented δ subunit expression. Low-dose THIP exposure, an agonist specific to δ subunit containing extrasynaptic GABARs, extended the lifespan, alleviated breathing abnormalities, enhanced motor function, and improved social behaviors of *Mecp2*$^{-/Y}$ mice. Such beneficial effects were associated with stabilization of brainstem neuronal hyperexcitability, including neurons in the LC and the mesencephalic trigeminal V nucleus (Me5), and improvement of norepinephrine (NE) biosynthesis. Such phenomena were found in symptomatic *Mecp2*$^{+/-}$ (s*Mecp2*$^{+/-}$) female mice model as well, in which the THIP exposure alleviated the hyperexcitability of both LC and Me5 neurons to a similar level as their counterparts in *Mecp2*$^{-/Y}$ mice, and improved breathing function. In identified LC neurons of s*Mecp2*$^{+/-}$ mice, the hyperexcitability appeared to be determined by both MeCP2 expression and their environmental cues. In conclusion, intervention to extrasynaptic $GABA_AR$ by chronic treatment with THIP might be a therapeutic approach to RTT-like symptoms in both *Mecp2*$^{-/Y}$ and *Mecp2*$^{+/-}$ mice models and perhaps in people with RTT as well.

INDEX WORDS: Rett Syndrome, *Mecp2*, extrasynaptic GABARs, THIP, imbalance of excitation and inhibition, locus coeruleus (LC), mesencephalic trigeminal neurons, breathing, social behaviors, motor function

INTERVENTION TO EXTRASYNAPTIC $GABA_A$ RECEPTORS FOR SYMPTOM RELIEF IN MOUSE MODELS OF RETT SYNDROME

by

WEIWEI ZHONG

A Dissertation Submitted in Partial Fulfillment of the Requirements for the Degree of

Doctor of Philosophy

in the College of Arts and Sciences

Georgia State University

2017

INTERVENTION TO EXTRASYNAPTIC $GABA_A$ RECEPTORS FOR SYMPTOM RELIEF IN MOUSE MODELS OF RETT SYNDROME

by

WEIWEI ZHONG

Committee Chair: Chun Jiang

Committee: Vincent Rehder

Deborah Baro

Electronic Version Approved:

Office of Graduate Studies

College of Arts and Sciences

Georgia State University

May 2017

ACKNOWLEDGEMENTS

With the recommendation of Dr. Fuxue Chen, I came to Dr. Chun Jiang lab oversea to pursue my PhD degree in August 2011. Five and a half years passed and when I come to write my dissertation, I would like express my appreciation to so many people that has helped me earn my PhD during the period.

Firstly, I would like to thank you to my advisor and mentor Dr. Chun Jiang. I was deeply impressed and inspired by his hard working and rigorous attitude on science. Without his supervise and motivation, I cannot achieve my goal and have the courage to continue my scientific career. Secondly, I would like to thank my committee members Dr. Rehder Vincent and Dr. Deborah Baro, for their valuable suggestions and continued support to help me shape my dissertation. I would also like to thank you to Dr. Anne Murphy. Although, she is not in my committee, she always provides me helpful suggestions about scientific data analysis to improve my research. Thank you to Dr. Albers Elliot for his valuable suggestions in my experiments. Thank you to Dr. Blaustein, Dr. Ulrich and Nancy for providing me such a wonderful teaching experience. I also acknowledge Brain and Behavior fellowship program for the financial support and wonderful seminars, which help me find my postdoc position. Meanwhile, thanks to my previous advisor in Shanghai University, Dr. Fuxue Chen. Without his encourage and recommendation, I would not came here and pursue my scientific career.

I also express my appreciation to my current and previous colleagues in Dr. Chun Jiang lab, including, but not limited to these people: Dr. Ningren Cui, Dr. Xin Jin, Dr. Max F. Oginsky, Dr. Xiaotao Jin, Dr. Lei Yu, Dr. Shuang Zhang, Dr. Shanshan Li, Yang Wu, Christopher M. Johnson, Hao Xing, Coline Arrowoo, and Brian Bondy. Also, my other GSU colleagues, Dr. Lei Zhong, Zhenda Shi, Anna Parker, Ngoc Nguyen. Here, I would like especially thank you to Dr.

Ningren Cui, Christopher M. Johnson and Yang Wu, who has been continuous supportive in my research, and Dr. Xin Jin, who is the first person guiding me to the scientific work when I first come to the lab.

Last but not the least, I would like to express my greatest appreciations to my family. Thank you to my husband, Zhuoli Lin, for his unconditional support and accompany during these years. We met in GSU and we have a lot of memories here. We study together, travel together, grow together and build our family together here. Without his accompany, I would miss a lot of happiness and touchness in these years. Thank you to my parents, Feng Zhong and Wenfeng Xu, for their support, financial generosity and their selfless love to me. Although they do not know much about science and they do not understand my decision to pursue PhD overseas, they always encourage me to be responsible to and do the best to all the decisions made by myself. Also, thank you to my parents in law, Yimin Lin and Xijun Chen, for their unconditional support in the critical period when my first baby was born. Here, I would like to dedicate my dissertation to my family.

TABLE OF CONTENTS

LIST OF TABLES

LIST OF FIGURES

ABBREVIATIONS

5-HT	5-hydroxytryptamine or serotonin
AAC	Augmentative and Alternative Communication
Ach	acetylcholine
aCSF	artificial cerebrospinal fluid
AHP	afterhyperpolarization
AMPA	α-amino-3-hydroxy-5-methyl-4-isoxazolepropionic acid
AP	action potential
a*Mecp2*$^{+/-}$	asymptomatic heterozygous female mouse model of Rett syndrome
BDNF	brain-derived neurotropic factor
BLA	basolateral amygdala
cAMP	cyclic adenosine monophosphate
CCRs	CO_2 central chemoreceptors
CDKL5	cyclin-dependent kinase-like 5
CNS	central nervous system
dmLC	dorsomedial nucleus of the LC
DBH	dopamine β hydroxylase
DE	delayed excitation
DMN	default mode network
DS2	4-chloro-N-[2-(2-thienyl) imidazo [1, 2-a] pyridin-3-yl] benzamide
EPSCs	excitatory postsynaptic currents
FOXG1	forkhead box protein G1
GABA	γ-aminobutyric acid
GABAR	GABA receptor
$GABA_AR$	$GABA_A$ receptor
GFAP	glial fibrillary acidic protein
GIRK	G protein-coupled inwardly rectifying potassium channels

HDAC	histone deacetylases
ICC	immunocytochemistry
IGF-1	insulin-like growth factor 1
iGluR	inotropic glutamate receptor
IPSCs	inhibitory postsynaptic currents
IQR	interquartile range
KA	kainite
KF	Kölliker-Fuse nucleus
LC	locus coeruleus
mAHP	medium afterhyperpolarization
MBD	methyl-binding domain
Me5	mesencephalic trigeminal V
MECP2	human *MECP2* gene
MeCP2	methyl CpG binding protein 2
Mecp2	animal *Mecp2* gene
$Mecp2^{+/-}$	heterozygous female with *Mecp2* gene disruption
$Mecp2^{+/+}$	WT female
$Mecp2^{-/Y}$	hemizygous male with *Mecp2* gene knockout
mGluR	metabotropic glutamate receptor
ncRNA	non-coding RNA
NE	norepinephrine
NMDA	N-methyl-D-aspartate
nTS	nucleus tractus solitaries
PBC	Pre-Bötzinger complex
PFC	prefrontal cortex
PIR	post-inhibitory rebound
qPCR	quantitative polymerase chain reaction
REM	rapid eye movement

RQ	relative quantity
RTT	Rett Syndrome
scPCR	single cell polymerase chain reaction
s*Mecp2*$^{+/-}$	symptomatic heterozygous female mouse model of Rett syndrome
SFA	spike frequency adaptation
SNpr	substantia nigra pars reticulate
TH	tyrosine hydroxylase
THIP	4,5,6,7-tetrahydroisoxazolo(5,4-c)pyridin-3-ol, or Gaboxadol
TRD	transcriptional repression domain
TrkB	tyrosine kinase receptor type 2
WT	wide type
XCI	X chromosome inactivation

1 SPECIFIC AIMS AND HYPOTHESES

Rett Syndrome (RTT) is a neurodevelopmental disease with ~0.01% morbidity rate in live-born females worldwide [1]. Mutations in the X-linked *MECP2* gene encoding methyl CpG binding protein 2 (MeCP2), a transcription repressor/regulator, accounts for >90% of RTT cases [1]. Mice with *Mecp2* knockout (*Mecp2*$^{-/Y}$ and *Mecp2*$^{+/-}$ mice) are widely used as RTT animal models.

Patients with RTT and mouse models show dysfunctions in the autonomic nervous system such as breathing instability, gastrointestinal disorders and cardiac arrhythmia [2, 3]. The norepinephrine (NE) system in the brainstem is affected. Recent studies have shown that in *Mecp2* $^{-/Y}$ mice, NE-ergic neurons in the locus coeruleus (LC), the major NE source in central nervous system (CNS), manifest themselves as hyperexcitability with reduced NE synthesis and impaired CO_2 chemosensitivity [4-9]. The inadequate synaptic GABAergic inhibition may contribute to the LC neuronal defects as well as the consequent breathing abnormalities [10, 11]. Indeed, several recent studies have shown that enhancing synaptic GABAergic inhibition alleviates breathing abnormalities in *Mecp2*$^{-/Y}$ mice [12, 13]. In addition to the synaptic $GABA_A$Rs, there is a group of extrasynaptic $GABA_A$Rs, interfere with which may potentially be another approach to the neuronal hyperexcitation. In contrast to the rich information of the synaptic $GABA_A$Rs in RTT research [10, 14-18], however, whether the extrasynaptic $GABA_A$Rs are affected by the *Mecp2* disruption remains unknown.

The extrasynaptic $GABA_A$Rs are characterized by their high sensitivity to GABA, capability to produce long-lasting hyperpolarization (tonic inhibition), and availability for modulation by conventional $GABA_A$R ligands as well as more selective extrasynaptic $GABA_A$R modulators [19, 20]. With these characteristics, the extrasynaptic $GABA_A$Rs may be a potential

novel target for pharmacological and behavioral therapies to alleviate RTT-like symptoms. Therefore, we proposed studies to test the hypothesis that **extrasynaptic $GABA_AR$s are potential therapeutical targets for alleviation of RTT-like symptoms in mouse models with RTT.** These studies addressed four specific aims:

1. **To demonstrate how *Mecp2* disruption affects LC neuronal excitability and breathing via extrasynaptic $GABA_AR$s.**
2. **To elucidate how intervention to the extrasynaptic $GABA_AR$s moderates RTT-like symptoms in *Mecp2*$^{-/Y}$ mice.**
3. **To determine the cellular mechanisms for the extrasynaptic $GABA_AR$ mediated symptom relieves in *Mecp2*$^{-/Y}$ mice.**
4. **To intervene to neuronal hyperexcitability by extrasynaptic $GABA_AR$ agonists in *Mecp2*$^{+/-}$ mice.**

2 GENERAL INTRODUCTION

2.1 Rett Syndrome

2.1.1 Overview

Rett Syndrome (RTT) is a neurodevelopmental disease with ~ 0.01% morbidity rate in live-born girls worldwide [1]. The disease was first described by Dr. Andreas Rett in 1966 and named after him. The genetic link was unknown until 1999 Zoghbi lab at Baylor reported that RTT patients showed mutations in *MECP2* gene in the X chromosome, demonstrating the underlying mechanism for most cases of the disease [21]. The RTT girls are diagnosed usually within 2 years after birth based on their symptoms and behaviors. Over 80% of the RTT suspects are further confirmed by genetic tests. Although there is no cure for RTT at present, multiple interventions are applied clinically, including physical therapy, speech therapy, occupational therapy and symptom-targeting medicine treatment. With optimal treatments, the RTT girls are expected to live in a better condition till middle Ages.

2.1.2 Mutations of Mecp2 gene

Mutations of the X-linked *MECP2* gene encoding methyl CpG binding protein 2 (MeCP2) underlie over 90% of RTT cases clinically, including T158M and R106W point mutations as well as C-terminal truncations [22]. The North American database shows that the missense mutations are slightly more common than nonsense ones in RTT clinical cases [22]. The other RTT cases were diagnosed clinically as atypical RTT caused mostly by mutations in Forkhead box protein G1 (FOXG1) and cyclin-dependent kinase-like 5 (CDKL5) genes [23]. As a general transcriptional regulator, MeCP2 has two major functioning domains: the methyl-binding domain (MBD) and the

transcriptional repression domain (TRD) where loss-of-function mutations mostly occur. As a transcriptional repressor, MeCP2 usually binds to methylated DNA, interacting with repressor complexes, including Histone deacetylases (HDAC), and reducing the gene transcription. On the other hand, some studies also reported other regulatory roles as a splicing modulator and transcriptional activator [24, 25]. MeCP2, expressed in universal cell types, is essential for the normal function of nerve cells and particularly important for neuron maturation of CNS. Mutations in the *MECP2* gene fail to regulate the downstream gene expressions, leading to the development of RTT.

2.1.3 Animal models

2.1.3.1 RTT male models

Targeting on the *Mecp2* gene, a variety of murine models has been developed in the RTT study. The most widely used mouse model is *Mecp2*$^{-/Y}$ with complete deletions of the functional exon 3 and 4 in *Mecp2* gene, generated first from Adrian Bird lab [26]. Although fetal death happens in humans carrying such mutations, these *Mecp2*-null mice survive with around 8-week lifespan, which allows the laboratory manipulation to uncover the pathology of RTT with a uniform genetic background. *Mecp2*$^{-/-}$ females cannot be produced as the *Mecp2*$^{-/Y}$ males are infertile. These animals suffer most of the severe RTT-like neurological symptoms at approximately six weeks old, including social defects and motor dysfunction. The life-threatening breathing abnormalities can be detected as early as 3 weeks of age [8, 27].

R168X is one of most prevalent *MECP2* mutations (11.5%) in clinical RTT cases[28]. A mouse model *Mecp2*^{R168X} was developed and widely accepted as well, with truncated protein at residue R168 and TRD missing. A study in our lab suggests the *Mecp2*^{R168X} male model

recapitulates the RTT-like neuronal and phenotypical characteristics as *Mecp2*$^{-/Y}$ mice [29]. Indeed, a variety of RTT mouse models manipulating the *Mecp2* gene has been generated for divergent study purposes. For example, to study the role of GABA system in the development of RTT, the mouse model with *Mecp2* deletion only in GABAergic neurons was created by Cre-Lox recombination system [11]. In addition, the mouse models with point mutations as *Mecp2*^{T158M}, *Mecp2*^{308}, *Mecp2*^{R106W} and models with *Mecp2* overexpression as *Mecp2*^{Tg1} [30] were generated and applied to laboratory research as well.

Recently a novel *Mecp2*-knockout rat model, the SD-*Mecp2*^{tm1sage} rat, has been developed by Sage Labs in Horizon Discovery Group (Boyertown, PA). These *Mecp2*$^{-/Y}$ rats recapitulate numerous RTT-like symptoms displaying growth retardation, malocclusion, anxiety, and breathing difficulties, defects in motor function and social interactions and short lifespan, which are comparable to those seen in the *Mecp2*$^{-/Y}$ mouse model, while some appeared more or less severe. Therefore, concerning the limitation for *in vivo* studies in mice due to their small size, the novel rat model provides a valuable alternative model in the RTT studies [31-33].

2.1.3.2 *Mecp2*$^{+/-}$ mice and rats

Although current studies are mostly performed in the male models that have a uniform genetic background, it is necessary to show how these research findings manifest themselves in the heterozygous *Mecp2*$^{+/-}$ females, which usually display phenotypic heterogeneity. This is particularly important when potential therapeutics are concerned.

The heterozygous *Mecp2*$^{+/-}$ mouse generated in Bird lab is the widely accepted female model, which recapitulates divergent RTT-like symptoms but exhibits a much later symptom onset as 6 months old. Somaco et al. reported that some of the phenotypes can be detected as early as 5 weeks old, such as apneic breathing difficulties [34]. Due to the X chromosome inactivation (XCI),

55%~85% *Mecp2* levels of wide-type (WT) littermate were maintained in the CNS of these heterozygous mice with variation of regions, which seems to enable heterozygous *Mecp2*$^{+/-}$ mouse to develop symptoms to a less severe level than the male model with *Mecp2* gene completely deleted [34]. The *Mecp2*$^{+/-}$ female rat model was demonstrated recently, which retains a half of the MeCP2 protein expression compared to their WT level [33]. Similar to the female mouse model, the *Mecp2*$^{+/-}$ rats display robust RTT-like behavioral and motor defects as well [32, 33], which provide a complementary tool for the cross-species study of RTT. In general, more studies of the pathophysiology in female RTT models are encouraged regarding their irreplaceable role in the potential disease-relevant preclinical study.

2.2 Symptom development

2.2.1 Physical condition and lifespan

RTT is almost exclusively a female disease, due to the fetal death of the male patients. Although live birth happens in some the RTT male cases, they cannot survive beyond 2 years. As a neurodevelopmental disease, RTT symptoms progress in four stages. In stage I, the retardation of the development of language and behavior skills is the characteristic symptom onset in the patients, which occurs from 6 to 18 months after birth. The deceleration of the head growth and the stereotypic movement appear in this stage as well. In stage II, usually happening between 1 to 4 years old, the girls exhibit the regression of development, including the deterioration of language skills and disinterest to other people. But such communication skills could be resumed at stage III, which usually lasts several years. Till Stage IV, more autism-like symptoms show up and may last up to decades, including anxiety, seizures, social defects, motor dysfunction and life-threatening breathing difficulties. The RTT girls do suffer shorter lifespan. But due to the great phenotype

variations among individuals, these girls can be expected to survive into the 40s, 50s and even beyond [35].

RTT murine models (*Mecp2*$^{-/Y}$ and *Mecp2*$^{+/-}$) recapitulate most of the RTT-like symptoms, enabling studies of the pathophysiology of the RTT and the potential clinic treatment. Distinct from the RTT male cases in human, *Mecp2*$^{-/Y}$ mice or rats are viable and appear normal at birth. Most of the symptoms exhibit from 2~3 weeks old, including malocclusion, hindlimb clasping, weight loss, shivering and irregular breathing. These male RTT models suffer short lifespan about 50-60 days as well [26]. The heterozygous female mice display hindlimb clasping and mobility problems starting at around 6 months, with much longer lifespan than the male models. Although the brain weight was significantly reduced in RTT female mice and rats, these two models do exhibit a protracted disease progression with large variations due to the remaining *Mecp2* containing X chromosome and XCI [36, 37].

2.2.2 Autonomic dysfunction

2.2.2.1 General phenotypes in animal models and patients, especially breathing abnormalities

The autonomic dysfunctions are commonly found in classic RTT cases, shown as breathing instability, gastrointestinal disorders, and cardiac arrhythmia. The cardiac rhythm abnormalities are described as bradycardic events, sinus pauses, atrioventricular block, premature ventricular contractions, non-sustained ventricular arrhythmias, and increased heart rate variability [38]. Gastroesophageal reflux, vomiting, gastroparesis, constipation and straining with bowel movement are the commonly seen as the gastrointestinal disorder in RTT patients.

A previous study reported that 26% of RTT patients died of unexplained causes [39]. The high rate of sudden death can be attributed to the breathing disorders, characterized by episodic

apnea, hypoventilation, hyperventilation and air swallowing, etc.[40, 41] Such breathing abnormalities in *Mecp2*$^{-/Y}$ mice occur at 2~3 weeks old and deteriorate with time. Indeed, long lasting apnea is often seen a few days before animal death [42]. Improving breathing regularities thus facilitates the survival of *Mecp2*$^{-/Y}$ mice [43, 44]. Therefore, the severity of breathing disturbances may be correlated with the lifespan of mutant mice. As one of the major challenges in the RTT, the life-threatening breathing abnormalities need to be concerned seriously.

2.2.2.2 Dysfunction in neuromodulation by norepinephrine and acetylcholine

Development of RTT-like breathing difficulties results from multiple neuronal defects, including the synaptic imbalance and modulatory disturbance. The neuronal hyperexcitation was found in the brainstem, where the respiratory centers are located, involving altered glutamatergic excitation and GABAergic inhibition [10, 36, 45]. The neuromodulator NE modulates the synaptic transmission, affecting the neuronal networks in the brainstem and the consequent phenotype. In the mouse model and patients with RTT, the NE level in the CNS was significantly reduced [46]. Pre-Bötzinger complex (PBC) is the respiratory rhythmic generator in the ventrolateral medulla of the brainstem. NE modulates the bursting activity and the frequency of PBC neurons via noradrenergic receptors respectively. Reduced NE level disturbs the modulation and leads to the breathing irregularities in RTT cases, and enhancing the NE content by desipramine, an NE reuptake blocker, significantly improves the breathing irregularities in *Mecp2*-null mice [44, 47].

A recent study showed that selective disruption of *Mecp2* in cholinergic neurons recapitulated some RTT phenotypes, such as the cardiac rhythm abnormalities, hypothermia, and early death, in the RTT mouse model, and restoration of the gene in cholinergic neurons rescued these phenotypes [48]. Thus, the defects in the acetylcholine (Ach) system are involved in the autonomic dysfunction, contributing to the early death in RTT. Indeed, Ach modulates the PBC

neurons via activation of muscarinic receptors, resulting in an increase in breathing frequency. Thus, the defect in cholinergic neurons contributes to the RTT-like breathing abnormalities as well.

2.2.2.3 Locus coeruleus nuclei

As the major NE source in the CNS, LC neurons show defects as altered intrinsic membrane prosperities, impaired chemosensitivity and deficit metabolic function in *Mecp2*-null mice [4, 6, 8]. Glutamate, GABA, glycine, Ach and serotonin send divergent signals to the LC nuclei, supporting their integrated function. Meanwhile, LC neurons project to divergent brain regions, such as the medulla, spinal cord, hypothalamus, and forebrain, affecting a series of behaviors. In *Mecp2*-null mice, both the GABAergic inhibition and Ach modulation in LC area were significantly reduced, leading to the neuronal hyperexcitability [10, 49]. This may contribute to the impaired NE synthesis and release in LC neurons, evidenced by the reduced expression of tyrosine hydroxylase (TH) and dopamine beta hydroxylase (DBH) in LC neurons and the reduced NE content in the brainstem [6, 50], and the consequent dysfunction of autonomic system in RTT mice. Interestingly, our study suggests that the severity of the breathing abnormalities is positively correlated to the neuronal hyperexcitability of LC neurons in *Mecp2*-null mice and stabilization of excessive firing in LC neurons alleviates the breathing difficulties [27]. Thus, the defects of LC neurons contribute to the development of autonomic dysfunction, especially breathing irregularities, via NE projections in RTT models.

2.2.3 Motor defects

2.2.3.1 General phenotype and the involved systems

A common feature of most RTT girls is the motor defect that keeps them in the wheelchair for the rest of their lives due to their deterioration of motor functions, including the loss of muscle tone, stereotypical hand movement, defects in motor coordination and mobility [26]. The abnormal gait (such as swaddling) and the retarded mobility are two major problems when scoring the phenotype severity of the RTT mouse models [51].

The cooperation among pyramidal, extrapyramidal and propriosensory systems ensures the normal motor function. The pyramidal motor system starts from the motor cortex, control the voluntary muscles by directly innervating the motor neurons in the brainstem or spinal cord. The extrapyramidal system is part of the motor system contributing to the coordinated movements, which is also involved in the regulation or modulation of the motor neurons in the spinal cord. The propriosensory neurons contribute to the motor activity by sending the feedback information to the motor neurons to ensure the coordinated movement. Increasing evidence suggests that the impaired pyramidal motor system results in the motor defects in the RTT patients and mouse models. The mitochondria in the skeleton muscle were reported to be dysfunctional due to the accumulation of the free radicals and the increase of oxidative stress [52]. In comparison to the rich information in the pyramidal motor system, the propriosensory neurons have not been well studied yet. Recent studies in our lab showed the propriosensory system was impaired as well, contributing to the RTT-like motor defects [53].

2.2.3.2 Mesencephalic trigeminal V nuclei

The Me5 neurons are the only group of propriosensory neurons with soma located in the CNS, which provide servo feedback control to the jaw muscles. The Me5 neurons project to the trigeminal motor nucleus, mediating the jaw jerk reflex. In *Mecp2*-null and *Mecp2*$^{168R/Y}$ mice, the neuronal hyperexcitation was detected in Me5 neurons [29]. *In vivo* studies in *Mecp2*$^{ZFN/Y}$ rats suggested the hyperexcitation of Me5 neurons contribute the impaired jaw jerk reflex, which is consistent with the malocclusion in RTT rats, and defects of chewing, drinking, and teeth grinding in RTT [53-56]. Although the reason of Me5 neuronal hyperexcitability in *Mecp2*-null mice is still unknown, the impaired intrinsic membrane properties may contribute [27].

2.2.4 Dysfunction in social behaviors

RTT girls developed autism-like social defects, showing a lack of interest in other people, preference to be alone, impairment in social communication, etc. These neurological phenotypes are usually progressive and long lasting. The mouse models of RTT displayed similar phenotypes, which can be achieved by a series of experimental tests, such as social interaction test and three - chamber test. Although the neurological mechanism underlying the social defects in RTT remains unclear, multiple brain regions are known to be involved, such as prefrontal cortex (PFC) and basolateral amygdala (BLA). A recent study in rats suggested a reduction of GABAergic inhibition in either medial PFC or BLA decreased sociability [57], which may underlie the social defects in RTT as the GABA transmission was globally declined in the CNS of RTT models. The impaired neuronal networks were widely seen in *Mecp2*-null mice. The autism-like social defects disorders were believed to be correlated to the weak connections in the default mode networks (DMN),

which is related to the self-reference, emotional processes, social activities and memory, involving the medial PFC and posterior cingulate cortex [58].

NE plays a role in regulating the social behaviors as well. NE-ergic neurons in the LC project broadly to the other brain regions, including the prefrontal cortex (PFC), BLA and other cortical areas [59]. In *Mecp2*-null mice, the normal functions of these regions receiving LC-NE projections may be impaired due to the reduced NE content, leading to the progression of the RTT-like phenotypes, including the social retard. A recent study also reported that the NE reuptake inhibitor atomoxetine decreased responding for social play in rats [60].

2.3 Potential cellular and molecular mechanisms underlying Symptom development

2.3.1 Imbalanced inhibition/excitation in the CNS in Mecp2$^{-/Y}$

2.3.1.1 Neuronal hyperexcitation/ hypoexcitation

The disruption of inhibition/excitation ratio in the CNS was believed as one of the mechanism of some psychiatric diseases, including schizophrenia, autism spectrum disease, Fragile X and Down syndrome [61, 62] [63-65]. In Fragile X syndrome, the reduced excitatory neuronal activity and the unaltered inhibitory neuronal activity in neocortical circuits result in the network hyperexcitability and consequent epilepsy and cognition problem [63]. In Down syndrome, the excessive synaptic inhibition contributes to the cognition impairment, and pharmacological innervation to the excitation/inhibition ratio rescued the behavior deficit [64]. Such an imbalance was found in mouse models of RTT as well, such as hypoexcited cortical activity, hyperexcited hippocampus network and hyperexcited neurons in pons [16, 53, 66, 67]. Thus, the imbalanced inhibition/excitation may underlie some pathology of the RTT-like symptoms, and maintaining the circuit homeostasis between excitation and inhibition may benefit

the patients and mouse models of RTT. Disturbances of the neurotransmission in the CNS caused by mutations of the *Mecp2* gene may contribute to the network alteration.

2.3.1.2 Neurotransmission abnormalities

Although the *Mecp2* gene was lost in all the cells in *Mecp2*-null mice, neurons do not show uniform responses. In general, the neuronal hyperexcitation is described in the brainstem nuclei, especially the neurons involved in the rhythmic respiration, whereas the neuronal hypoexcitation is a feature in the forebrain and midbrain [68]. The imbalanced excitation/inhibition ratio was attributed to the abnormal neurotransmission system, which involves GABA and glutamate.

The GABAergic inhibition is reported to be reduced in the CNS, including the neurons of the brainstem, such as the Kölliker-Fuse (KF) and LC [10, 69], resulting in the neuronal hyperexcitability. The enhanced excitatory transmission contributes to the hyperexcitation as well in the nucleus tractus solitarius (nTS) [70]. The hyperexcitation in these nuclei is associated with defects in the autonomic system in RTT patients and mouse models, such as the RTT-like breathing abnormalities. On the other hand, the elevated glutamatergic excitation was reported in girls and mouse models with RTT [71]. In the forebrain, although the glutamatergic excitation was locally enhanced, the overall neuronal output show a hypoexcitation, consequent in the RTT-like cognition impairment, which may be related to the potential disinhibition in the neuronal network [68]. The downregulated excitatory postsynaptic currents (EPSCs) and the unchanged inhibitory postsynaptic currents (IPSCs) lead to the reduced cortical activity [16]. Indeed, ketamine, a NMDA glutamate receptor antagonist, rescued the phenotypes in the RTT mouse model [72]. Such a defect in the synaptic plasticity was reported as spatial and temporal related, which is consistent with the development of the symptoms. Therefore, correction of the disrupted excitation/inhibition ratio in

the mouse models and patients with RTT by innervating the GABAergic inhibition or glutamatergic excitation may be beneficial for the brain development.

2.3.2 GABAergic inhibition in Mecp2$^{-/Y}$ mice

2.3.2.1 GABAergic inhibition (synaptic and extrasynaptic)

Previous study suggested selective deletion of the *Mecp2* gene in GABA-ergic neurons recapitulates most RTT phenotypes in mice [11], and selective restoration of the gene in these GABAergic neurons resumed the multiple RTT-like symptoms in mouse models [73]. These indicate the crucial role of GABA system in the development of the RTT symptoms.

As the most prominent inhibitory neurotransmitter in the brain, GABA acts via both synaptic and extrasynaptic GABARs. Activation of the synaptic $GABA_ARs$, usually located in the postsynaptic membranes, produces fast IPSCs and hyperpolarizes the postsynaptic cells. The extrasynaptic $GABA_ARs$ known as tonic receptors are characterized by their extrasynaptic location, high sensitivity to GABA, and the capability to produce tonic currents with long-lasting hyperpolarization [19, 20].

Both of the synaptic and extrasynaptic $GABA_ARs$ are pentamers, usually composed of 2-3 heteromeric subunits of a total 19 (α1-6, β1-3, γ1-3, δ, θ, ε, π, and ρ1-3) subunits [19]. The combination pattern of $GABA_ARs$ shows spatial specificity. The γ2 -containing receptors are mainly localized at the synapse, playing a key role in the GABAergic synaptic transmission. The δ subunit, usually assembled with 2 α and 2 β subunits, is located exclusively out of the synaptic cleft [74]. These receptors are responsible for tonic GABAergic inhibition without interfering with synaptic transmission, which is due to their high affinity to GABA and weak desensitization.

2.3.2.2 Defects of the GABAergic neurons in *Mecp2*$^{-/Y}$ mice

The impaired GABAergic inhibition is widely reported in patients with RTT and mouse models and mouse models. In RTT patients, a marked reduction in $GABA_AR$ density in the brain was reported. [75, 76]. In RTT animal models, the reduced synaptic GABAergic inhibition was found in multiple brain regions, including the hippocampus, substantia nigra pars reticulate (SNpr), cerebellum and brainstem [10, 17, 66]. Such a GABA deficit showed location-specific and age-dependent variations in the CNS of RTT mouse model [17, 77]. An epigenetic study in a mouse model of RTT indicates that the $GABA_AR$ β3 subunit expression is reduced in the cerebellum, which was confirmed by another molecular study [78, 79]. In the ventrolateral medulla, where contains the respiration rhythm generators such as the pre-Bötzinger complex (PBC), the presynaptic GABAergic inhibition was defective and postsynaptic GABAergic inhibition was also impaired with reduced expression of α2 and α4 subunits in *Mecp2*-null mice. Such a defect in synaptic GABA system was found as early as 7 days in *Mecp2*-null mice before the RTT symptoms developed [18]. In LC, both $GABA_A$ and $GABA_B$ receptor mediated postsynaptic inhibition are reduced, and the GABA release from presynaptic terminals is significantly low [10], contributing to a rise in the excitability of the cells.

In contrast to the widespread reduction of synaptic GABAergic inhibition, the extrasynaptic $GABA_ARs$ seem well remained in the *Mecp2*-null mice. The extrasynaptic $GABA_A$ receptor-mediated tonic inhibition was dose-dependently enhanced in null mice, showing larger tonic GABA currents and higher expression level of δ subunit, a marker of extrasynaptic $GABA_ARs$ [67]. The reason causing the different expression of synaptic and extrasynaptic $GABA_ARs$ remains unclear. Considering the characteristic that the extrasynaptic $GABA_ARs$ have the capability to change dynamically their expression levels under different physiological and

pathophysiological conditions [80], it is possible that compensatory neuroadaptation is involved. Indeed, such an enhancement of the extrasynaptic $GABA_A$ receptor-mediated tonic inhibition was found in Fragile X syndrome and Angelman syndrome as well, which share many phenotypical similarities with RTT [81, 82].

Taking the advantage of the GABA system defects, pharmacological interventions have been attempted in the RTT mouse models. The therapeutic synaptic $GABA_AR$ activators diazepines and the GABA reuptake blocker NNC-711 improved the RTT-like breathing abnormalities in animal models [12, 13]. However, intervening to the synaptic GABARs may lead to the several side effects, including sedation, tolerance and addiction. The extrasynaptic GABARs can provide an alternative to avoid such potential side effect, as manipulations of these receptors with selective agents do not interrupt GABAergic synaptic transmission. Indeed, exposure to the extrasynaptic $GABA_AR$ agonist THIP (also called Gaboxadol) relieves multiple RTT-symptoms in *Mecp2*$^{-/Y}$ mice, including the breathing abnormalities [67, 83].

2.3.3 Glutamatergic excitation in Mecp2$^{-/Y}$ *mice*

2.3.3.1 Glutamatergic transmission

The imbalanced inhibition/excitation ratio in RTT may be attributable to the defected excitatory neurotransmission as well. As the major excitatory neurotransmitter present in over 50% neurons, glutamate usually depolarizes the postsynaptic cells by activating their metabotropic (mGluR) and inotropic receptors (iGluR). The iGluRs form the ion channel pore by four subunits, which tend to produce fast excitatory postsynaptic currents (EPSCs). According to their different affinity to agonists, the iGluRs are further classified into N-methyl-D-aspartate (NMDA) receptor, α -amino-3-hydroxy-5-methyl-4-isoxazolepropionic acid (AMPA) receptor and kainate (KA)

receptor. The mGluRs, G -protein -coupled receptors, indirectly activate ion channels through signaling cascades that involves G proteins, which favors producing a prolonged stimulus. Activation of the mGluR hyperpolarizes the postsynaptic cells by altering the K^+ permeability and turning off the cyclic adenosine monophosphate (cAMP) -dependent pathway.

The defects in glutamatergic signaling are believed to contribute to the autism-like characteristics. The enhanced glutamatergic transmission elevated the excitation/inhibition ratio, which is associated with epilepsy [84]. Down-regulation of the mGluR5 signaling to 50% rebalanced the excitation/inhibition and alleviated the symptoms in Fragile X syndrome [85]. Thus, glutamatergic dysfunction affects the excitation/inhibition balance, attributable to the development of RTT.

2.3.3.2 Defects of glutamate system in *Mecp2*$^{-/Y}$ mice

A recent study showed that selective deletion of the *Mecp2* gene in glutamatergic neurons produced some RTT-like symptoms, including premature death, obesity, tremor and anxiety-like behaviors, which is different from the phenomena in animals without *Mecp2* gene only in GABAergic neurons, and restoration of the gene rescued the phenotypes in RTT mouse models [45]. Thus, the defects of glutamatergic excitation contributes to the development of RTT symptoms in a distinct way from the impaired GABAergic system.

The alteration of NMDA receptor density was reported to increase in RTT girls under 8 years old and a reduction in girls older than 10 [71]. Such an alteration of NMDA receptor expression was found with location specificity as well in RTT mouse models. In the *Mecp2*-null mice, the age -dependent change of NMDA receptors was reported as bi-phasic in the visual cortex, whereas enhanced expression of NMDA receptors was found regardless of age in the thalamus [86]. Thus, mutations in the *Mecp2* gene altered the glutamate transmission in the CNS as temporal

and spatial specificity, which contributes to the RTT-like phenotypes. Furthermore, in the nTS, the enhanced glutamatergic excitation leads to the neuronal hyperexcitation and the consequent breathing abnormalities [68, 70] in the mouse model with RTT. In the hippocampus, accompany with the reduced GABAergic inhibition, enhanced glutamatergic excitation was believed to contribute to the network hyperexcitability, consequent in the impairment of learning and memory. The altered synaptic trafficking of AMPA receptors contributes to the hyperexcited synaptic activity in hippocampus as well [87]. In general, in patients with RTT and mouse models, the glutamate level and the glutamate receptor expression were elevated [88], which may lead to the neuronal hyperexcitation in different brain regions, underling the disturbed inhibition/excitation ratio. Interestingly, *Mecp2* mutation enhanced glutamatergic excitation in the forebrain, leading to the local hypoexcitation, instead of hyperexcitation, and exposure to the NMDA receptor antagonist ketamine alleviated the RTT - like phenotypes, which may be related to disinhibition by presynaptic GABAergic neurons [68].

2.3.4 Brain-derived neurotrophic factor and Insulin-like growth factor-1

BDNF, as a member of growth factors, is involved in the neuronal survival, maturation, differentiation and synapse plasticity by activation of neurotrophic tyrosine kinase receptor type 2 (TrkB) via signaling pathways, including PLCγ, PI3K/Akt, and MAPK/ERK.

Previous genetic studies suggest MeCP2 acts as a transcriptional repressor of BDNF by binding to their promoter IV until MeCP2 is phosphorylated and released [89]. Mutations of the *Mecp2* gene lead an early increase in BDNF content in MeCP2-deficient neurons, followed by the progressive reduction in total cellular BDNF in multiple brain regions, which is consistent with the delayed onset and the pathological phenotypes deterioration in a mouse model of RTT [90].

One of the major consequences caused by the abnormal BDNF in *Mecp2* mutated mice is the respiratory irregularity. In *Mecp2*-null mice, BDNF is critical for the normal development and maintenance in the brainstem and nodose ganglia, which are crucial in cardiorespiratory homeostasis and autonomic control [91]. The KF, PBC and nTS in the pons and brainstem, where the respiratory center located, are modulated by BDNF as well [70, 92, 93]. Reduced BDNF content in *Mecp2* deficit mice results in the RTT-like breathing abnormalities and restoration of normal BDNF level rescued the defects [70, 91].

In addition, the abnormal BDNF level in the MeCP2 deficit CNS modulates the synaptic transmission improperly, contributing to the imbalanced excitation/inhibition ratio and the consequent RTT-like symptoms. For example, in KF neurons, application of BDNF significantly reduced the IPSCs frequency [92]. BDNF modulates the glutamatergic transmission in nTS neurons as a strong reduction of AMPA receptor mediated currents by activating the TrkB receptors [94]. In *Mecp2*-null mice, indeed, the reduced BDNF resulted in the enhanced EPSCs in nTS, and exogenous application of BDNF rescued the synaptic defect by reducing the abnormal EPSCs [70].

Similar to BDNF, the insulin-like growth factor 1 (IGF-1) is widespread in the CNS and contributes to the neuron survival and synapse maturation. Studies in mouse models and patients with Rett syndrome also reported the beneficial effects of IGF-1, which share similar signaling pathways with BDNF [95]. Defects in synaptic structure and plasticity have been demonstrated in RTT [89]. IGF-1 treatment increased the synaptic growth and rescued a number of RTT-like symptoms in RTT mouse models [96]. Unlike BDNF, the capability of penetrating the blood - brain barrier (BBB) makes IGF-1 a better candidate for clinical trials.

2.3.5 Epigenetic modification

Epigenetics is a genetic process that changes the gene expression, which is heritable and not involved in the changes of DNA sequences. Methylation of genes, modification of histones and non-coding RNA (ncRNA)-associated gene silencing are the major types of mechanisms, leading to the phenotype changes without alteration in the genotype. Because of their methyl-CpG binding domain, MeCP2 binds to methylated DNA and forms a complex with histone deacetylase 1 (HDAC1) to removes acetyl groups, leading to the chromatin condense and gene regulation. There are two methylated forms of DNA: hydroxymethylcytosine (hmC) and methylated cytosine followed by a nucleotide (mCH, where H = A, C or T) [97, 98]. These two marks on chromatin accumulate during the neuronal maturation and their accumulation is coincident with the increased MeCP2 expression. Thus, in RTT patients or mouse models, *Mecp2* mutations may lead to the less binding to hmC and mCH markers, resulting in the onset of RTT [99]. In addition, in the *Mecp2* deficit neurons, the chromatin disorganization, evidenced by the differential localization of chromatin remodeling protein, coincides with phenotypic progression [100]. In general, the epigenetic mechanisms might contribute to the delayed onset of the RTT-like symptoms and the symptom progression [99].

2.3.6 X inactivation in Mecp2$^{+/-}$ mice

2.3.6.1 General information

In female mammalians, only one copy of X chromosomes is active and the other is transcriptionally silenced or inactivated. Such a phenomenon is known as X chromosome random inactivation (XCI), which leads to the mosaic expression of the X-linked genes in the cells of female animals. Thematically, the X chromosomes from maternal or paternal origin

share the same probability to be inactivated, which renders half of the cells to express maternal or paternal X chromosome randomly in the early embryogenesis. However, such XCI is not always balanced, so that the nonrandom or skewed XCI has been reported, especially in RTT patients [101, 102]. Although the classic law of inheritance cannot explain XCI and the genetic mechanism remains unclear so far, a mathematical model of genetically influenced choice was proposed to fit the XCI pattern distributions [103].

2.3.6.2 Nonrandom X chromosome inactivation and the impact on phenotypes

RTT is mostly caused by the mutations of the X-linked *Mecp2* gene in heterozygous females. Instead of a uniform expression, central neurons show mosaic patterns of MeCP2 expression in the *Mecp2*$^{+/-}$ mice due to the XCI, which vary among regions and animal ages [104]. The XCI was believed to impact the phenotypic outcome in human patients and female animal models [105]. In many cases, RTT girls show random XCI with equal numbers of MeCP2 negative or positive cells, which theoretically renders 50% of *Mecp2*$^{+/-}$ individuals to carry the mutated gene. However, nonrandom XCI has been reported to contribute to clinical symptom variations in some RTT patients as well [106]. Skewed XCI to the WT may lead to the milder phenotypes in the RTT mouse model [102]. Our previous study also suggests that only ~20% the *Mecp2*$^{+/-}$ mice developed breathing disorders [107], which is consistent with the skewed XCI in RTT. Thus, nonrandom or preferential XCI may play a role in the phenotypic and individual variations of RTT.

In addition, in heterozygous females, the MeCP2-negative neurons generally displays different morphology from MeCP2–positive cells as shorter dendritic length and smaller cell size [108]. The more skewed XCI from the WT allele, the more severe neuronal phenotype of the MeCP2-negative cells would be. On the other hand, the MeCP2-negative cells affect the development of surrounding WT cells in *Mecp2*$^{+/-}$ mice as well [109], Therefore, the nonrandom

XCI may contribute to the cross-interaction of the MeCP2-negative and –positive cells on structural and functional outcomes, depending on the skewed condition.

2.3.7 Locus Coeruleus Nuclei

2.3.7.1 Intrinsic membrane properties and CO_2 chemosensitivity

LC is located bilaterally in the dorsal area of the rostral pons, which is involved in many behaviors via the widespread projections, especially the regulating the autonomic function as breathing activity. Defects of LC neurons are involved in multiple neuropsychiatric disorders, including Parkinson's disease, Alzheimer's disease and posttraumatic stress disorder [110, 111]. Recent studies in our and other labs have shown that the LC neurons in *Mecp2*-null mice are defective as well, which underlie the pathology of some RTT-like phenotypes. The defect manifests itself as abnormal intrinsic membrane prosperities and impaired CO_2 chemosensitivity [112, 113]. The intrinsic membrane properties of LC neurons were impaired by showing the shorter time constant, stronger inward rectification and smaller medium afterhyperpolarization (mAHP) amplitude, which may contribute to the LC dysfunction as excessive firing and reduced metabolic function [4, 10]. The CO_2 central chemoreceptors (CCRs) were found in the brainstem, including the LC, which play a critical role in respiratory and cardiovascular controls. In *Mecp2*-null mice, the CO_2 chemosensitivity of LC neurons was defective, showing the abnormal response to mild hypercapnia but normal response to the severe hypercapnia. The overexpression of Kir4.1 channel, which reduced the pH sensitivity, in LC area may contribute, allowing the neurons detect CO2 until severe hypercapnia develops [8]. Such a defect in LC neurons contributes to the RTT-like breathing abnormalities, including high breathing frequency variation, apnea, and hyperventilation.

2.3.7.2 Norepinephrine biosynthesis and the homeostasis

As the prominent NE recourses, LC produces ~70% NE throughout the CNS. In patients with RTT and mouse models, the monoamine level was significantly reduced, including NE [46], leading to the RTT-like phenotypes, such as abnormal breathing activity. It was confirmed by the later studies that the expression levels of tyrosine hydroxylase (TH) and dopamine beta hydroxylase (DBH), the rate-limiting enzyme in the NE synthesis, were significantly reduced in *Mecp2*-null LC neurons [114]. Desipramine, an inhibitor of NE reuptake, can improve respiratory rhythm activity, increases the number of NE containing neurons, and extends the lifespan of *Mecp2*-null mice [44, 47].

The cause of the NE deficit remains unknown. Mutations of the *Mecp2* gene, the general transcriptional regulator, may affect the enzyme expressions. The persistent hyperexcitation of LC neurons may contribute as well. There may be a homeostatic state between LC neuronal excitability and NE biosynthesis, allowing a stable release of NE at synapses. Although high LC neuronal excitation may lead to more NE release, persistent hyperexcitability may have adverse effects. In *Mecp2*-null mice, the excessive firing of LC neurons may contribute to their metabolic dysfunction by disturbing the homeostasis of NE synthesis, the NE production and NE release from presynaptic terminals. The idea is supported by our recent study that further stimulation of NE-ergic terminals in a mouse model with *Mecp2* null did not improve the NE modulation to their target nuclei [115]. Coincidently, the LC neurons in *Mecp2*-null mice showed the age-dependent deterioration [27] and the TH expression level was also progressively reduced [50], which is consistent with the homeostasis idea as well. Interestingly, our study has shown that the severity of breathing abnormalities increases with the increased LC firing rate in the symptomatic *Mecp2*-null mice at similar ages [27], which also indicate the potential linkage

between the neuronal hyperexcitability and the declining metabolic function. Other studies also reported the tight linkage between the neuronal firing activity and the behaviors of the animals. LC cells usually active firing during awake and become silence during rapid eye movement (REM) sleep [116]. The altered metabolic function or NE synthesis and release of LC neurons may underlie such linkage. In general, in patients with RTT and mouse models, the metabolic function of LC was impaired, which may be due to the imbalanced neuronal firing activity and NE synthesis.

2.3.7.3 Defects of cell communications

As the major NE-ergic nuclei, LC neurons receives signals from and projects to the broad brain regions and spinal cord, affecting diverse behaviors, such as breathing, cognition, attention, sleep, learning and memory [117]. The LC-NE system sends output to the medulla, where the respiratory centers are located, and regulates the breathing activities. The prefrontal cortex receives the LC-NE projection as well, which contributes to the cognitive functions, seizure and social behaviors [118]. Although previous studies indicate that the LC neurons may function as individual cells to innervate divergent brain area distinctively, a viral-genetic tracing study suggests LC-NE circuit receives convergent signals from many brain regions through axon projections, including cerebellar Purkinje cells, intervening the LC-NE modulation in the target regions and the associated behaviors [59]. GABA and glutamate are the major inhibitory and excitatory neurotransmitters regulating the LC-NE circuits. One study in our lab reported a local group of GABAergic neurons in the dorsomedial area of LC (dmLC) involves the direct or indirect regulation in LC-NE output [119]. In patients with RTT and mouse models, the abnormal synaptic input affects the normal outcome of LC-NE circuit [10, 14, 49, 67]. Together with their internal defects, the abnormal LC-NE circuit makes the system unable to maintain the

normal function and leads to multiple RTT-like symptoms. Improving the NE-LC circuits by innervating the inputs may benefit their target regions, leading to the alleviation of the associated abnormal behaviors in RTT.

2.4 Therapeutical attempts

2.4.1 Pharmaceutical intervention

Since murine models with RTT were generated, pathophysiology of the RTT has been studied for decades. Increasing evidence reported the imbalanced neuronal excitation/inhibition may underlie the development of the disease. Targeting on the involved neurotransmitters may help to alleviate multiple RTT-like symptoms. As the major inhibitory neurotransmitter, GABA level was significantly reduced in RTT CNS, and global reduction of GABAergic inhibition shifts the excitation/inhibition ratio to the hyperexcitation side. The GABA reuptake blocker (NNC711), synaptic GABA receptor agonist (diazepam) and extrasynaptic GABA receptor agonist (THIP) significantly alleviate the symptoms, especially breathing irregularities [12]. The overall enhanced glutamatergic excitation leads to the skewed excitation/inhibition in the CNS. Ketamine, a glutamate receptor antagonist, alleviated the RTT-like phenotypes in the RTT as a disinhibition in the forebrain neuronal network [120]. Another weak NMDA receptor blocker, memantine, restored the post-tetanic potentiation and paired-pulse facilitation, favors the function reinstallation in RTT [121]. Although preclinical trials have not tested these pharmaceutical treatments via GABA or glutamate system, the beneficial effects on RTT mouse models demonstrated their potentiation.

The reduced monoamine level was widely reported in patients with RTT and mouse models, including NE, dopamine, and serotonin, and increasing their level in the CNS alleviated

the RTT-like symptoms. Desipramine, an NE reuptake blocker, significantly ameliorated the breathing disorders and expanded their lifespan in *Mecp2*-null mice [44, 47]. Selective 5-HT1a receptor agonists F1599 and 8-OH-DPAT decreased apnea, corrected breathing irregularity and improved hand stereotypy and social skills via G protein-coupled inwardly rectifying potassium (GIRK) channels in both female and male RTT mouse models [122, 123]. The selective serotonin 5-HT7 receptor agonist LP-211 rescued multiple RTT-related defective performances, including anxiety, motor disabilities, exploratory behavior and memory [124]. As a clinical medicine for l-dopa-induced dyskinesia, Sarizotan, a 5-HT1a agonist and a dopamine D2-like agonist, was shown to have beneficial effects on breathing activity and locomotion in mouse models with RTT as well [125].

BDNF, involved in the neuronal survival and synaptic plasticity, has been widely demonstrated as an overall reduction in the *Mecp2*-null CNS by both multiple biochemistry and genetic methods. Application of exogenous BDNF rescued the synaptic dysfunction in nucleus tractors solitaries, leading to the alleviation of cardiorespiratory disorder in RTT [70]. CX546 is an ampakine drug, which promotes the activation of AMPA receptors. Chronic treatment of the CX546 resulted in the increased BDNF levels in the brainstem and nodose cranial sensory ganglia, leading to the rescue of normal respiration in *Mecp2*-null mice [70]. Environment enrichment, a physical intervention that enhances the synapse formation and plasticity, augmented the endogenous BDNF in RTT models and ameliorated several RTT-like symptoms, such motor coordination, motor learning, memory deficits and anxiety-related behaviors [126]. In general, mouse models and patients with RTT benefit from the restoration of normal BDNF level in their CNS. In addition, to overcome the limitation of the low-penetration to the BBB for BDNF, BDNF can mimic by its alternatives with similar functions were studied. Chronic administration of 7,8-

dihydroxyflavone, which is able to activate the high -affinity BDNF receptor (TrkB), delayed the body weight loss, increased neuronal nuclei size, alleviated the locomotion defects and the breathing abnormalities in the RTT mouse model [127]. Insulin-like Growth Factor (IGF-1) was also reported to be beneficial to the RTT. In the RTT mouse model, treatment of an active peptide fragment of IGF-1 ameliorated the locomotor dysfunction, breathing abnormalities and the cardiac irregularities, leading to the extended lifespan [96].

In general, although more pharmacokinetics and pharmacodynamics work would be required before the clinical trials, these lab studies provide us multiple alternative targets and potential treatments for the RTT patients.

2.4.2 Genetic restoration

Genetic intervention has been shown to rescue certain phenotypes of RTT as well. Taking advantage of current genetic methods, such as Cre-Lox recombination system, the *Mecp2* gene could be restored in specific nuclei or the whole CNS in RTT mouse models. Selectively restoration of *Mecp2* gene in GABAergic neurons enhanced GABAergic inhibition, expanded lifespan, rescued motor defects and social abnormalities, but tremor or anxiety was not rescued in *Mecp2*-null mice. Such rescue was also detected in *Mecp2*$^{+/-}$ mice, although less dramatic [73]. Conditional mouse models with *Mecp2* re-expressionon in glutamatergic neurons showed the enhanced abnormal EPSCs and the alleviation of RTT-like phenotypes [45]. Delayed global restoration of *Mecp2* gene in the brain and body by crossing *Mecp2*$^{+/-}$ mice containing a “stop-flox” cassette in *Mecp2* gene of one allele with transgenic mice containing the tamoxifen-inducible estrogen receptor/Cre transgene in the ROSA26 locus improves the general phenotypic severity, rescued multiple RTT-like motor and social behaviors, and improves EEG oscillatory activity in *Mecp2*-deficient mice [128]. However, overexpression of *Mecp2* gene in neurons leads to the

severe progressive neurological phenotypes as MeCP2 duplication symptom, although opposite changes in synaptic transmission were triggered in comparison to the *Mecp2* deficiency (22781840). Therefore, the precise regulation of MeCP2 expression level is critical in rescuing the RTT-like symptoms in patients and mouse models.

2.4.3 Other therapy

In current clinical trials, multiple interventions have been applied aiming to improve the living quality of the RTT patients and their families, including physical therapy, speech therapy, and occupational therapy. Although these RTT patients have to limit achievements due to their neurological problems, proper physical interventions favor to maintain motor skills and transitional skills, alleviate deformities, discomfort and irritability and improve their independence [129]. The language retardation of these RTT girls is one of the major challenges in their daily life, which may obstacle the potential treatment due to the improper communication. Speech-language pathologists proposed the Augmentative and Alternative Communication (AAC), a communication method used in place of speech, could be used as the communication innervation in these RTT girls. Written language, body language, and facial expressions, as the typical examples of AAC can be used to communicate with the RTT patients [130]. Due to the deterioration of the symptoms, RTT girls may lose their independence gradually by reducing the meaningful activities in their daily life [131]. Thus, occupational therapy encourages them to maintain or improve these functional activities, as this has been shown to improve health. Therefore, although, there is no cure for the RTT, multiple innervations have been applied in the clinical trials and the RTT girls would benefit from the combination of the treatment.

3 SIGNIFICANCE

Rett Syndrome (RTT) is a neurodevelopmental disease affecting 1 out of 10,000 female children worldwide. People with RTT usually develop autism symptoms, including extreme social anxiety and repetitive stereotype hand movements, which make RTT a serious clinical problem [1, 132]. Currently, there is no cure for the disease, neither a therapeutic agent for symptom relieves. Thus, studies of seeking for therapeutic modalities are innovative and highly significant.

Compared to synaptic $GABA_AR$s, the extrasynaptic $GABA_AR$s are characterized by their extrasynaptic location, high sensitivity to GABA, the capability to produce tonic currents, long-lasting hyperpolarization, and availability for modulation by conventional $GABA_AR$ ligands as well as more selective extrasynaptic $GABA_AR$ modulators [19, 20]. Therefore, it is possible that the extrasynaptic $GABA_AR$s are potential targets for novel pharmacological and behavioral therapies for RTT symptom alleviation.

THIP (also known as Gaboxadol), an agonist specific extrasynaptic $GABA_AR$s [133, 134], is an investigational drug, originally developed for insomnia. Clinical trials suggest that THIP (10mg/day) has no significant effects on sleep onset and total sleep time [135]. It does have effects on these measures in a higher dose (15mg) where the effects are inconsistent between genders, and side effects emerge including sedation and disorientation [135, 136]. Therefore, Merck and Lundbeck canceled further development of the drug. It is not unusual, however, that a preclinical drug fails in one application, but succeeds in another. The low efficacy of THIP on insomnia indeed may be beneficial for its applications to RTT, as the unnecessary sedation can be avoided. We have found that exposure of low-dose THIP alleviated the RTT-like breathing abnormalities, motor dysfunction, social impairment and extends lifespans of *Mecp2*-null mice [67]. Besides, THIP is currently under clinical trials for the Angelman Syndrome and Fragile X Syndrome, which share

many similarities with RTT. Therefore, pre-clinical studies of the drug in RTT-models as proposed in our studies are significant.

4 MATERIAL AND METHODS

4.1 Animal models

Female heterozygous mice (Genotype: *Mecp2*$^{+/-}$; Strain name: B6.129P2(C)-*Mecp2*tm1.1Bird/J; Stock number 003890, Jackson Lab) from were crossbred with male C57BL/6 mice to produce the RTT model mice with the genotype *Mecp2*$^{+/-}$ and *Mecp2*$^{-/Y}$ for further study. The PCR protocol from Jackson Lab was used to identify the genotypes. All experimental procedures were conducted in accordance with the National Institutes of Health (NIH) Guide for the Care and Use of Laboratory Animals and were approved by the Georgia State University Institutional Animal Care and Use Committee.

4.2 THIP Administration

THIP was delivered to the test animals orally in the drinking water. THIP was given to the mother in her drinking water (200mg/L), and then passed to pups of WT and *Mecp2*$^{-/Y}$ male mice via lactation [15]. This will last till weaning at P18. After that, THIP was given through pup's drinking water (20mg/L) for another 5 weeks. In the vehicle control group, THIP was replaced by regular water.

In *Mecp2*$^{+/-}$ mice, identification of RTT-like symptoms was done at 6-9 months of age. Then, the symptomatic mice were divided into two groups treated with THIP (20mg/L in drinking water with the calculated dose: 6.3 mg/kg/day in animals) or water alone (vehicle) for 5 consecutive weeks. The same protocol was applied to WT females as controls.

4.3 Brain slice Preparation

Mice were decapitated after deep anesthesia with inhalation of saturated isoflurane. The brain stem was obtained and immediately placed in ice-cold and sucrose-rich artificial cerebrospinal fluid (aCSF) containing (in mM): 220 sucrose, 1.9 KCl, 0.5 $CaCl_2$, 6 $MgCl_2$, 33 $NaHCO_3$, 1.2 NaH_2PO_4 and 10 D-glucose. The solution was bubbled with 95% O_2 balanced with 5% CO_2 (pH 7. 40). The transverse pontine sections (150-250 μm) containing the LC area were obtained using a vibratome sectioning system and then recovered at 33°C for 60min in normal aCSF containing (in mM): 124 NaCl, 3 KCl, 2 $CaCl_2$, 2 $MgCl_2$, 26 $NaHCO_3$, 1.3 NaH_2PO_4 and 10 D-glucose. The brain slices were kept at room temperature before use. During recording, the slices were perfused with oxygenated aCSF at a rate of 2 ml/min and maintained at 34°C in a recording chamber by a dual automatic temperature control (Warner Instruments).

4.4 Electrophysiology

LC and Me5 neurons were identified as described previously [14, 53]. Whole-cell voltage clamp and whole-cell current clamp were performed with patch pipettes. Sutter pipette puller (Model P-97, Novato, CA) was used to pull the patch pipettes with resistance as 3–5 MΩ. Only the neurons with membrane potential less than -40 mV (LC) or -50mV (Me5) and action potential (AP) over 65 mV were accepted for further experiments. In voltage clamp, the pipettes were filled with solution containing in mM: 50 KCl, 85 CsCl, 2 MgCl2, 2 Mg-ATP, 1 Na-GTP, 10 HEPES, 0.5 EGTA (pH 7.30). The brain slices were perfused with oxygenated aCSF containing in mM: 130 NaCl, 3.5 KCl, 1.25 NaH_2PO4, 1.5 $MgSO_4$, 10 D-glucose, 24 $NaHCO_3$, 2 $CaCl_2$ (pH 7.40). $GABA_AR$-mediated inhibitory postsynaptic currents (IPSCs) and tonic currents were isolated with following agents in the bath solution: 6-cyano-7-nitroquinoxaline-2, 3-dione (CNQX, 10 μM,

Tocris, Minneapolis, MN, disodium salt), the α-amino-3-hydroxy-5-methyl-4-isoxazolepropionic acid (AMPA) receptor antagonist; DL-2-amino-5-phosphonopentanoic acid (DL-APV, 10 μM, Tocris, sodium salt), the N-methyl-D-aspartate (NMDA) receptor antagonist; and strychnine (1 μM, Sigma-Aldrich, St. Louis, MO), the glycine receptor antagonist. All recordings were performed at a holding potential of –70 mV. Tetrahydroisoxazolo [5, 4-c] pyridin-3-ol hydrochloride (THIP, also known as gaboxadol, Tocris, hydrochloride), 4-chloro-N-[2-(2-thienyl) imidazo [1, 2-a] pyridin-3-yl] benzamide (DS2, Tocris), bicuculline (Tocris) and picrotoxin (Sigma-Aldrich) were used to measure the tonic current in the study. In current clamp, the pipette solution containing in mM: 130 K gluconate, 10 KCl, 10 HEPES, 2 Mg-ATP, 0.3 Na-GTP and 0.4 EGTA (pH 7. 3). The bath solution was normal aCSF bubbled with 95% O_2 and 5% CO_2 (pH 7. 40). Recorded signals were amplified with an Axopatch 200B amplifier (Molecular Devices, Union City, CA), digitized at 10 kHz, filtered at 1 kHz, and collected with the Clampex 8.2 data acquisition software (Molecular Devices). The temperature was maintained at 33°C during recording by a dual automatic temperature control (Warner Instruments, New Haven, CT).

Membrane potentials were measured without any current injection. In LC neurons, the input resistance was calculated as the slope of the linear portion in the I-V curve in response to a series of injected pulse hyperpolarized currents (typically from 0.15nA to 0nA). The AP overshoot was measured as the amplitude from 0mV to the peak of more than 20 events. The threshold was determined at the initiation point of at least 20 spontaneous action potentials. In Me5 neurons, APs were evoked with depolarizing pulses. AP properties (threshold, amplitude, rise time and D50) were analyzed from the first evoked APs.

4.5 Molecule experiments

4.5.1 Quantitative PCR

Brain slices were obtained from 3-4 week old mice. Transcripts were obtained from micropunches (~ 1.5mm in diameter) from the LC area, and cDNAs were synthesized with the high-capacity cDNA reverse transcription kit (Life Technologies, Grand Island, NY). PCR primers for GAPDH, δ subunit, α4 subunit, α5 subunit, α6 subunit, β1 subunit, β2 subunit, β3 subunit, TH and DBH were designed with the primer express software and synthesized from Sigma Genesis (Sigma-Aldrich). The Quantitative PCR (qPCR) was performed with Fast SYBR® Green Master Mix (Applied Biosystems, Life Technologies) following the manufacturer's instructions in a Fast Real-time PCR system (Applied Biosystems 7500) for 40 cycles. GAPDH was used as the internal control for the quantification.

4.5.2 Single cell PCR

Transcripts were obtained from single LC neurons that had been studied in whole-cell current clamp experiments. The cDNAs were synthesized with the high-capacity cDNA reverse transcription kit (Life Technologies, Grand Island, NY). Three microliters of reverse transcription product were used to perform PCR with Taq DNA Polymerase (Promega, Madison, WI) for 30 cycles following the manufacturer's instructions. Three microliters of the PCR product were performed using the same PCR cycling protocol as before. The second PCR product was run on 2% agarose gels, which was then imaged using an Alpha Innotech AlphaImager 3400 Multi-Function Gel Imager (Alpha Innotech, Santa Clara, CA). Glial fibrillary acidic protein (GFAP) was used as the negative control. Primers for *Mecp2* were designed with online primer-BLAST and synthesized from Sigma (Sigma-Aldrich, St. Louis, MO).

4.5.3 Western Blot

Pontine slices (300 μm thick) containing the LC area were obtained from 3- to 4-week-old mice by vibratome sectioning system and the pons was processed in RIPA buffer (Sigma-Aldrich) with 1% protease inhibitor. BCA protein assay reagent (Pierce, Rockford, IL) was used to estimate the protein concentrations and 30 μg proteins were used to detect δ subunit signals in 10% SDS-PAGE gels and electrophoretically transferred to nitrocellulose membranes. The membranes were then blocked for 2 h in 5% non-fat milk and incubated overnight at 4 °C with rabbit GAPDH primary antibody (1:10000, Sigma-Aldrich) and rabbit δ subunit primary antibody (1:1000, EMD Millipore, Billerica, MA) [137]. After washed in PBS Tween, the membranes were incubated by HRP-conjugate goat anti-rabbit secondary antibody (1:10000, Life Technologies) for 1h at RT. The chemiluminescent detection system (Pierce) was used to expose the membrane to films (Hy Blot CL; Denville, Metuchen, NJ) and the photographs were scanned. The immunoblotting signals were quantified using the ImageJ software (NIH). The δ subunit signals were normalized to the internal GAPDH controls.

4.5.4 Immunocytochemistry

Mice were anesthetized by inhalation of saturated isoflurane and transcardially perfused with 0.9% saline and 4% (w/v) paraformaldehyde in 0.1M PBS, sequentially. Then, the brain was removed, fixed with 4% (w/v) paraformaldehyde for 2 hour and transferred to a 30% sucrose solution in 0.1M PBS. Pontine transverse sections (30 μm) containing the LC region were obtained on a cryostat (Leica, Wetzlar, Germany). Catecholaminergic neurons were labeled with anti-dopamine β-hydroxylase (TH) and cells. MeCP2 expression was detected with anti-MeCP2 antibodies. Briefly, the sections were incubated with primary anti-TH antibodies (mouse; 1:4,000;

Sigma, St. Louis, MO) and anti-MeCP2 antibodies (Rabbit; 1:1,000; Sigma, St. Louis, MO), followed by Alexa Fluor 488-conjugated donkey anti-mouse (1:400; Life Technologies) and Alexa Fluor 647-conjugated goat anti-rabbit (1:500; Life Technologies) secondary antibodies. All the steps were performed at room temperature.

For quantification of TH or MeCP2 immunoreactivity, each slices were captured as two images, which were then analyzed using ImageJ software. Around 10 images were used in each animal, and the immunoreactivity of each cell was scored and recorded. In general, 4 animals in each group were used in the experiments. The median of TH-positive cell numbers in each image is ~25 in each image and percentages of MeCP2-positive and MeCP2–negative cells were analyzed.

4.6 Behavior Tests

4.6.1 Plethysmograph

The breathing activities of unanesthetized mice were recorded by the plethysmograph system with a ~ 40 ml plethsmograph chamber and a connected reference chamber. The individual animal was kept in the plethysmograph chamber flowed by air at a rate of 60ml/min for at least 20 min for adaptation followed by a 20 min recording. The breathing activities were recorded continuously as the barometrical changes between the plethysmograph chamber and the reference chamber with a force-electricity transducer. The signal was amplified and collected with Pclamp 9 software. The animals were monitored via a video camera to ensure the awake status during tests. The data analysis was done blindly to the treatment. Apnea was considered only if the breathing cycle lasts twice or longer than the previous cycle. Breathing frequency variation was calculated as the division of standard deviation (SD) of the frequency by their

arithmetic mean. All of were measured from 200~300 successive breathing events, which were randomly sampled from three or four stretches with at least 50 breaths in each.

4.6.2 Grip Strength

When lifted by the tail, the forelimbs of a mouse (age 5-6 weeks) were allowed to grasp the sensor lever of a force-electricity transducer. The mouse was then gently pulled upward by the tail until it released the grip. Forces were continuously recorded with the Clampex 9 software. The grip strength of each mouse was measured as the maximum force before lever release, and averaged from three consecutive trails.

4.6.3 Grid Walking

A mouse (age 5-6 weeks) was placed on the metal rigid floor of a trial box (32 cm × 20 cm × 20 cm). The box was elevated by 50 cm with the floor made of 11 × 11 mm metal mesh. Mouse walking on the metal mesh floor was videotaped for 5 minutes. In the video record, the limb placement error was counted. A footfault was counted only when a limb missed the metal floor bar (0.5mm in diameter) completely and went through the grid opening. The footfault ratio was calculated by the overall numbers of footfaults divided by the total steps including both forelimbs and hindlimbs.

4.6.4 Open Field test of spontaneous locomotion

The experiment was performed as we described previously [31]. Mice aged 5-6 weeks were tested in an open field chamber made of white plexiglass boards (50 cm L × 50 cm W × 30 cm H) with 10 cm × 10 cm square lines. Test animals were kept in their home cages and habituated for 30 min in the test room before testing. When tested, each animal was placed in the center square

and allowed to move freely in the chamber. Spontaneous locomotion activity was monitored by a video camera for 5 min. With the video record, square crosses (all four paws cross) were measured in each mouse. To eliminate potential residual odors and potential contaminants, 70 % ethanol was used to clean the apparatus followed by dd H_2O rinse after each test.

4.6.5 Three Chamber (Social Interaction)

Mice, age 6-7 weeks, were tested in a box (60 cm L × 30 cm W × 40 cm H), in which there were three chambers (20 cm L × 30 cm W × 40 cm H) separated with transparent walls. A door was arranged diagonally in each wall allowing the tested mouse to travel freely in the chambers. Before test, mice were placed in the test room for 30 min habituation. Then sequential tests were performed in each mouse. Firstly, the tested mouse was placed in the center chamber, and allowed to move freely over all three chambers for 10 min. Its chamber preference was analyzed by the time spent in each chamber. Secondly, the social behavior test was performed by introducing a random littermate in one of the side chambers for 10 min, while times that the tested mice spent with the mice were measured. The littermate was randomly assigned in either side of the chamber to avoid the side bias. Lastly, the social novelty test was performed by introducing a new stranger mouse in the chamber and switching the familiar littermate to the other chamber. The time spent in both side the chambers were analyzed subsequently [138].

4.6.6 Lifespan

Mecp2$^{-/Y}$ mice used in the experiment were randomly selected and divided into two groups. One group was treated with THIP containing water, and the other treated with regular water as vehicle control. Their lifespan were monitored under the identical living condition. Their daily activity and general physical conditions, including feeding, movement, body weight, interaction

with other mice, were observed. Death date of each mouse was recorded when it occurred naturally or reached the humane end point that was determined by staff members in the animal facility at Georgia State University without any consultation with the investigators. One outlier, which was 1.5 interquartile range (IQR) above the third quantile and below the first quantile, was removed from each group to minimize data variations.

4.6.7 Phenotype scoring system

To separate the *Mecp2*$^{+/-}$ mice, a two-step identification procedure was used. Firstly, we adopted the scoring system proposed previously [51] with modifications to determine potential symptomatic *Mecp2*$^{+/-}$ mice, which consisted of 1) abnormal mobility, 2) abnormal gait, 3) hindlimb clasping, 4) tremor, 5) abnormal breathing, and 6) weak general condition. Score 0 was assigned to a mouse if none of these signs was found; the animal was scored 1 if any one of the 6 signs was shown to be mild (score 6 if the mouse showed all); score 2 if any of the signs was severe (maximum 12). The *Mecp2*$^{+/-}$ mouse was placed in the potential symptomatic group if it received 3 scores or more. Secondly, the mouse was considered to be symptomatic when it also showed breathing abnormality in the plethysmograph test as we reported previously [107]. Only were the symptomatic *Mecp2*$^{+/-}$ (s*Mecp2*$^{+/-}$) mice used in the present study, which were divided into two groups and treated with vehicle or THIP.

4.7 Double Blind

The animals used in the study were randomly separated into vehicle group and THIP group. The patch experiments were done double-blindly by two to three people without information of mouse genotype and treatment. All the data analysis of behavior experiments, including breathing

activity, motor function and social behavior were done with no information of the genotype and treatment.

4.8 Data Statistics

The electrophysiological data and the plethysmograph data were analyzed with Clampfit 10.3 software. The sample sizes in the experiments were examined with G-Power Analysis to yield sufficient statistical power [139]. Data are presented as means ± SE or median ± IQR. Mantel-Cox test was used in the lifespan experiment. Two-tailed Student's *t*-test, ANOVA, Tukey's or Fisher's LSD post-hoc, Kruskal-Wallis test, Pearson correlation and Spearman's correlation were used to perform the statistical analysis. Difference was considered significant when $P < 0.05$.

Table 4.1: Primers for PCRs

Target gene	Primers Sequences
GAPDH	Fw: CCAGCCTCGTCCCGTAGA
	Re: TGCCGTGAGTGGAGTCATACTG
δ subunit	Fw: GGCTTCTTGGGCTTTACC
	Re: CACCCCCACTGTTTTTCTC
α4 subunit	Fw: GTGGGAAATCACTCCAGCAAG
	Re: AATGCAGGGCGAGTGGAAG
α5 subunit	Fw: CAAAAGAGCAGCCTCCAG
	Re: GAAAGTGCCAAACAAGATGG
α6 subunit	Fw: GACTTTGCCCATCGTTCC
	Re: TGCAAAAGCTACTGGGAAGAG
β1 subunit	Fw: TGGTTTTCGATCTTGTGTGTCAG
	Re: AGCCACCTCTCTCTTTGTGTTTG
β2 subunit	Fw: TTCCCACTGCTGTTTCTCACATAC
	Re: ATCCTAACCACTTCTCCTTTTTTCC
β3 subunit	Fw: GTTGAGTGGTTGTGTTGCCAATG
	Re: ATGTCCCCGTGTTGGCATC
TH	Fw: TGGCTGACCGCACATTTG
	Re: CCTGCACCGTAAGCCTTCA
DBH	Fw: TACCACAACCCACGGAAGATA
	Re: CGGTCAACACAAAGGCAGTCT
Mecp2	Fw: CCAAATCTCCCAAAGCTCCA
	Re: GCTTGGAAAGGCATCTTGAC

GAPDH; glyceraldehyde 3-phosphate dehydrogenase, TH; tyrosine hydroxylase, DBH; dopamine b-hydroxylase.

5 CHAPTER1: *MECP2* GENE DISRUPTION AUGMENTS $GABA_AR$ MEDIATED INHIBITION IN LOCUS COERULEUS NEURONS: IMPACT ON NEURONAL EXCITABILITY AND BREATHING

Publication: **Zhong W**, Cui N, Jin X, Oginsky MF, Wu Y, Zhang S, Bondy B, Johnson CM and Jiang C. (2015) Methyl CpG binding protein-2 gene disruption augments tonic currents of γ-aminobutyric acid receptors in locus coeruleus neurons: Impact on neuronal excitability and breathing. *Journal of Biological Chemistry*, 290(30):18400-11.

Contribution disclosure: Weiwei Zhong and Dr. Chun Jiang designed the research and write the article. Weiwei Zhong performed the experiments and analyzed the data. Ningren Cui, Xin Jin, Max F Oginsky, Brain Bondy and Christopher M Johnson assisted in the electrophysiology experiments. Yang Wu and Shuang Zhang assisted in the molecular experiments.

5.1 Abstract

People with Rett Syndrome (RTT) and mouse models show autonomic dysfunction involving brainstem locus coeruleus (LC). Neurons in the LC of *Mecp2*-null mice are overly excited, likely to result from defect in neuronal intrinsic membrane properties and deficiency in GABA synaptic inhibition. In addition to the synaptic GABA receptors, there is a group of $GABA_A$ receptors ($GABA_A$Rs), which is located extrasynaptically, and mediates tonic inhibition. Here we show evidence for augmentation of the extrasynaptic $GABA_A$Rs in *Mecp2*-null mice. In brain slices, exposure of LC neurons to $GABA_A$R agonists increased tonic currents that were blocked by $GABA_A$R antagonists. With 10 μM GABA, the bicuculline-sensitive tonic currents were ~ 4 folds larger in *Mecp2*-null LC neurons than the wild-type (WT). Single-cell PCR analysis showed that δ subunit, the principal subunit of extrasynaptic $GABA_A$Rs, was present in LC neurons. Expression levels of the δ were ~ 50% higher in *Mecp2*-null neurons than in the WT. Also increased in expression in *Mecp2*-null mice was another extrasynaptic $GABA_A$R subunit α6 by ~ 4 folds. The δ subunit-selective agonists THIP and DS2 activated the tonic $GABA_A$ currents in LC neurons and reduced neuronal excitability to a greater degree in *Mecp2*-null mice than in the WT. Consistent with these findings, in-vivo application of THIP alleviated breathing abnormalities of conscious *Mecp2*-null mice. These results suggest that extrasynaptic $GABA_A$Rs seem to be augmented with *Mecp2* disruption, which may be a compensatory response to the deficiency in GABA-ergic synaptic inhibition and allow a control of neuronal excitability and breathing abnormalities.

5.2 Introduction

Rett Syndrome (RTT) is a neurodevelopmental disease with ~ 0.01% morbidity rate in live-born females worldwide [1]. Over 90% of RTT cases are caused by mutations of the X-linked *MECP2* gene encoding methyl CpG binding protein 2 (MeCP2), a transcription regulator [1]. People with RTT usually develop autism-like symptoms 6 to 18 months after birth, which include stereotypical repetitive hand movements, social anxiety and seizures. Dysfunctions in the autonomic nervous system such as breathing instability, gastrointestinal disorders and cardiac arrhythmia are common [2, 3].

The NE system in the brainstem is involved in autonomic function, especially NE-ergic neurons in the locus coeruleus (LC). Recent studies in our and other labs have shown that the LC neurons in *Mecp2*-null mice are abnormal or defective. The defect manifests itself as reduced expression of NE synthetic enzymes, hyperexcitability and impaired CO_2 chemosensitivity [4-9]. The hyperexcitability of LC neurons is attributable to the intrinsic membrane properties of the cells and a decrease in synaptic inhibition mediated by γ-aminobutyric acid (GABA) [4, 10]. Both $GABA_A$ and $GABA_B$ receptor mediated postsynaptic inhibition are reduced, and the GABA release from presynaptic terminals is significantly low [10]. Consistent with these observations, defects in the $GABA_A$ receptor ($GABA_AR$) system are also found in other brain regions [17, 18, 78, 140]. Selective deletion of the *Mecp2* gene in GABA-ergic neurons recapitulates most RTT phenotypes in mice [11]. These findings indicate that the GABA system plays an important role in the development of RTT.

GABA is the most prominent inhibitory neurotransmitter in the brain acting on both synaptic and extrasynaptic GABARs. The synaptic $GABA_ARs$ are found in postsynaptic membranes of neurons. In adult neurons, activation of the synaptic $GABA_ARs$ produces fast

inhibitory postsynaptic currents and hyperpolarization of the postsynaptic cells. The extrasynaptic $GABA_AR$s known as tonic receptors are characterized by their extrasynaptic location, high sensitivity to GABA, capability to produce tonic currents with long-lasting hyperpolarization, and availability for modulation by conventional $GABA_AR$ ligands as well as more selective extrasynaptic $GABA_AR$ modulators [19, 20].

Both of the synaptic and extrasynaptic $GABA_AR$s are pentamers, usually composed of 2-3 heteromeric subunits with a total 19 (α1-6, β1-3, γ1-3, δ, θ, ε, π, and ρ1-3) [19]. $GABA_AR$s with different combinations of subunits are found in different neurons. γ2 containing receptors are mainly localized at the synapse, playing a key role in the GABA synaptic transmission [141, 142]. The δ subunit, usually assembled with 2 α and 2 β subunits, is the major contributor of the extrasynaptic $GABA_AR$s [20, 142]. These receptors are responsible for tonic GABA inhibition without interfering with synaptic transmission, which is due to their high affinity to GABA and weak desensitization.

The findings of defects in synaptic $GABA_AR$-mediated synaptic inhibition in *Mecp2*-null mice are encouraging because therapeutical $GABA_AR$ activators are widely available. These drugs may be used to correct the defects in the GABA system and relieve RTT-like symptoms. Indeed, several recent studies have shown that the breathing disorders of *Mecp2*-null mice can be alleviated by augmenting GABA synaptic inhibition [12, 13]. In contrast to the rich information of the synaptic $GABA_AR$s in RTT research [10, 14-18], how the extrasynaptic $GABA_AR$s are affected by the *Mecp2* disruption remains unknown. The capability of these tonic $GABA_AR$s to reduce neuronal excitability without interrupting synaptic transmission suggests that these receptors may allow an alternative therapeutic intervention to RTT. Therefore, we studied the extrasynaptic $GABA_A$ currents in LC neurons in wild-type (WT) and the mouse model of RTT.

5.3 Results

5.3.1 $GABA_A$-ergic tonic currents in WT neurons

To determine the $GABA_A$ tonic currents in LC neurons, whole-cell voltage clamp was performed in brain slices of WT mice. Inward Cl^- currents were studied, with 135 mM Cl^- in both the pipette and bath solutions at a holding potential of -70 mV, with glutamatergic and glycinergic currents were blocked (see Methods). Under this condition, the LC neurons showed spontaneous GABA-ergic IPSCs that were blocked by bicuculline (50 μM) or picrotoxin (20 μM). Meanwhile, we found that these $GABA_A$-R blockers also suppressed tonic inward currents. Thus, we studied the $GABA_A$-ergic tonic currents. The currents histograms were generated at stable condition before and after $GABA_AR$ blockade, which were then fit with Gaussian distribution. The opening of the ionotropic receptors also increases the current noise levels, which were measured as the standard variation of the Gaussian distribution. We analyzed the ratio of noise levels before vs after a treatment with $GABA_AR$ blockers.

Bicuculline reduced the tonic currents by 2.9 ± 0.6 pA (n = 5), and the noise ratio is 1.31 ± 0.06 (n = 5) (Fig. 5-1B). Similar results were obtained with picrotoxin (Fig. 5-1A). The effects of bicuculline on the tonic currents and the noise ratio were more obvious in the presence of GABA in the perfusion solution. A pre-treatment with 1 μM GABA augmented the tonic currents to 5.0 ± 1.0 pA, and the noise ratio to 1.37 ± 0.08 (n = 5) (Fig 5-1C). With 10 μM GABA, the tonic currents were raised to 13.6 ± 1.4 pA (n = 6), and the noise ratio to 3.97 ± 0.76 (n = 6) (Fig 5-1D). The bicuculline sensitive tonic currents and noise augmentation increased dose-dependently with increased GABA concentrations ($P < 0.001$, One-way ANOVA) (Fig. 5-1E, F, G).

5.3.2 Enhancement of $GABA_A$-ergic tonic currents in Mecp2-null mice

At baseline, the bicuculline-sensitive tonic currents were significantly larger in *Mecp2*-null mice than in WT mice (6.4 ± 0.8 pA, n = 5 vs. 2.9 ± 0.6 pA, n = 5; P < 0.01, Student's *t*-test; Fig. 5-2A, D, E). These tonic currents in *Mecp2*-null mice became even greater in the presence of 1 μM or 10 μM GABA, which were 13.5 ± 1.7 pA (n = 5) and 49.8 ±10.7 pA (n = 6) respectively. Both were significantly higher than in the WT neurons (P < 0.001 and P < 0.01, Student's *t*-test; Fig. 5-2B, C, D, E). In *Mecp2*-null mice, the noise ratio also increased dose-dependently with these GABA concentrations (1.74 ± 0.08 and 7.77 ± 1.21, respectively; P < 0.01 and P < 0.05, respectively; Student's *t*-test; Fig. 5-2F) although significant difference was not found at baseline. These results suggest that the bicuculline-sensitive tonic currents are significantly increased in *Mecp2*-null LC neurons.

5.3.3 Effects of specific agonists for extrasynaptic $GABA_ARs$

The $GABA_A$-ergic tonic currents are likely to be mediated by extrasynaptic $GABA_ARs$ expressed in the LC neurons. Because the molecular compositions of extrasynaptic $GABA_ARs$ are different from those of synaptic $GABA_ARs$, these extrasynaptic receptors can be activated with selective agonists such as THIP and DS2 that do not affect the synaptic $GABA_ARs$ [133, 134]. In the presence of 1 μM THIP in the bath solution, the $GABA_A$-ergic tonic currents (18.6 ± 2.9 pA, n = 5) and noise ratio (1.94 ± 0.07, n = 5) were both augmented in WT neurons (Fig. 5-3A). In *Mecp2*-null neurons the same concentration of THIP raised the tonic currents (55.3 ± 6.6 pA, n = 5) and the noise ratio (2.91 ± 0.29, n = 5) to significantly greater degrees than in the WT neurons (P < 0.001 and P < 0.01, respectively, Student's *t*-test; Fig. 5-3B-E). THIP did not affect frequency

and amplitude of the GABA-ergic IPSCs in both WT and *Mecp2*-null LC neurons (Student's *t*-test; Fig. 5-3F-I).

Similarly, application of DS2 (20 μM), a positive allosteric modulator of extrasynaptic $GABA_A$Rs, augmented the tonic currents and noise ratio. This effect was larger in *Mecp2*-null mice (19.5 ± 2.3 pA, 2.32 ± 0.21, respectively; n = 5) than in the WT mice (8.5 ± 1.2 pA, 1.53 ± 0.07, respectively; n = 5; $P < 0.01$ and $P < 0.01$, respectively, Student's *t*-test; Fig. 5-4A-E). Unlike THIP, DS2 augmented the frequency and amplitude of the GABA-ergic IPSCs in LC neurons, which may be attributed to their affinity for the αβ type $GABA_A$Rs. Despite this, we did not find significant differences between WT and *Mecp2*-null mice (Student's *t*-test; Fig. 5-4F-I). These results indicate that the extrasynaptic $GABA_A$Rs existing in LC neurons seem to have a greater effect on LC neuronal activity in *Mecp2*-null mice.

5.3.4 Differential expression of $GABA_A$R subunits in WT and Mecp2-null mice

The δ subunit is the principal component of extrasynaptic $GABA_A$Rs, which is localized exclusively outside of the synaptic cleft, mediating the $GABA_A$-ergic tonic currents [143]. If *Mecp2*-null LC neurons have more extrasynaptic $GABA_A$Rs, the δ subunit should be expressed in these cells at a higher level than in the WT neurons. To test this possibility, we studied the δ subunit expression in mRNA and protein levels. Single-cell PCR analysis showed that the δ subunit was expressed in most LC neurons in both WT and *Mecp2*-null mice (14 of 14 WT neurons and 15 of 17 *Mecp2*-null cells; Fig. 5-5A), consistent with the presence of $GABA_A$-ergic tonic currents in the LC neurons.

In quantitative PCR (qPCR), the δ subunit was found to be expressed in the WT LC neurons with the $2^{-\Delta Ct}$ method. With the $2^{-\Delta\Delta Ct}$ method, the expression level of the δ subunit increased by

1.8 ± 0.5 folds in LC tissue micropunches obtained from *Mecp2*-null mice in comparison to the WT (n = 9, P < 0.01, Student's t-test; Fig. 5-5B-D). The Western blot analysis showed that the δ subunit protein expression was increased by 1.6 ± 0.1 folds in *Mecp2*-null mice over the WT (n = 6, P < 0.01; Student's t-test, Fig. 5-5E, F). These results suggest that the δ subunit is expressed in LC neurons, and its increased expression in *Mecp2*-null mice may contribute to the abundant tonic $GABA_A$ currents.

The α5 subunit is another important contributor to the extrasynaptic $GABA_A$Rs [144, 145]. In single-cell PCR, the α5 transcript was barely detected in LC neurons (0 out of 14 in WT and 2 out of 17 in *Mecp2*-null). The qPCR analysis showed that α5 expression in LC neurons was only about one third of δ subunit expression in WT mice. There was a significant reduction of α5 expression in *Mecp2*-null mice (n = 5, P < 0.05, Student's t-test; Fig. 5-5B-D), suggesting that the large tonic currents in *Mecp2*-null mice were unlikely to be produced by increased α5 expression.

The δ containing extrasynaptic $GABA_A$Rs are usually composed of 2 α and 2 β subunits. Previous studies report that all the 3 β subunits (β 1 – 3) and α4, α6 subunits contribute to the assembling of extrasynaptic $GABA_A$Rs [20, 74, 146]. In qPCR, α6 expression was increased by ~ 4 folds in *Mecp2*-null mice over the WT levels, while α4 expression was reduced (n = 4, P < 0.001, Student's t-test; Fig. 5-5H). Transcript levels of β1 and β2 subunits were both reduced (n = 5, P < 0.001, Student's t-test), while β3 transcript did not change (Fig. 5-5H).

5.3.5 Modulation of LC neuronal firing activity by extrasynaptic $GABA_A$R agonists

LC neuronal electrophysiological activity was studied in current clamp. In WT mice, THIP reduced the input resistance (Rm) from 480.5 ± 7.1 MΩ to 458.7 ± 7.6 MΩ. Meanwhile, THIP hyperpolarized the cells by 1.1 ± 0.4 mV and decreased firing rate by 17.3 ± 3.3% (n = 14, Fig. 5-

6A_1-A_3, C, D, E). In *Mecp2*-null mice, the same THIP treatment reduced the input resistance from 500.5 ± 8.7 MΩ to 424.9 ± 17.7 MΩ, hyperpolarized the cells by 3.0 ± 0.5 mV, and lowered the firing rate from 5.1 ± 1.3 Hz to 3.6 ± 1.6 Hz (n = 9; $P < 0.05$, $P < 0.05$ and $P < 0.05$, respectively, Student's *t*-test; Fig. 5-6B_1-B_3, C, D, E), which is approximate to the baseline level in WT LC neurons (2.9 ± 0.2 Hz in WT baseline, n = 14, Fig 5-6E). All these percentile changes were significantly greater than in the WT neurons ($P < 0.01$, $P < 0.01$ and $P < 0.05$, respectively, Student's *t*-test; Fig. 5-6F-H).

In either WT or *Mecp2*-null mice, 1 μM THIP did not affect the super-threshold and repetitive firing properties, including action potential morphology, afterhyperpolarization (Fig. 5-7), spike frequency adaptation (Fig. 5-8), and delayed excitation (Fig. 5-9), when synaptic transmission was deliberately blocked. Post inhibitory rebound and bursting activity were not found in LC neurons before and after THIP treatment in neither WT mice nor *Mecp2*-null mice. Taken together, these results indicate that activation of δ-subunit containing $GABA_A$Rs leads to an inhibition of LC neurons, an effect that is greater in *Mecp2*-null mice than in the WT, which brings the neuronal firing from hyperexcitable status to the level of WT neurons.

5.3.6 The effect of extrasynaptic $GABA_A$R agonist on breathing

Previously studies indicate that LC neurons are sensitive to high CO_2 and low pH, and they play an important role in regulating the breathing activity [8]. In *Mecp2*-null mice, several groups of neurons including the LC neurons are hyper-excitable [4, 12, 15, 147], which appears to contribute to the breathing disorders in *Mecp2*-null mice. To test whether activation of the extrasynaptic $GABA_A$Rs can alleviate the breathing abnormities, we studied breathing activity using plethysmography in conscious *Mecp2*-null mice. The mice were divided into two groups with one

receiving THIP injections (10 mg/kg, i.p.), and the other was given saline injection. At the 3 weeks of age, *Mecp2*-null mice start to develop breathing disorders with obvious breathing frequency variation and frequent apneas. Therefore, we monitored the breathing activity of *Mecp2*-mull mice with THIP/saline injection once a day for 7 consecutive days starting from 26 days of age. After the 7 day treatment, *Mecp2*-null mice with saline injection continued to develop severe breathing disorders with 89 ± 16 apneas/hour, a ~ 50% increase compared to day 0 (n = 5, Fig. 5-10A, C), and 0.29 ± 0.03 F variation, a ~ 20% increase (n = 5, Fig. 5-10A, D). THIP treatment markedly reduced breathing disorders to 46 ± 6 apnea/hour, a 18% reduction compared to day 0 (n = 5, Fig. 5-10B, C), and 0.17 ± 0.04 F variation, a 32% reduction (n = 5, 6-. 5-10B, D). Both the breathing parameters are significantly improved in the THIP group over their saline counterparts (Fig. 5-10C, D, two-way ANOVA and Tukey's post-hoc test). Therefore, the results suggest that the extrasynaptic $GABA_AR$ agonist THIP alleviates the breathing disorders of *Mecp2*-null mice.

5.4 Discussion

To our knowledge, this is the first demonstration of extrasynaptic $GABA_A$ currents in the mouse model of RTT. Our results have shown that tonic $GABA_A$ currents in LC neurons are significantly larger in *Mecp2*-null neurons than in the WT, likely to be due to the overexpression of the $GABA_AR$ species containing δ and α6 subunits. Furthermore, activation of the extrasynaptic $GABA_ARs$ appears to reduce neuronal excitability and alleviate breathing abnormalities of *Mecp2*-null mice.

5.4.1 Defects in synaptic $GABA_A$Rs in Mecp2-null mice

Previous studies have shown that the $GABA_A$ system is defective in *Mecp2*-null mice and people with RTT. In mice, this is associated with multiple RTT-like phenotypes, including progressive motor dysfunction and abnormal breathing [11]. In GABA-ergic neurons, impaired GABA synthesis and the consequent reduction in the GABA quanta release have been found [10, 11, 18]. In postsynaptic cells, there is a marked reduction in $GABA_A$R density in the brain of RTT patients and *Mecp2*-null mice [75, 76]. An epigenetic study in a mouse model of RTT indicates that the $GABA_A$R β3 subunit expression is reduced in the cerebellum, and another molecular study confirmed the down-regulation of β3 subunit in cerebellum [78, 79]. The α1 subunit in the frontal cortex, and α2 and α4 subunits in the ventrolateral medulla were also reduced in *Mecp2*-null mice [18]. In LC neurons our previous studies have shown that the postsynaptic $GABA_A$ and $GABA_B$ currents both are defective in *Mecp2*-null mice [10]. Consistent with these findings, the therapeutic $GABA_A$R activators diazepines and the reuptake blocker NO-711 improve RTT symptoms in animal models, including breathing [12, 13]. However, it is still unclear how the extrasynaptic $GABA_A$Rs are affected in *Mecp2*-null mice, which makes our present study remarkable.

5.4.2 Presence of extrasynaptic $GABA_A$Rs in LC neurons

Extrasynaptic $GABA_A$Rs were first described in cerebellar cortical grey matter [148], and later found in many other brain areas, such as cerebral cortex, dentate gyrus granule, thalamus and neocortex [149-154]. The extrasynaptic $GABA_A$Rs are sensitive to low levels of ambient GABA with little desensitization. They are likely key targets for neurosteroids and alcohol [143, 155-157], and useful targets for the treatment of some neuronal disease such as sleep disorders, epilepsy, stroke and Parkinson's disease [158, 159]. The δ subunit is the primary component of extrasynaptic

$GABA_AR$s found exclusively in extrasynaptic locations meditating tonic inhibition [20, 142]. Some other $GABA_AR$ subtypes may be also involved in extrasynaptic $GABA_AR$s, such as α5-subunit containing receptors [144, 145, 160]. Our results from this study suggest that extrasynaptic $GABA_AR$s are also present in LC neurons. Activation of these receptors results in tonic hyperpolarizing currents that are sensitive to GABA and the $GABA_AR$ blockers bicuculline and picrotoxin. Consistent with these electrophysiological studies, our molecular biological evidence indicates that the δ subunit is expressed in LC neurons.

Accompanying with the δ subunit are another 2 α and 3 β subunits forming pentameric extrasynaptic $GABA_AR$s. Our qPCR results suggest that the α6 containing extrasynaptic $GABA_AR$s seem to play a major role in *Mecp2*-null LC neurons, which has been described in mature cerebellar granule cells [161]. The β1 – 3 subunits are necessary components in both extrasynaptic and synaptic $GABA_AR$s. Previous studies report a ~ 30% reduction in postsynaptic GABAergic IPSCs in *Mecp2*-null LC neurons. The reduced α4 level found in this study is thus consistent with the deficiency in synaptic $GABA_AR$s. Regarding the increase in the α6 transcript level, it is possible that deletion of *Mecp2* leads to reorganization of the GABA receptor species in LC neurons by increasing the α6 subunit expression and reducing the expression of other α subunits. Similar reorganization has been found in nicotinic ACh receptors in *Mecp2*-null LC neurons [49]. The increased α6 subunits may assemble the extrasynaptic receptors together with the δ subunit as well as synaptic $GABA_AR$s with β and γ subunits. Because all the β subunits contribute to the synaptic $GABA_AR$s, and because the synaptic $GABA_AR$s are lowered with the *Mecp2* knockout, it is possible that their overall reduction masks the potential up-regulation of some subunits in the extrasynaptic location. Another possibility is that the extrasynaptic $GABA_AR$s in *Mecp2*-null mice might be composed of more than 2 α subunits, which may explain

the reduced expression of β subunits and the unproportionally increased expression of α6 subunits although the 2 α, 2 β, and 1 δ stoichiometry of $GABA_AR$s has previously been shown in an exogenous expression system [162]. Despite the uncertainty of β subunits, it is likely that the overly expressed $GABA_AR$ species in *Mecp2*-null mice appears to contain δ and α6 subunits.

5.4.3 Tonic $GABA_A$ currents in Mecp2-null mice

The presence of tonic $GABA_A$ currents in LC neurons motivated us to study the extrasynaptic $GABA_AR$s in *Mecp2*-null mice. We found that the bicuculline-sensitive $GABA_A$-ergic tonic currents not only existed in *Mecp2*-null mice, but also were markedly enhanced, as extrasynaptic $GABA_AR$ agonists also elicited significantly larger tonic $GABA_A$ currents in *Mecp2*-null neurons. What underlies the large tonic $GABA_A$ currents in *Mecp2*-null neurons is unclear, which may result from a relief of direct transcription repression by MeCP2 or its indirect effects on other transcriptional regulators and second messenger systems as a result of the *Mecp2* disruption. It is also possible that the increased $GABA_A$ tonic currents result from compensatory mechanisms for insufficient GABA synaptic input in *Mecp2*-null neurons [10]. Multiple types of neurons are hyperexcitable in *Mecp2*-null mice, such as hippocampal neurons, neocortical neurons, LC neurons, hypoglossal neurons, etc. [4, 12, 18, 147, 163-165], which is likely to be due to impaired synaptic transmission and intrinsic membrane properties. The highly excitable state of some of these neurons seems to contribute to cognitive defects, motor abnormality and breathing disturbances [8, 12, 163, 164]. Clearly, such an over-excitation in central neurons can be alleviated by GABA-ergic inhibition, in which excessive extrasynaptic $GABA_AR$s are beneficial. Interestingly, this seemingly compensatory up-regulation of GABA-ergic inhibition has been reported in the synaptic $GABA_A$ system [16, 166, 167]. In neocortical layer 5 neurons of *Mecp2*-null mice, an increase of spontaneous IPSCs were recorded, which seems to result from the deficit

in GABA release from presynaptic terminals [16]. Therefore, the large tonic $GABA_A$-ergic currents in LC neurons of *Mecp2*-null mice found in the present study might be a compensatory response to the deficient GABA synaptic inhibition.

Although the expression level suggests that the large tonic $GABA_A$ currents in *Mecp2*-null mice are likely to be due to the overexpression of δ subunit-containing receptors, our data cannot rule out the possibilities that other expression patterns of $GABA_A$Rs or a change in GABA affinity could also contribute to the enhanced tonic GABA inhibition in *Mecp2*-null mice. Nevertheless, RTT patients and *Mecp2*-null mice with insufficient GABA-ergic inhibition may benefit from these overexpressed extrasynaptic $GABA_A$Rs, as they may provide alternative targets for pharmaceutical interventions in addition to synaptic $GABA_A$Rs.

5.4.4 Modulation of neuronal activity and breathing

Experimental evidence suggests that LC neurons play an important role in brainstem CO_2 chemosensitivity and breathing regulation [8, 42, 147]. Several groups of respiratory neurons and motoneurons are modulated by NE, in which NE augments cellular excitability via α adrenoceptors [168, 169]. This NE-ergic modulation relies on firing activity and NE biosynthesis in LC neurons. It is possible that there is a homeostatic state between LC neuronal excitability and NE biosynthesis, allowing a stable release of NE at synapses. Although high LC neuronal excitability may lead to more NE release, persistent hyperexcitability may have adverse effects. Hyperexcitability often leads to Ca^{++} overload, while a persistent elevation of cytosolic Ca^{++} can activate a variety of degradative enzymes including proteases, lipases and endonucleases [170, 171]. These may trigger a cascade of events leading to abnormal cellular activity and metabolic dysfunction, which may paradoxically compromise NE biosynthesis.

Mecp2 disruption in mice also causes hyperexcitability in LC neurons and impaired metabolic activity, which is attributable to the defects in neuronal intrinsic membrane properties and insufficient GABA inputs [4, 8, 147]. Consistent with these findings, treatment with GABA or diazepam rebalances the hyperexcitability of expiratory neurons, and improves the breathing activity in *Mecp2*-null mice [12, 13]. In the present study, we have found that administration of THIP activates extrasynaptic $GABA_A$Rs and reduces excitability of LC neurons as well. Like diazepam, the THIP treatment alleviates the breathing abnormalities of *Mecp2*-null mice. Therefore, the excitability stabilization appears crucial for reinstallation of brainstem autonomic function. To avoid potential effects of THIP on arousal states, we monitored the animal activity with a video camera during plethysmograph recordings and confirmed that they were not in behavioral sleep.

In *Mecp2*-null mice, over-excitation of LC neurons may contribute to their metabolic dysfunction by disturbing the homeostasis of NE synthesis, the NE production and NE release by presynaptic terminals. A previous study reported that in Cos-7 cells, chronic over-excitation impaired the homeostatic synaptic plasticity by decreasing the AMPA receptors expression [172]. Indeed, decreased expression of tyrosine hydroxylase (TH) and dopamine β hydroxylase (DBH) are known to occur in LC neurons of *Mecp2*-null mice, leading to insufficient NE biosynthesis [6, 50]. THIP application seems to correct the LC neuronal hyperexcitability by activation of extrasynaptic $GABA_A$Rs as shown in this study, which we believe may stabilize neuronal activity and metabolism rebalancing the homeostatic state and improving the NE biosynthesis.

In conclusion, bicuculline-sensitive tonic currents were recorded from LC neurons, which were increased dose-dependently with increased GABA concentrations. In comparison to WT mice, these $GABA_A$-ergic tonic currents were increased significantly in *Mecp2*-null mice.

Agonists specific to extrasynaptic $GABA_AR$s triggered larger tonic $GABA_A$ currents in *Mecp2*-null LC neurons. Consistently, the δ subunit, the principal component of extrasynaptic $GABA_AR$s, was expressed in LC neurons, whose expression level together with the α6 expression in the LC area became higher in *Mecp2*-null mice than in the WT, which may contribute to the enhanced tonic $GABA_A$ currents. The presence of extrasynaptic $GABA_AR$s in *Mecp2*-null mice seems to allow a control of neuronal excitability and breathing abnormalities with $GABA_AR$ activators.

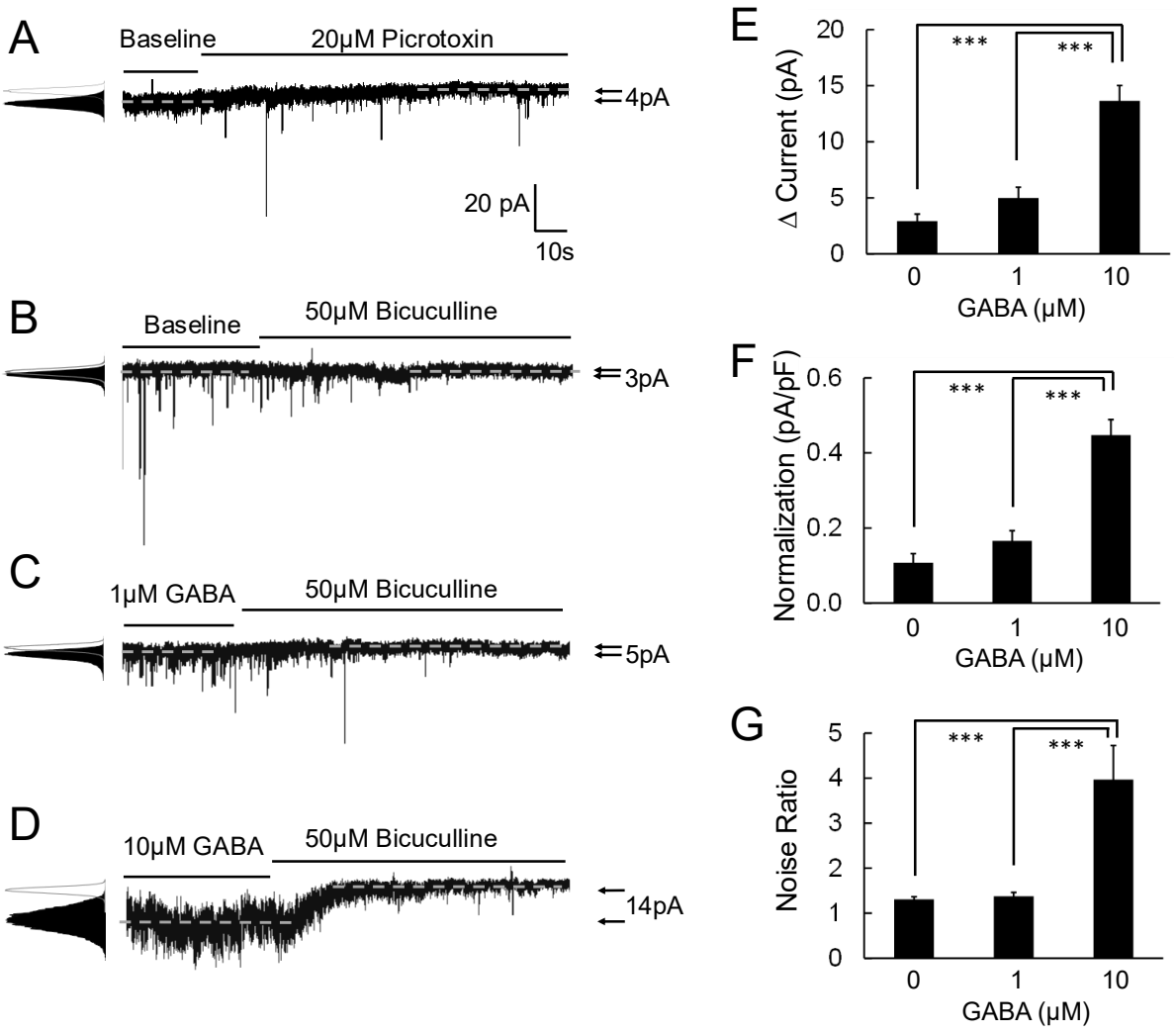

Figure 5- 1. $GABA_AR$ antagonists reduce the tonic currents of LC neurons in WT mice. Tonic $GABA_A$ currents were recorded in whole-cell voltage clamp by ion substitution and selective receptor blockers. **(A-B)** In the absence of exogenous GABA in the bath solution (baseline), tonic currents were measured as the difference before and after treatment of $GABA_ARs$ antagonists. Picrotoxin (20 μM) and bicuculline (50 μM) reduced the both the synaptic $GABA_A$ currents (IPSCs) and the tonic $GABA_A$ currents of LC neurons in WT mice. Noise was measured as standard deviation of the currents, and shown as a ratio with vs. without $GABA_ARs$ antagonist treatment. The noise level was reduced with the treatment of these two $GABA_ARs$ antagonists. **(C-D)** Pre-treatments with 1 μM and 10 μM GABA boost larger

bicuculline-sensitive tonic current in WT LC neurons. **(E-G)** The effects of bicuculline on the tonic currents and noise ratio increased dose-dependently with an increased in GABA concentrations (*, $P < 0.05$; **, $P < 0.01$; ***, $P < 0.001$; One-way ANOVA).

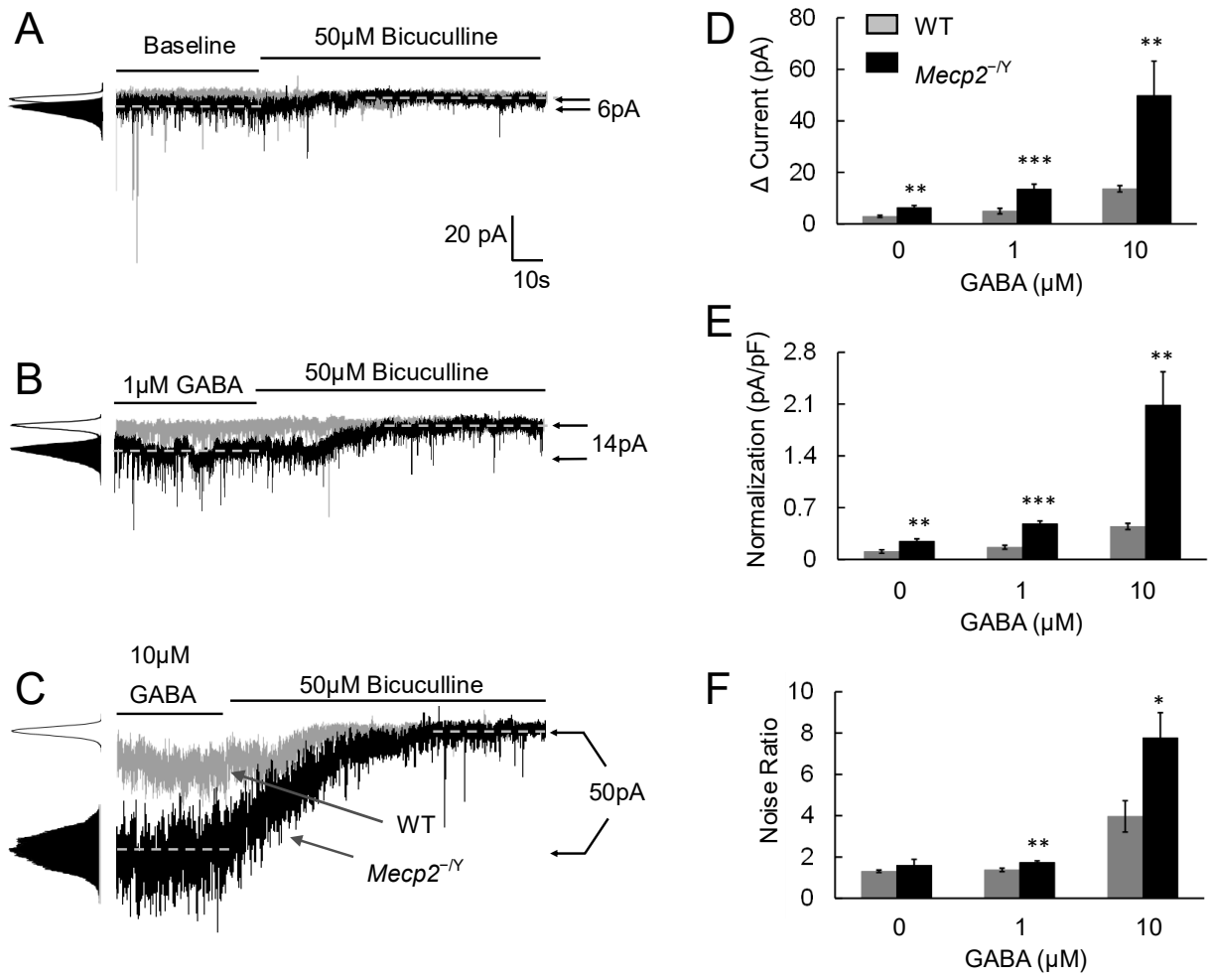

Figure 5- 2. Bicuculline sensitive tonic currents are increased in *Mecp2*$^{-/Y}$ mice.

(A) In comparison to WT mice, bicuculline (50 μM) reduced more tonic currents and noise in *Mecp2*-null mice in the absence of exogenous GABA (baseline). **(B-C)** In the presence of 1 μM or 10 μM GABA, the bicuculline effects on the tonic currents and noise ratio were significantly even larger in *Mecp2*-null neurons than the WT. **(D-F)** Both tonic currents and the noise ratio increased dose-dependently with an increase in GABA concentrations. Such effects were more obvious in *Mecp2*-null mice (*, $P < 0.05$; **, $P < 0.01$; ***, $P < 0.001$; Student's t-test).

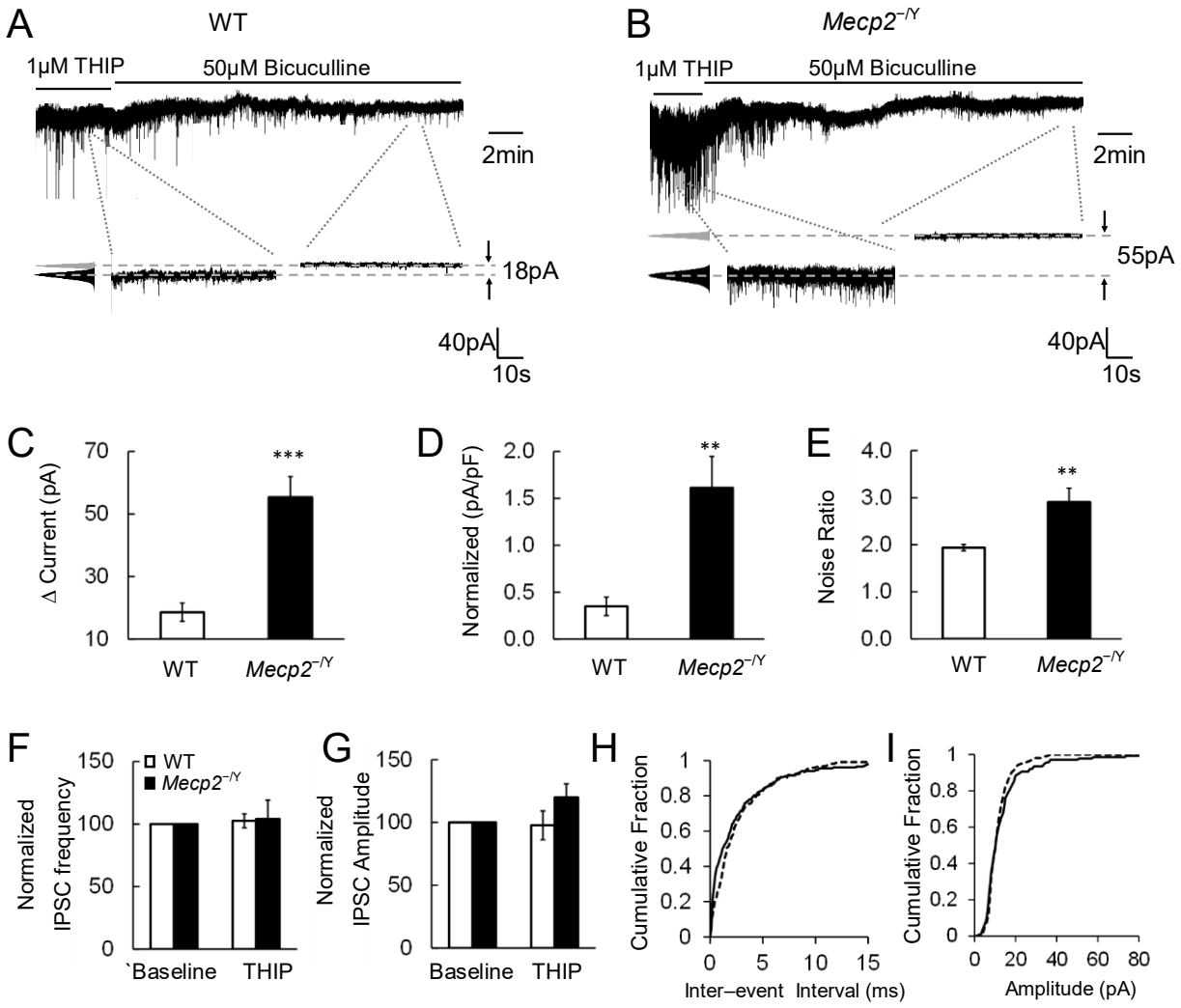

Figure 5- 3. THIP boosts larger tonic currents in *Mecp2*$^{-/Y}$ mice.

(A-E) THIP (1 μM) applied to the bath solution triggered bicuculline-sensitive tonic currents measured 18.6 ± 2.9 pA and noise ratio 1.94 ± 0.07 in WT neurons. In *Mecp2*-null neurons, the THIP activated tonic currents were augmented by 3 folds compared to WT cells, and the noise ratio was also significantly increased. **(F-G)** The effects of THIP on IPSC frequency and amplitude were not significantly different between WT and *Mecp2*-null LC neurons. **(H-I)** Analysis of cumulative fraction of IPSCs showed that 1 μM THIP treatment did not alter the inter-event interval and amplitude of GABA-ergic IPSCs in WT neurons; (*, $P < 0.05$; **, $P < 0.01$; ***, $P < 0.001$; Student's *t*-test).

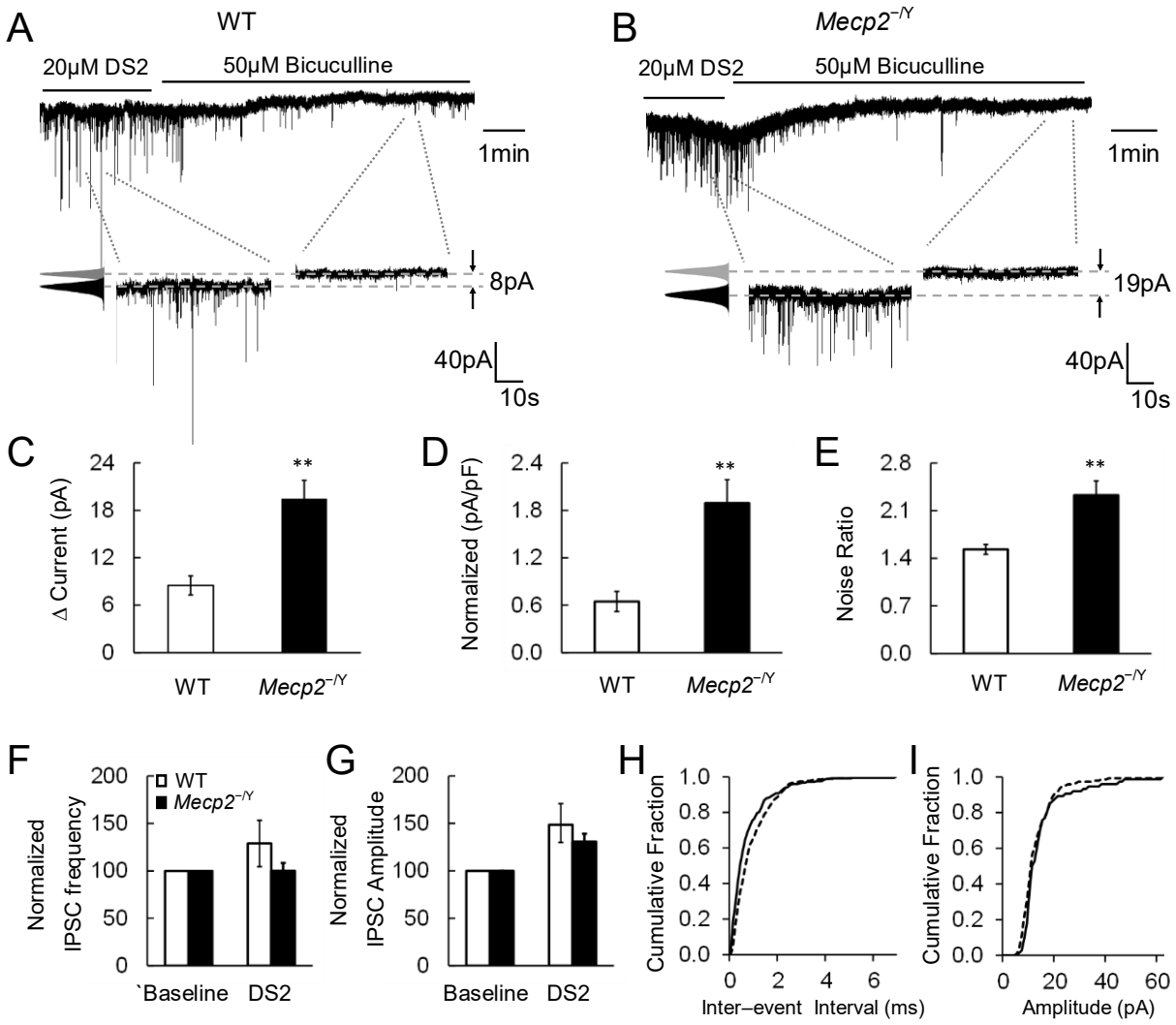

Figure 5- 4. DS2 raises tonic currents in *Mecp2*$^{-/Y}$ mice.

(A-E) Application of DS2 (20 μM) enhanced the tonic currents by ~ 3 folds and raised the noise ratio to a significantly greater degree in *Mecp2*-null neurons than in the WT. **(F-G)** The effects of DS2 on IPSC frequency and amplitude were not significantly different between WT and *Mecp2*-null LC neurons. **(H-I)** The cumulative analysis of IPSCs showed that DS2 shifted the inter-event interval to the higher frequency range without altering the amplitude of IPSC in WT LC neurons (**, $P < 0.01$; Student's *t*-test).

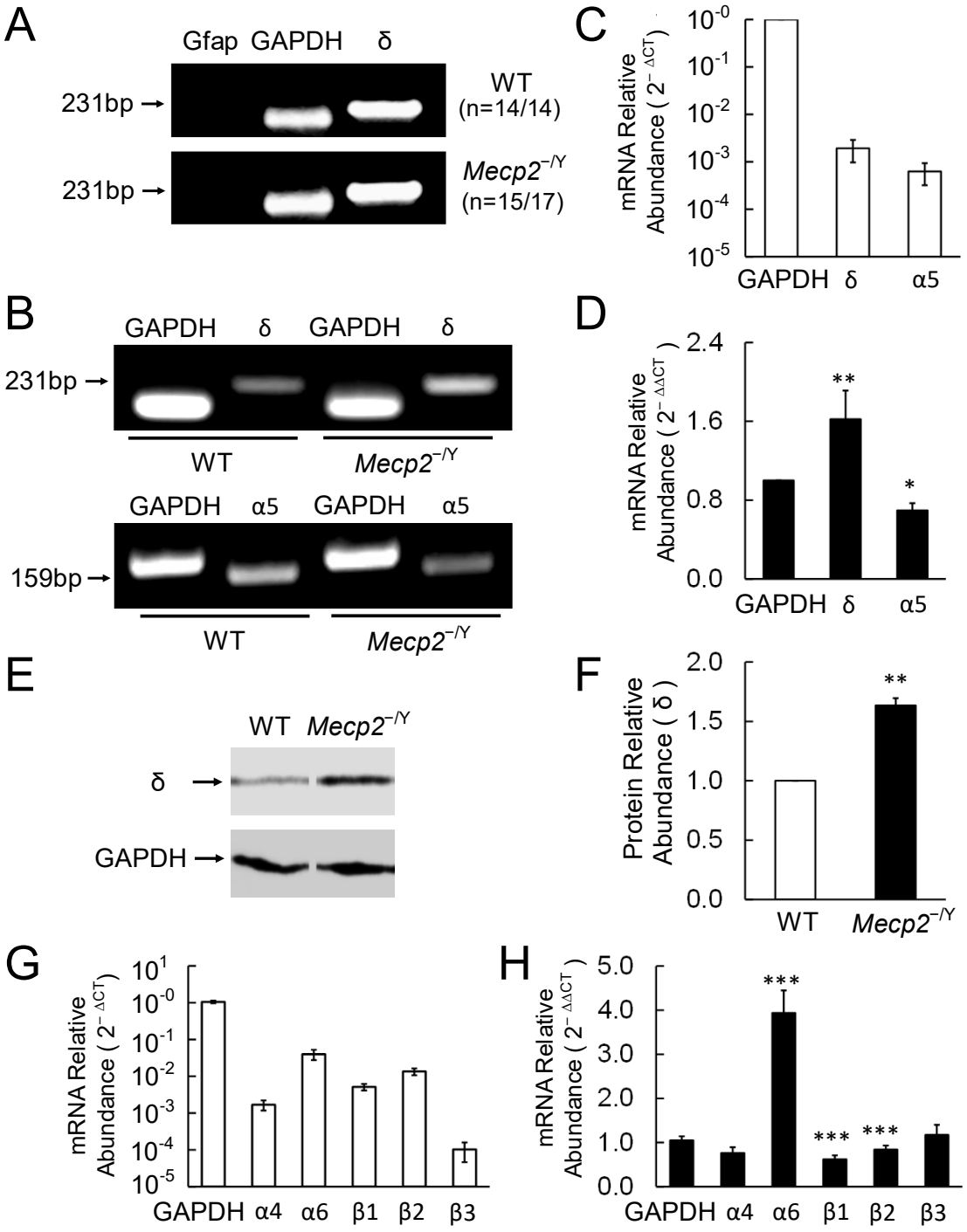

Figure 5- 5. $GABA_AR$ δ subunit was overexpressed in the LC region of *Mecp2*$^{-/Y}$ mice.

(A) Single-cell PCR showed δ subunit, the essential subunit for extrasynaptic $GABA_ARs$, was expressed in most LC neurons with negative GFAP and positive GAPDH expression in both WT

and *Mecp2*-null mice**. (B-D)** qPCR analysis indicated the expression level of the δ and α5 subunits in WT mice **(B**, $2^{-\Delta Ct}$). The δ subunit level was significantly increased and α5 subunit level was significantly reduced in *Mecp2*-null mice (**C**, $2^{-\Delta\Delta Ct}$); *E-F*: Western analysis showed a significant increase of δ subunit protein expression in *Mecp2*-null mice; **(G-H)** qPCR analysis showed the transcript level of α4, α6, β1 – 3 subunits in WT mice (**G**, $2^{-\Delta Ct}$). The α6 subunit level was significantly increased in *Mecp2*-null mice (**H**, $2^{-\Delta\Delta Ct}$). (*, $P < 0.05$; **, $P < 0.01$; Student's *t*-test)

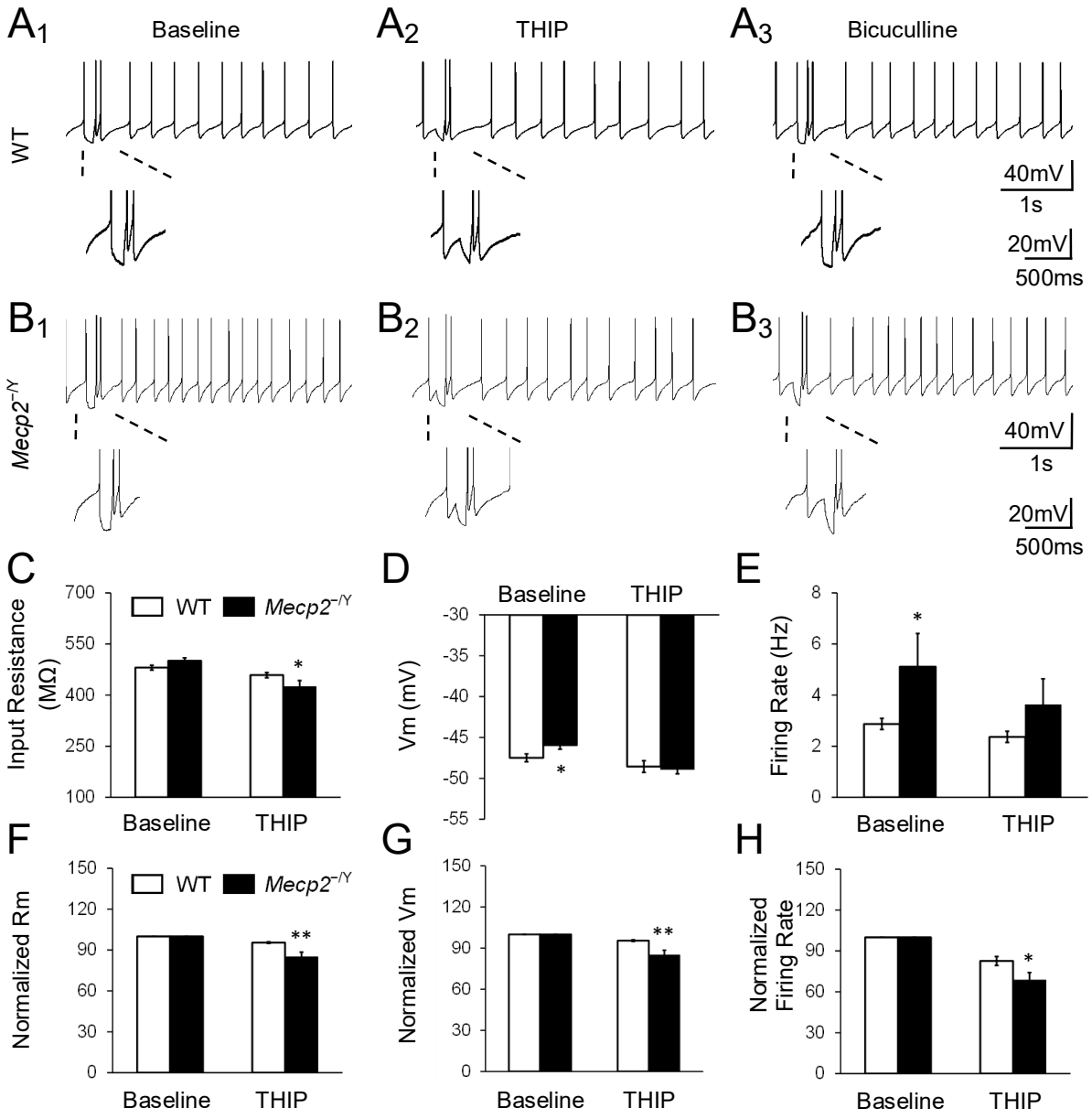

Figure 5- 6. THIP inhibits the LC firing activity by activating extrasynaptic $GABA_A$Rs.

(A_1-A_3) Application of 1μM THIP suppressed the spontaneous firing activity with a hyperpolarization and a decrease in input resistance (Rm) of LC neurons in WT mice. The effects were abolished in the presence of bicuculline. Magnified inset with hyperpolarizing current injection indicates the input resistance. **(B1-B3)** LC neurons in *Mecp2*-null mice showed the similar response to 1 μM THIP; **(C-E)** Membrane potential and firing rate showed significant

differences at the baseline (normal aCSF without exogenous GABA) between WT and *Mecp2*-null neurons, and THIP abolished the differences. THIP treatment also produced a significant decrease in input resistance. **(F-H)** In comparison to the WT, THIP had significantly larger effects on input resistance, membrane potential and firing rate in *Mecp2*-null neurons (*, $P < 0.05$; **, $P < 0.01$; Student's *t*-test).

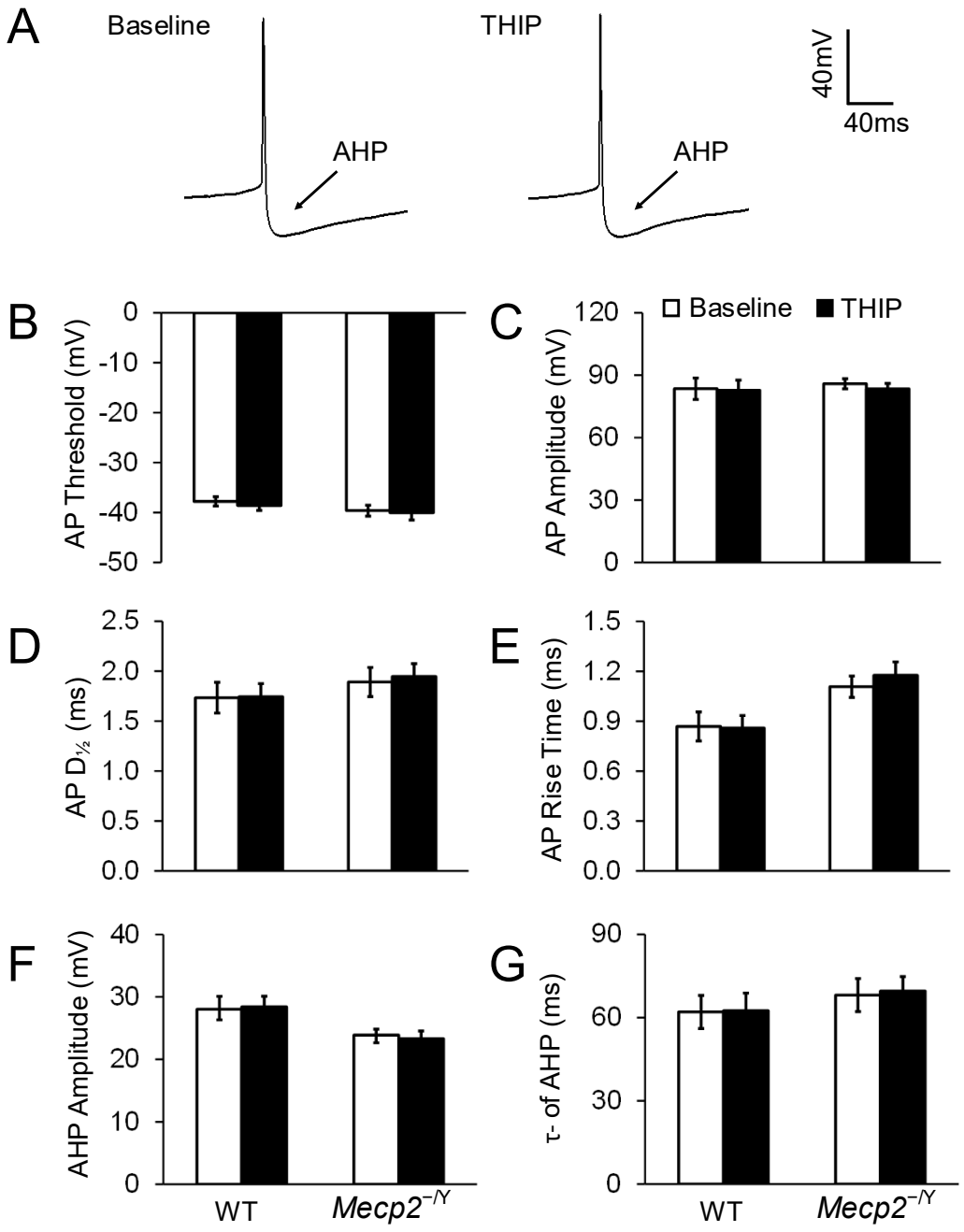

Figure 5- 7. THIP does not affect the morphology of action potential (AP) and afterhyperpolarization (AHP) in either WT or *Mecp2*-null neurons.

(A) Spontaneous APs recorded from an LC neuron. No obvious changes in AP morphology were found after exposure to THIP. **(B-E)** In the presence of ionotropic receptor blockers (AP5, CNQX and strychnine) in the bath solution, THIP did not change the AP threshold (the potential at AP

initiation point), AP amplitude (the amplitude from threshold to peak), rise time and half width (D1/2, measured at 50% amplitude) of APs in either WT or *Mecp2*-null neurons (n = 7 and n = 12; P > 0.05 and P > 0.05, respectively; Student's t-test). **(F-G)** In the presence of ionotropic receptor blockers, AHP was also not affected by THIP in WT and *Mecp2*-null neurons. AHP amplitude was measured from AP threshold to the lowest hyperpolarization point, and the time constant of AHP was described with single exponential in the period from 10% to 90% of the AHP amplitude (n = 7 and n = 12; P > 0.05 and P > 0.05, respectively; Student's t-test).

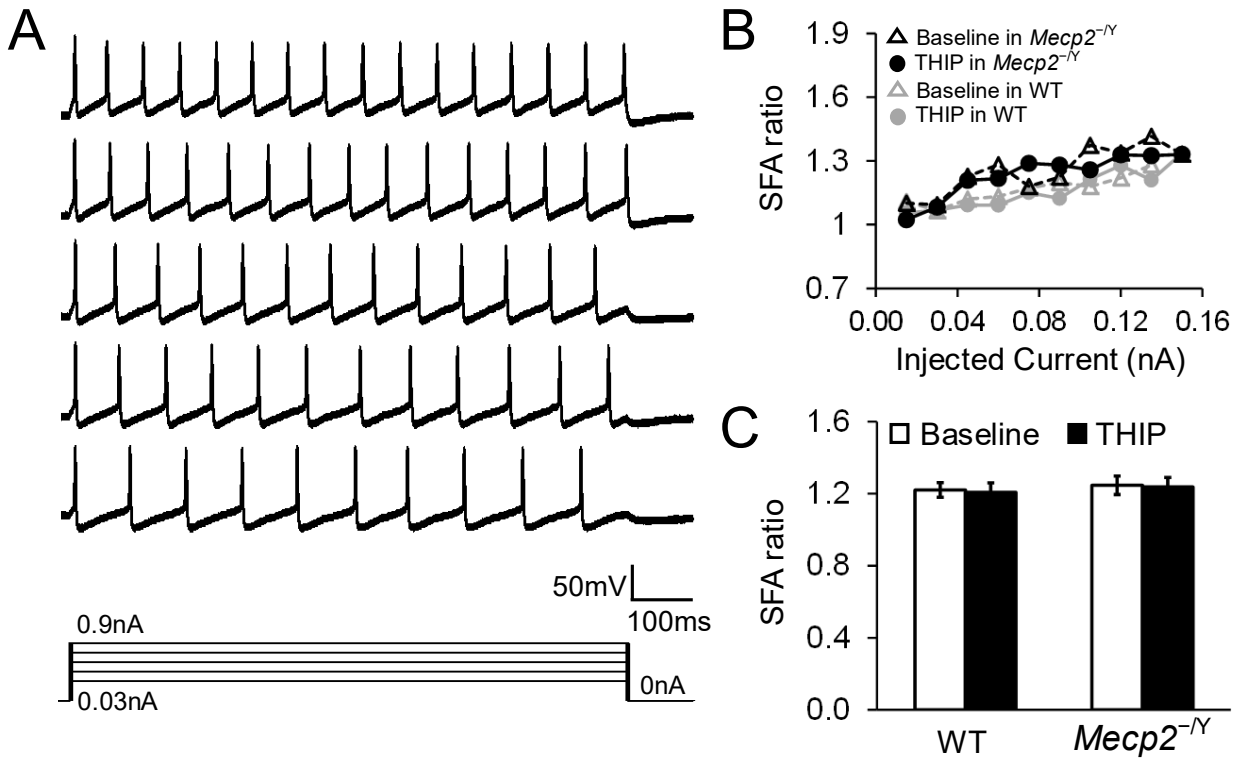

Figure 5- 8. THIP does not affect the spike frequency adaptation (SFA) in either WT or *Mecp2*-null neurons.

(A) The SFA was studied with series of depolarizing currents (0 – 0.15 nA). The firing rate of the neurons declined with a long period of depolarization. **(B)** The SFA ratio was obtained by division of peak frequency, measured between the first two APs, by steady state frequency, measured between the last two APs with the same current injection. The SFA ratio was increased with the increasing depolarizing currents. THIP treatment did not affect the SFA ratio in both WT and *Mecp2*-null neurons. **(C)** With a 0.06 nA current injection, THIP affected the SFA ratio neither in WT nor *Mecp2*-null neurons (n = 6 and n = 9; P > 0.05 and P > 0.05, respectively; Student's t-test).

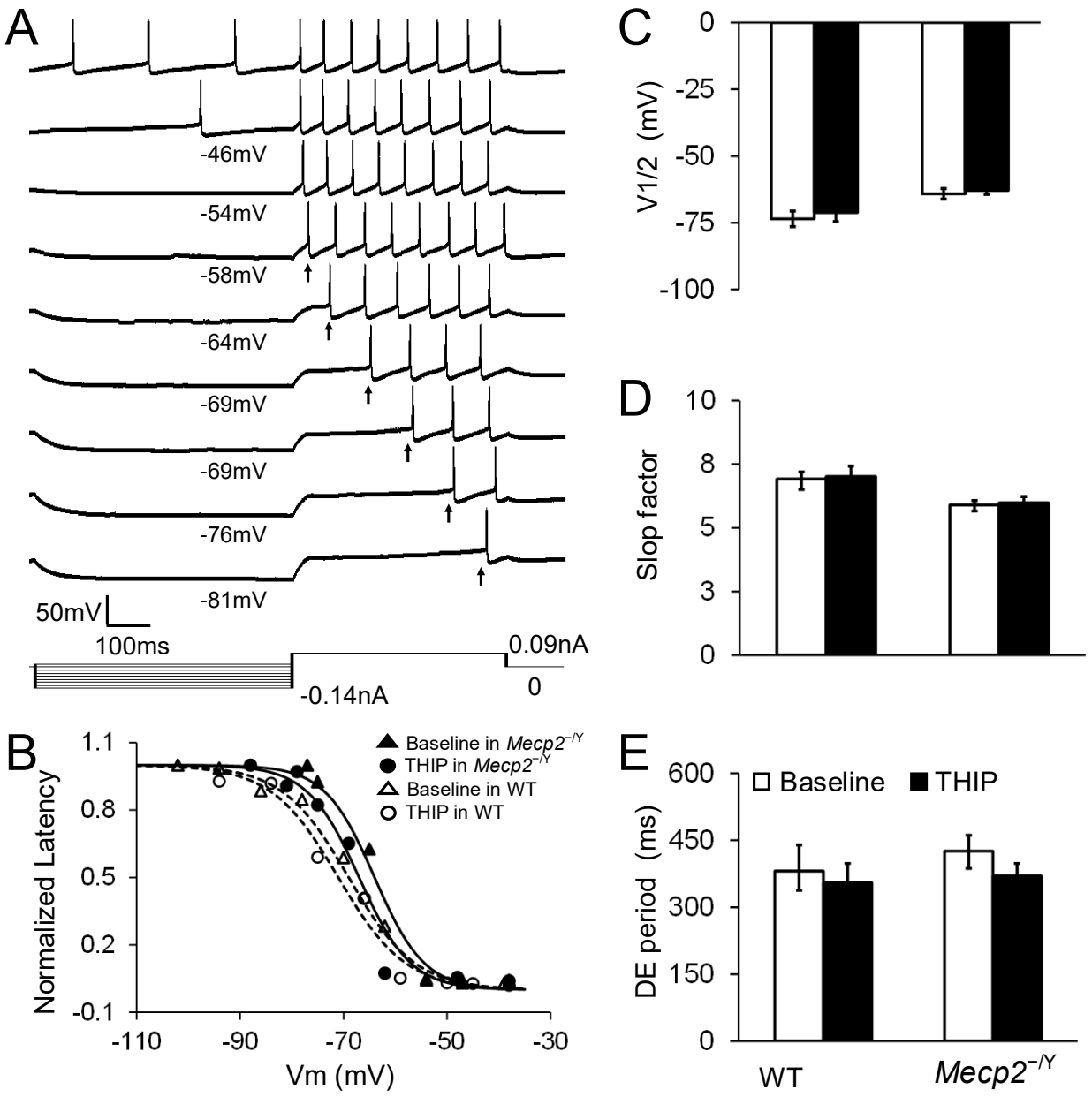

Figure 5- 9. THIP does not affect the delayed excitation (DE) in both WT and *Mecp2*-null neurons.

(A) The DE was measured as the time delay between the starting point of depolarization pulse and initiation of the first action potential after a prior hyperpolarization. (**B)** The DE was described as the function of the conditioning hyperpolarization, which was fit with Boltzmann

Equation as D = Dmax/{1+exp[(V-V1/2)/k]}, where Dmax is the maximum DE period, V is the hyperpolarizing membrane potential, V1/2 is the half-inactivation, and k is the Boltzmann constant or slop factor. **(C-E)** Neither WT nor *Mecp2*-null neurons showed significant difference on V1/2, slop factor and DE period before and after THIP treatment (n = 8 and n=7; $P > 0.05$ and $P > 0.05$, respectively; Student's t-test).

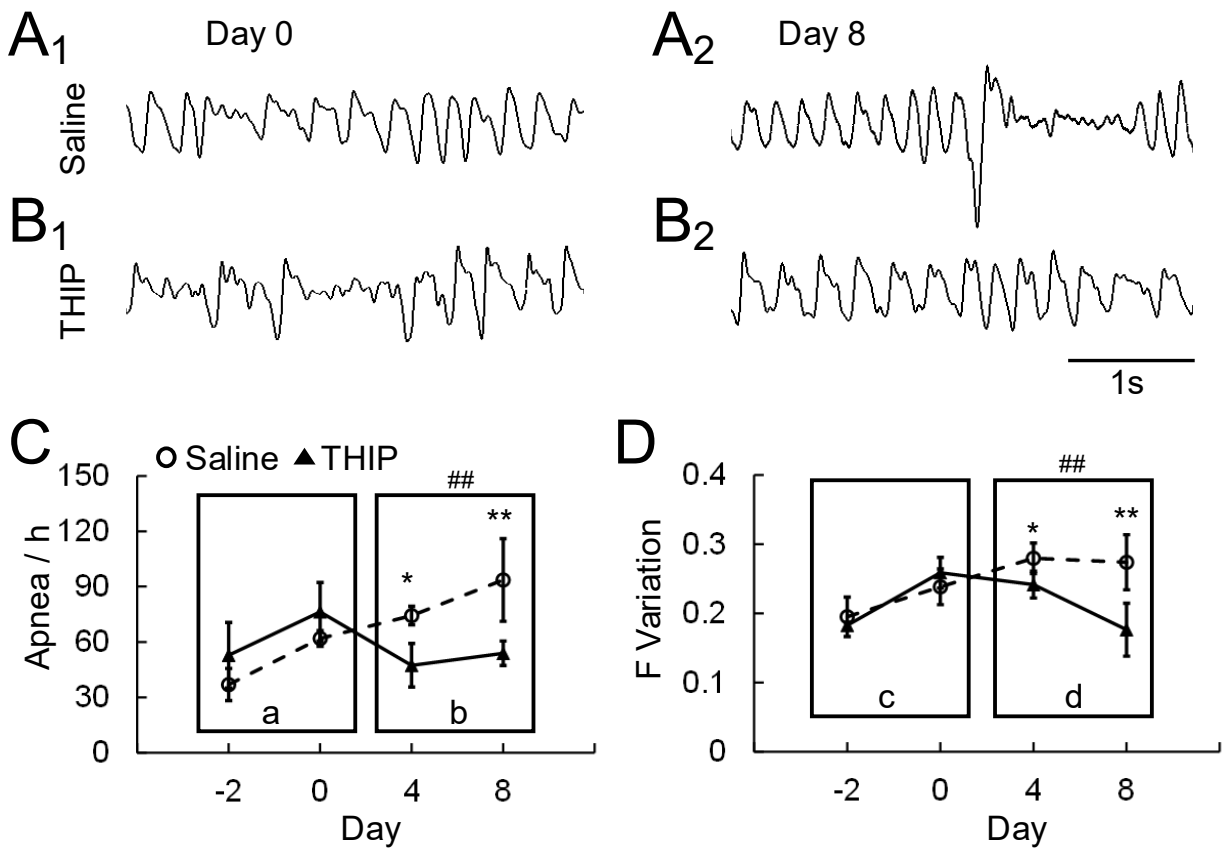

Figure 5- 10. THIP alleviates the breathing abnormalities in *Mecp2*$^{-/Y}$ mice.

(A-B) The *Mecp2*-null mice were injected with THIP (10 mg/kg, i.p.) or saline for 7 consecutive days. Breathing activity was recorded in plethysmograph system 2 days before the injection. The injection started at Day 0 when mice were 26 days after birth. All the animals developed breathing disorders before THIP injection, showing apnea and clear breathing frequency (f) variation at day 0. At Day 8, both were alleviated after the THIP treatment for 7 days by showing less apnea and smaller breathing f variation. **(C-D)** When apnea occurrence (events/h, **C**) and breathing f variation (SD/mean, **D**) were compared between THIP and saline injected groups, THIP improved significantly both apnea and f variation in *Mecp2*-null mice. In *box a & box c*, there was no significant difference (NS) in the main effect, neither significant interaction. In *box b & box d*, there was significant difference in the main effect (##, $P < 0.01$; Two-way ANOVA) of drug

treatment. No significant effect of age and no significant age-drug interaction were found (*, $P < 0.05$; **, $P < 0.01$; Tukey's post-hoc test).

6 CHAPTER2: THE BENEFICIAL EFFECTS OF EARLY INTERVENTION TO THE EXTRASYNAPTIC $GABA_A$RS ON PHENOTYPE DEVELOPMENT IN THE *MECP2*-NULL MOUSE MODEL OF RETT SYNDROME

Publication: **Zhong W,** Johnson CM, Cui N, Wu Y, Xing H, Zhang S and Jiang C. (2016) Effects of early exposure to gaboxadol on phenotype development in a mouse model of Rett syndrome. *J Neurodev Disord.* 2016 Oct 19;8:37

Contribution disclosure: Weiwei Zhong and Dr. Chun Jiang designed the research and write the article. Weiwei Zhong performed the experiments and analyzed the data. Christopher M Johnson and Ningren Cui assisted in the electrophysiology experiments. Christopher M Johnson and Yang Wu assisted in the behavior and molecular experiments. Christopher M Johnson, Ningren Cui, Yang Wu, Hao Xing and Shuang Zhang assisted in the behavior data analysis.

6.1 Abstract

Rett Syndrome (RTT) is a neurodevelopmental disorder caused mostly by disruptions in the *MECP2* gene. *Mecp2*-null mice show imbalances in neuronal excitability and synaptic communications. Several previous studies indicate that augmenting synaptic GABA receptors ($GABA_ARs$) can alleviate RTT-like symptoms in mice. In addition to the synaptic $GABA_ARs$, there is a group of $GABA_ARs$ found outside synaptic cleft with the capability to produce sustained inhibition, which may be potential therapeutic targets for the control of neuronal excitability in RTT. Enhancing the GABARergic synaptic inhibition alleviated the RTT-like breathing difficulties. It is possible that intervention to such extrasynaptic $GABA_ARs$ would have beneficial effects on RTT-like symptoms in *Mecp2*-null mice as well. Therefore, in our study, we randomly divided wild-type and *Mecp2*-null mice into four groups, which received the extrasynaptic $GABA_AR$ agonist THIP and vehicle control, respectively. Low-dose THIP was administered to neonatal mice through lactation. RTT-like symptoms including lifespan, breathing, motor function and social behaviors were studied when mice became mature. Changes in neuronal excitability and NE biosynthesis enzyme expression were studied in electrophysiology and molecular biology. With no evident sedation and other adverse side-effects, early-life exposure to THIP extended the lifespan, alleviated breathing abnormalities, enhanced motor function, and improved social behaviors of *Mecp2*-null mice. Such beneficial effects were associated with stabilization of locus coeruleus neuronal excitability and improvement of NE biosynthesis enzyme expression. In conclusion, THIP treatment in early lives might be a therapeutic approach to RTT-like symptoms in *Mecp2*-null mice and perhaps in people with RTT as well.

6.2 Introduction

Rett Syndrome (RTT) caused mostly by disruptions in the *Mecp2* gene is a neurodevelopmental disorder occurring in 1/10,000 live female births [1]. One of the major consequences of the *Mecp2* disruption is dysfunction of brainstem neurons [3, 107, 147, 173]. In *Mecp2*-null mice, several groups of brainstem neurons including those in the locus coeruleus (LC) show increased membrane excitability. As a result of the excessive neuronal excitability, the balance of excitation and inhibition in local neuronal networks is impaired, affecting normal brainstem functions for breathing control, cardiovascular regulation, gastrointestinal activity, arousal and locomotion, consistent with RTT manifestations in humans [3, 8].

The increased neuronal excitability in the brainstem is attributable to abnormal intrinsic membrane properties and deficiency in GABAergic synaptic inhibitions [4, 10, 14, 18, 49]. In *Mecp2*-null mice, both $GABA_A$ and $GABA_B$ synaptic currents are reduced in LC neurons [10]. In contrast, our recent studies indicate that extrasynaptic $GABA_A$ currents are well retained in LC neurons of *Mecp2*-null mice [67], which is encouraging as the extrasynaptic $GABA_A$Rs may provide an alternative pharmaceutical target to relieve the excessive neuronal excitability and its associated RTT symptoms. Indeed, we have found that the extrasynaptic $GABA_A$R agonist THIP (tetrahydroisoxazolo [5,4-c]-pyridin-3-ol) is beneficial to RTT-like symptom relief in *Mecp2*$^{-/Y}$ mice.

THIP or gaboxadol is an investigational drug, originally developed for insomnia, Clinical trials suggest that THIP (10mg/day) has no significant effects on sleep onset and total sleep time [135]. It does have effects on these measures in a higher dose (15mg) where the effects are inconsistent between genders, and side effects emerge including sedation and disorientation [135, 136]. Therefore, Merck and Lundbeck canceled further development of the drug. It is not unusual,

however, that a preclinical drug fails in one application, but succeeds in another. The low efficacy of THIP on insomnia indeed may be beneficial for its applications to RTT, as the unnecessary sedation can be avoided. We have found that intraperitoneal injection of THIP alleviates the breathing abnormalities and extends lifespans of *Mecp2*-null mice [67]. However, intraperitoneal injection may introduce stress and subject the animals to infection. To overcome this potential problem, oral administration was given to mice in this study. Also we chose to use a low and non-sedative dose of THIP to avoid potential side-effects. RTT symptoms start in 6-18 months after birth, causing a loss of certain acquired motor and language skills in humans. To intervene to this early period of development, we exposed neonatal mice to THIP one day after birth before the RTT-like symptoms manifest themselves. Therefore, this study was conducted in a way that was close to therapeutic condition and very much different from our previous study [67].

6.3 Results

6.3.1 THIP Administration

Symptoms of RTT patients and mouse models start after a period of postnatal development. In *Mecp2*-null mice, breathing disorders started at 2-3 weeks after birth, and defects in motor and social behaviors begin at 4-6 weeks [42, 174]. Early intervention to extrasynaptic $GABA_AR$s may affect the development of the symptoms. Therefore, we started the THIP treatment of *Mecp2*-null mice from the birth day, and maintained the level till mice were fully mature.

Following strategies were used to determine THIP dosing. a) Based on water consumptions in our studies, the dose given to the mother was 61.0 ± 2.2 mg/kg/day. Consistent with previous studies, the mother with this dose did not show any evident sedation, neither had any behavioral

alterations [175]. The infants received maximally one tenth of the dose to the mother via lactation [176-178], i.e., ~6 mg/kg/day. After weaning, these mice received 6.3 ± 0.4 mg/kg/day THIP in their drinking water, which were also calculated based on their daily water intake. b) According to a THIP patent report, the LD50 in mice is 320mg/kg orally, which is 2.2 times higher than i.p. (LD50 145mg/kg) [179]. The THIP dose used in mouse models of Angelman syndrome and Fragile X syndrome is 2-3mg/kg i.p. [81, 82, 180], equivalent to 5-7 mg/kg in oral after multiplication by 2.2, which is approximately the same as used in our studies. c) THIP pharmacokinetics has been well studied in humans and laboratory animals [181-184]. According to the visual observation, THIP treatment had no evident effects on feeding, movement, body weight, and other general physical conditions in both WT and *Mecp2*-null mice.

6.3.2 Lifespan

Lifespan of the mice was studied with THIP or vehicle treatment. In the vehicle group, about 50% of the *Mecp2*-null animals died at P52 with only 1 out of 14 tested animals surviving beyond P80. In contrast, *Mecp2*-null mice with THIP treatment reached 50% fatality (LD50) on P82, and one third (5 out of 15) mice lived beyond P90 (Fig. 6-1A-B). When comparing LD50, the THIP administration extended the lifespan of *Mecp2*-null mice by over 50%, which was statistically significant as well (Fig. 6-1A; $P = 0.004$, Mantel-Cox test). The same THIP and vehicle treatments did not cause any lethality in WT mice.

6.3.3 Breathing Abnormalities

Like people with RTT, *Mecp2*-null mice developed severe breathing abnormalities by showing significantly high apnea rate and high breathing frequency variation [8, 185], which may lead to the early death or unexpected sudden death seen in RTT patients and the RTT mouse model.

It is possible that the extended lifespan in *Mecp2*-null mice is attributable to the alleviation of breathing abnormalities through THIP treatment. Therefore, we studied mouse breathing activity using plethysmography. Early-life administration of THIP prevented the development of breathing abnormalities in *Mecp2*-null mice (Fig. 6-2B, D). In age 6 – 8 weeks, both the apnea rate and breathing frequency variation were significantly reduced in *Mecp2*-null mice treated with THIP (Fig. 6-2A_1, A_2, C, E).

6.3.4 Motor Function

The grip strength and grid walking tests were performed to evaluate muscle strength and motor coordination, respectively. Our results showed that in 5-6 week-old *Mecp2*-null mice, THIP treatment improved the grip strength from 58.5 ± 2.1 g to 74.0 ± 1.7 g (Fig. 6-3A), and the footfault ratio from 4.3 ± 0.5 % to 2.7 ± 0.2 % (Fig. 6-3B). Both were significantly different from those of the vehicle controls. These results were unlikely to be due to the sedative effects of THIP, as in the open field test THIP did not affect the spontaneous locomotion of either WT or *Mecp2*-null mice (Fig. 6-3C). Therefore, chronic treatment of THIP moderated certain motor defects in *Mecp2*-null mice, such as muscle strength and motor coordination.

6.3.5 Social Behaviors

The three-chambered tests are used widely in the studies of sociability and social novelty [138]. In our current study, only the animals showing no preference to either side chamber during the exploration period were used for further testing (Fig. 6-4A). Both of the WT and *Mecp2*-null mice in the experiments showed the similar time spending in the side chambers, indicating that none of the animals were in the sedative state. THIP treatment did not alter the chamber transitions or the chamber preference either (Fig. 6-4B).

In the sociability test, we found that WT mice tended to spend significantly longer time in the chamber with an animal than without (267.9 ± 16.7 sec in the animal chamber vs. 155.9 ± 14.6 sec in the empty chamber), whereas *Mecp2*-null mice in the vehicle group did not show such preference (252.7 ± 36.3 sec in the animal chamber 1 vs. 240.0 ± 39.4 sec in the empty). THIP administration improved significantly the social interaction or sociability of the *Mecp2*-null mice (313.5 ± 43.1 sec in the animal chamber 1 vs. 153.5 ± 35.9 sec in the empty) (Fig; 6-4C).

In the social novelty preference test, WT mice spent significantly more time in the chamber with novel animals than the chamber with the familiar one (349.3 ± 32.1 sec in the animal 1 chamber vs. 138.4 ± 22.8 sec in the animal 2 chamber), whereas the *Mecp2*-null mice did not show such a preference (321.7 ± 44.1 sec in the animal 1 chamber vs. 200.9 ± 50.9 sec in the animal 2 chamber). THIP treatment improved significantly the social novelty preference of the *Mecp2*-null mice (386.7 ± 29.1 sec in the animal 1 chamber vs. 122.2 ± 22.6 sec in the animal 2 chamber) (Fig. 6-4D), suggesting that THIP treatment seems to alleviate the defects of sociability and social novelty as well.

6.4 Discussion

In these studies, we have shown that early-life exposure of the *Mecp2*-null mice to a non-sedative dose of the extrasynaptic $GABA_A$Rs agonist THIP has several beneficial effects on lifespan, breathing activity, motor function and social behaviors.

The extrasynaptic $GABA_A$Rs have several properties different from the synaptic $GABA_A$Rs, which may be unique in interventions to neuronal excitability. They are located outside the synaptic area, produce tonic or long-lasting Cl^- currents, show very little desensitization upon activation, and are sensitive to some synaptic $GABA_A$R agonists and extrasynaptic $GABA_A$R-

specific agonists [20, 141, 186]. They have the capability to change dynamically their expression levels under different physiological and pathophysiological conditions [67, 80, 187]. Manipulations of these receptors with selective agents do not interrupt GABAergic synaptic transmission mediated by the synaptic $GABA_ARs$. Thus, therapeutic activation of these extrasynaptic $GABA_ARs$ may avoid several side effects of the synaptic $GABA_AR$ activators including sedation, tolerance and addiction.

To minimize potential side-effects of THIP, we chose to use THIP chronically in low dosage. Although pharmacokinetic studies were not performed in this report, such information has been collected in previous studies on mice, rats, dogs and humans [181-184]. With a daily dose of 10 mg in humans, THIP reaches the maximum plasma concentration ~140ng/ml in 2.0 h, and the terminal plasma half-life time is 1.7 h [181]. Another preclinical study in humans, rats and mice shows a rapid and complete absorption of THIP with the peak concentration reached within 0.5 h in several organs include the brain [29]. A clinical report indicates that therapeutic dosages of THIP by long-term oral administration range from 20-120mg daily in human patients [188]. Higher doses of THIP may cause adverse side effects, including sedation, confusion and dizziness [136]. In our present study, the oral dose of THIP was calculated to be ~ 6 mg, which appears effective for alleviating multiple RTT-like symptoms in *Mecp2*-null mice. Our test of spontaneous locomotion supports the non-sedative effects of the dosage. The dosage given to the mother during lactation was 61.0 ± 2.2 mg/kg/day, which was also reported to have no sedative effects and neither behavioral alterations [175].

Similar to the dosages that we used in the study, several previous studies have reported to use THIP for treatment of mouse models of Fragile X syndrome and Angelman Syndrome. Since these diseases share multiple similarities to RTT, such as impaired GABA system, neuronal

hyperexcitability and autism-like symptoms [81, 82, 189], the information shown in the present study is likely to benefit to moving the drug for further clinical trials in all these diseases.

The impaired neuron networks were widely seen in *Mecp2*-null mice [80, 190]. The social defects of autism spectrum disorders were believed to be correlated to the weak connections in the default networks including the medial prefrontal cortex and posterior cingulate cortex [58]. With the beneficial effects found in this study, we speculate that THIP might contribute to reinforcement of these connections as well as amelioration of the phenotypes.

In comparison to the *Mecp2*-null mice the most widely used RTT mouse model, the *Mecp2*$^{+/-}$ mice tend to display large variations in RTT-like symptoms due to the random X-chromosome inactivation. According to our previous study, only 15-20% *Mecp2*$^{+/-}$ mice showed the RTT-like symptom of breathing abnormalities, suggesting that the wild-type allele is not randomly inactivated [107]. Generally, ~50% the neurons in the CNS of *Mecp2*$^{+/-}$ mice retained MeCP2 expression [102, 191], which may allow the *Mecp2*$^{+/-}$ mice to recapitulate the normal behaviors to some degree, compared to the *Mecp2*-null mice. However, the MeCP2 mosaic expression pattern is not uniform in the CNS, and it varies between individuals, ages and brain regions [102, 191]. Regional expression levels of MeCP2 was reported be correlated to the specific symptoms in the *Mecp2*$^{+/-}$ mice. Hippocampus MeCP2 expression is related to the exploratory activity behaviors and anxiety-like behaviors. Cortical MeCP2 expression affects the general symptomatic severity [104]. The age-dependent mosaic pattern suggests that even the X-chromosome inactivation ratio may also be affected by MeCP2 deficiency in the RTT mice brain and the consequent variation of postnatal brain functions in RTT [191]. Thus, the age-dependent and region-specific expression pattern of MeCP2 in the CNS contributes to the large variation of the phenotypic outcome in *Mecp2*$^{+/-}$ mice, which all need to be considered in studies of female

RTT models. Furthermore, *Mecp2*$^{+/-}$ mice usually develop the diagnostic symptoms when they become sexually mature. The periodical hormone alternations in *Mecp2*$^{+/-}$ mice may affect mouse performance in the behavioral tests complicating the interpretation of the THIP effects. A previous study reports significant variations in the open field, tail flick and suspension tests in female mice during their estrous cycle [192]. With all these complications in the female models, therefore, studies under *Mecp2*-null condition in the male model seems beneficial as the first step of investigation before sophisticated preclinical trials are conducted, which can be based on *Mecp2*$^{+/-}$ female mice and may benefit from the experimental evidence obtained from the male RTT models.

Selective restoration of *Mecp2* in GABAergic neurons rescues multiple phenotypes in both *Mecp2*$^{-/Y}$ and *Mecp2*$^{+/-}$ mice [73], which suggests that the GABA system is a feasible target to manipulate in RTT female mouse model and RTT patients. Although the sexual difference of LC neurons might be a concern of the potential effects of THIP, a morphological study suggested female LC neurons showed a higher frequency of communication with dmLC neurons in comparison to the male [119, 193], indicating that THIP may have a greater effect in female RTT mouse model or patients. A previous study reports that for some unknown reasons, THIP tends to have a greater efficacy in women than in men [135], further suggesting that the potential beneficial effects of THIP in RTT female mouse model and patients. Nevertheless, further studies on *Mecp2*$^{+/-}$ mice are needed, which may be conducted as deliberate, thorough and systematic investigations that might benefit from our findings in the male model.

In conclusion, consistent with our previous study showing that the daily injection of THIP in a high dose alleviates breathing abnormalities by stabilizing the neuronal activity [67], our current study shows that early-life exposure to a low dose of THIP affects multiple RTT-like symptoms. The early-life exposure to THIP extends the lifespan of *Mecp2*-null mice, reduces

breathing disorders and motor dysfunction, and improves social behaviors. These results suggest that THIP has beneficial effects on RTT-like symptoms in the mouse model with complete knockout of the *Mecp2* gene.

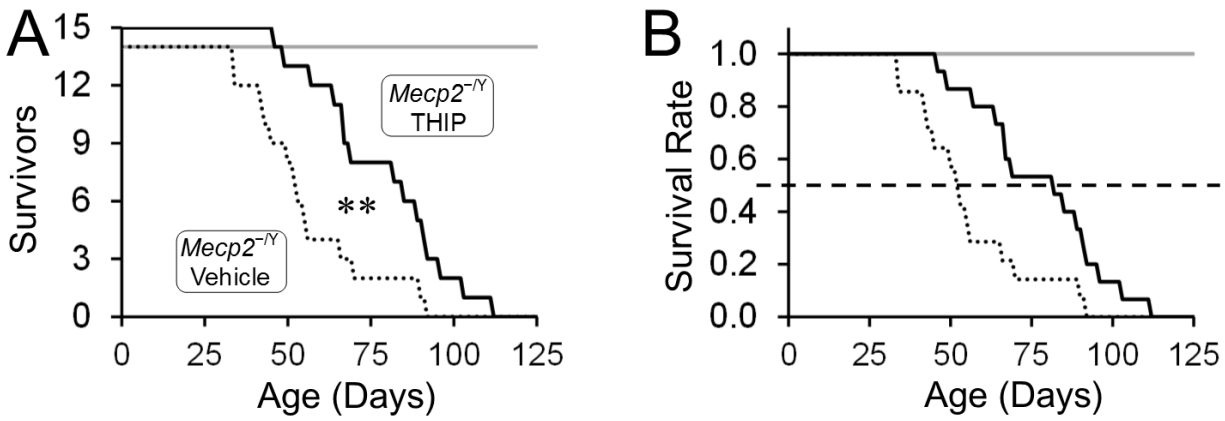

Figure 6- 1. THIP administration extended the lifespan of *Mecp2*-null mice.

(A) Twenty-nine *Mecp2-null* mice were used in the survival experiment and fourteen of them were delivered THIP orally (solid line) and thirteen without THIP treatment (dash line). (** $P <$ 0.01; Mantel-Cox test). **(B)** Percentage of survival in the tested mice. In the vehicle group, 50% *Mecp2*-null mice died within 52 days, while THIP treatment expanded the 50% lifespan to 82 days.

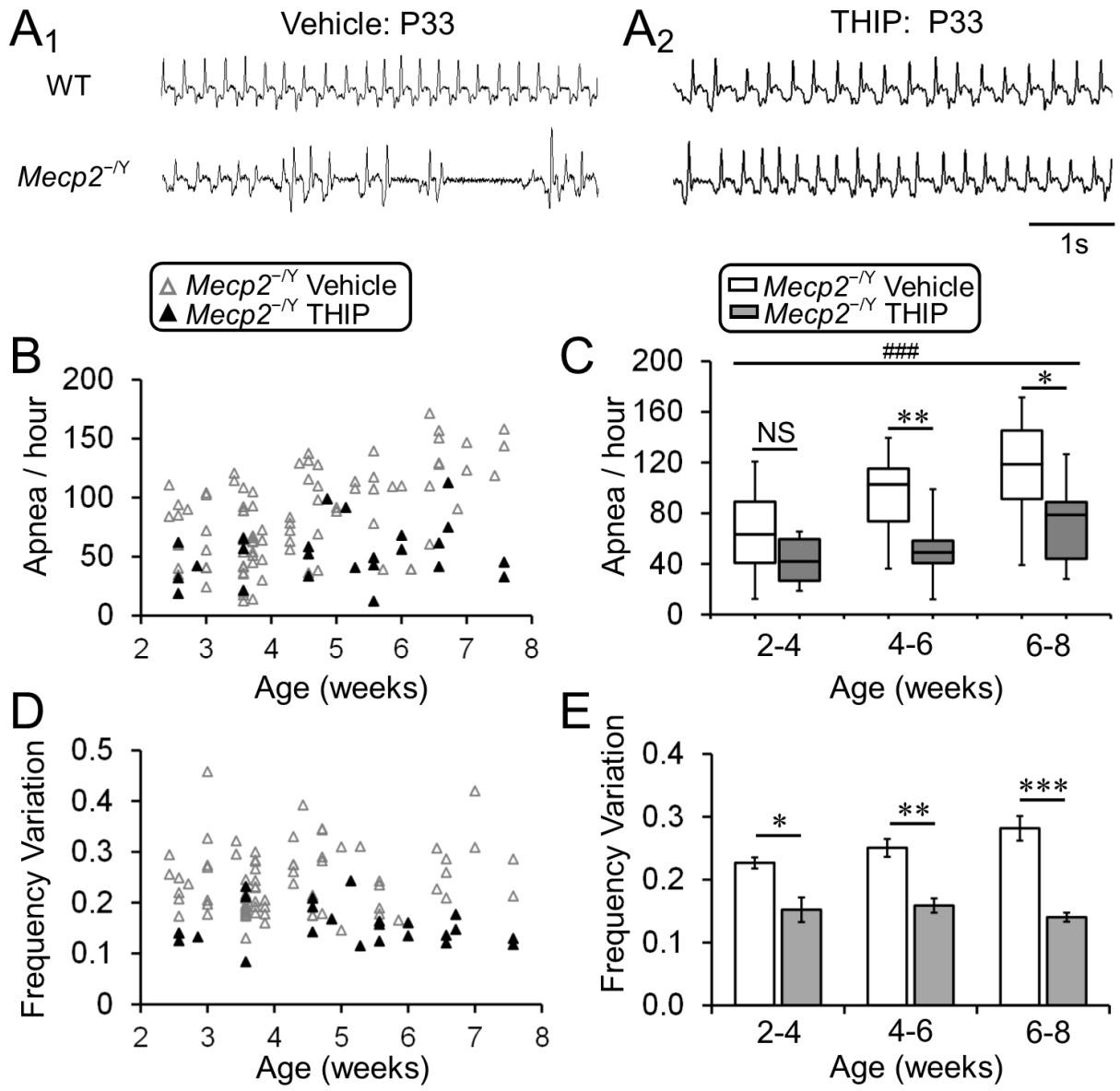

Figure 6- 2. THIP administration alleviated the breathing abnormalities in *Mecp2*-null mice.

(A1-A2) Typical records of breathing activity from both WT and *Mecp2*-null mice with and without THIP administration. **(B)** Distributions of apnea count in different aged *Mecp2*-null mice with and without THIP treatment. **(C)** In *Mecp2*-null mice, THIP administration significantly reduced the apnea count at ages of 4-6 weeks (vehicle: n = 26, THIP: n = 8, $P = 0.002$) and 6-8 weeks (vehicle: n = 19, THIP: n = 8, $P = 0.021$), although the significance was not found in 2-4

weeks (vehicle: n = 45, THIP: n = 7, $P = 0.081$; ### $P < 0.001$ in Kruskal-Wallis test; * $P < 0.05$, ** $P < 0.01$ in Mann-Whitney post hoc comparison). **(D-E)** Similar effects of THIP treatment on breathing frequency variation was observed in these mice (2-4 weeks: $P = 0.037$; 4-6 weeks: $P = 0.004$; 6-8 weeks: $P < 0.001$; * $P < 0.05$, ** $P < 0.01$, *** $P < 0.001$; One-way ANOVA and Tukey's post-hoc).

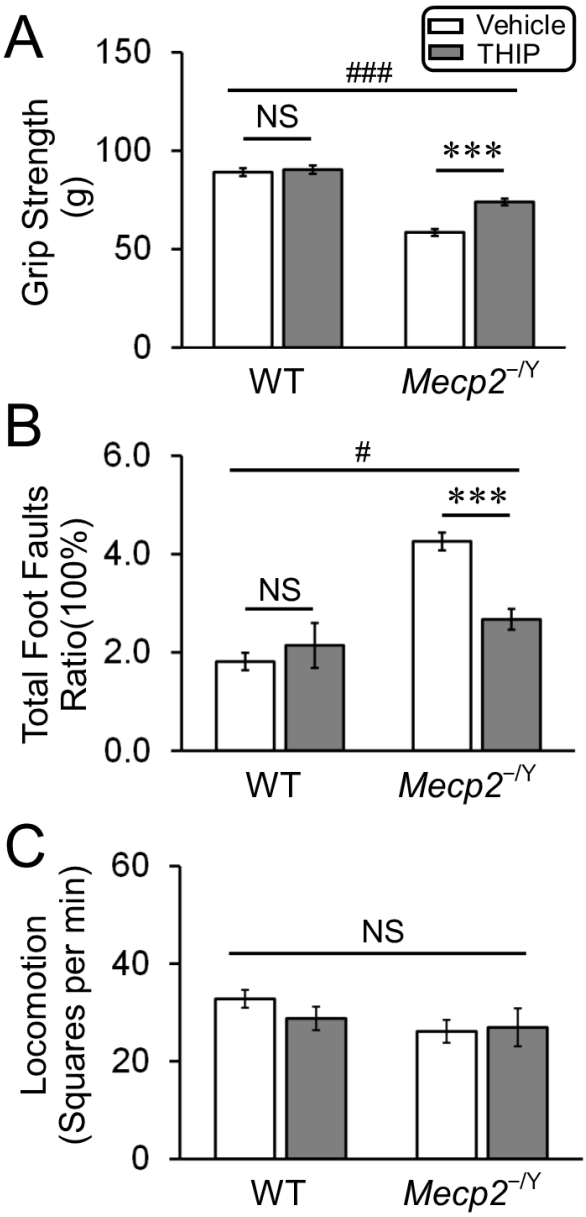

Figure 6- 3. THIP administration improved motor function of *Mecp2*-null mice.

(A) Significant main effects of THIP treatment (F = 23.74, *df* = 1, *P* < 0.001) and genotype (F = 147.85, *df* = 1, *P* < 0.001) were observed, as well as a significant interaction (F = 12.04, *df* = 1, *P* < 0.001). (### *P* < 0.001, Two-way ANOVA) The grip strength of *Mecp2*-null mice was significantly increased with THIP treatment (WT: n = 18 and n = 18 mice; *Mecp2*-null: n = 23 and n = 22; vehicle and THIP, respectively; *** *P* < 0.001, Tukey's post hoc). **(B)** Significant

main effects of THIP treatment (F = 5.26, *df* = 1, *P* < 0.05) and genotype (F = 30.4, *df* = 1, *P* < 0.001) were observed, as well as a significant interaction (F = 13.25, *df* = 1, *P* < 0.001) (# *P* < 0.05, Two-way ANOVA). THIP administration significantly reduced the footfault ratio (including both hindlimb and forelimb) of *Mecp2*-null mice (WT: n = 22 and n = 23 mice; *Mecp2*-null: n = 20 and n = 25; vehicle and THIP, respectively; *** *P* < 0.001, Tukey's post hoc) **(C)** The spontaneous locomotion of WT and *Mecp2*-null mice was not significantly affected by THIP treatment. The main effect of THIP treatment was not significant (F = 0.26, *df* = 1, *P* = 0.614), as the main effect of genotype (F = 3.00, *df* = 1, *P* = 0.095). The interaction of these two factors was not significant (F = 0.99, *df* = 1, *P* = 0.329) (WT: n = 8 and n = 7 mice; *Mecp2*-null: n = 9 and n = 6; vehicle and THIP, respectively; Two-way ANOVA).

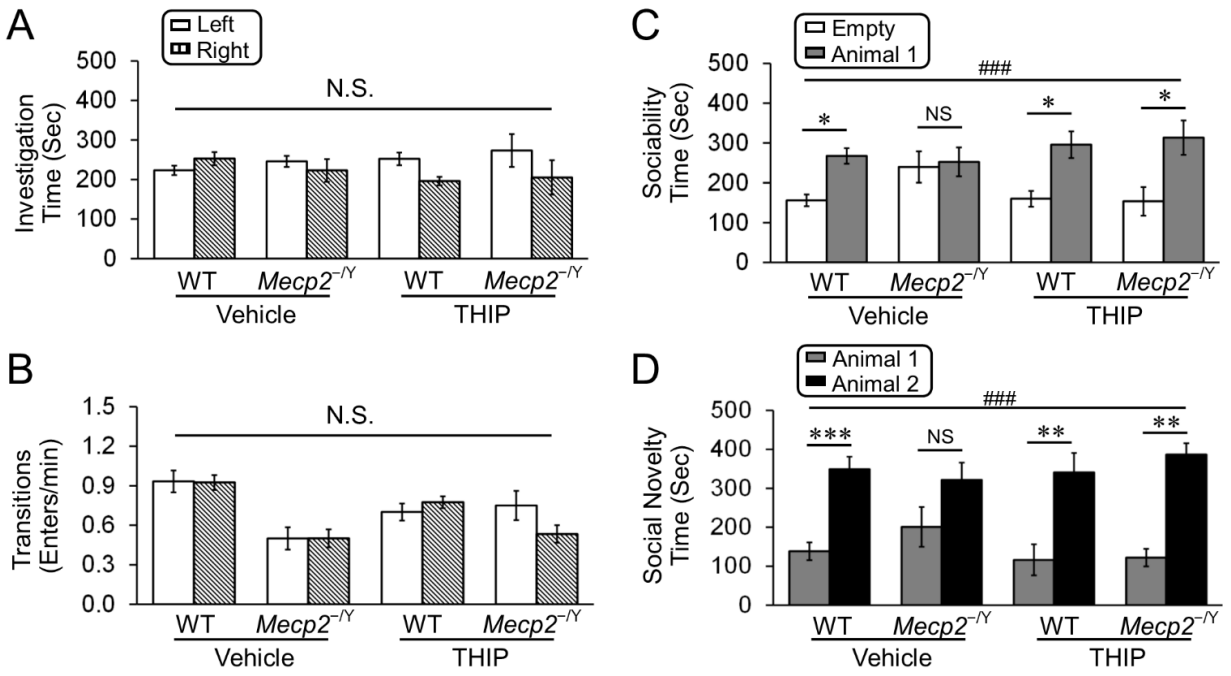

Figure 6- 4. THIP administration alleviated the defects of social behaviors in *Mecp2*-null mice.

(A-B) During the habituation period in the three chamber test, both WT and null mice took similar amount of times (A) and transitions (B) in either side of the chambers indicating no preference. The main effect preference was not significant. (A: F = 1.72, *df* = 1, *P* = 0.195; B: F = 0.20, *df* = 1, *P* = 0.656; Three-way ANOVA). The transitions between the chambers also suggested that the tested animals are not in a sedative state. **(C)** In the sociability test, a significant difference was detected within the main factor of preference (F = 23.31, *df* = 1, ### *P* < 0.001, three-way ANOVA). WT mice spent significantly more time in the chamber containing an animal than the empty one, whereas the *Mecp2*-null mice lost such a preference. THIP administration increased the time expenditure of *Mecp2*-null mice in interacting with another mouse (* *P* < 0.05; Tukey's post hoc). No significant differences were found in the main factor of genotype (F = 1.20, *df* = 1, *P* = 0.278) or THIP treatment (F = 0.03, *df* = 1, *P* = 0.863). The interactions of genotype × treatment (F = 0.46, *df* = 1, *P* = 0.500), genotype × preference (F =

1.41, *df* = 1, *P* = 0.239), treatment × preference (F = 3.31, *df* = 1, *P* = 0.074) or genotype × THIP treatment × preference (F = 2.08, *df* = 1, *P* = 0.155) were not significant as well (Three-way ANOVA). **(D)** In the social novelty test, the main factor of preference showed a significant difference (F = 54.48, *df* = 1, ### *P* < 0.001, three-way ANOVA). WT mice spent significantly more time in the chamber with a novel animal than the chamber with a familiar one, whereas the *Mecp2*-null mice did not show the preference to either chamber. With THIP treatment the novelty preference was improved in the *Mecp2*-null mice; (** *P* < 0.01, *** *P* < 0.001; Tukey's post hoc). No significant differences were found in the main factor of genotype (F = 0.57, *df* = 1, *P* = 0.453) or THIP treatment (F = 0.17, *df* = 1, *P* = 0.681). The interactions of genotype × treatment (F = 0.02, *df* = 1, *P* = 0.888), genotype × preference (F = 0.49, *df* = 1, *P* = 0.487), treatment × preference (F = 1.58, *df* = 1, *P* = 0.213) or genotype × THIP treatment × preference (F = 1.35, *df* = 1, *P* = 0.250) were not significant as well (Vehicle: n = 12 and n = 9; THIP: n = 8 and n = 6; WT and *Mecp2*-null, respectively; Three-way ANOVA).

7 CHAPTER3: CELLULAR MECHANISMS OF THE BENEFICIAL EFFECTS OF EARLY-LIFE EXPOSURE TO THE EXTRASYNAPTIC GABAAR AGONIST THIP IN THE *MECP2*-NULL MOUSE MODEL OF RETT SYNDROME BEFORE

Publication: **Zhong W,** Johnson CM, Cui N, Oginsky MF, Wu Y and Jiang C. (2016) Effects of early-life exposure to THIP on brainstem neuronal excitability in the *Mecp2*-null mouse model of Rett syndrome before and after drug withdrawal. *Physiological Reports.* 2017 Jan;5(2). pii: e13110.

Contribution disclosure: Weiwei Zhong and Dr. Chun Jiang designed the research and write the article. Weiwei Zhong performed the experiments and analyzed the data. Christopher M Johnson, Ningren Cui and Max F Oginsky assisted in the electrophysiology experiments. Yang Wu assisted in the breathing experiments.

7.1 Abstract

Rett syndrome (RTT) is mostly caused by mutations of the X-linked *MECP2* gene. Although the causal neuronal mechanisms are still unclear, accumulating experimental evidence obtained from *Mecp2*$^{-/Y}$ mice suggests that imbalanced excitation/inhibition in central neurons plays a major role. Several approaches may help to rebalance the excitation/inhibition, including agonists of $GABA_A$ receptors ($GABA_AR$). Indeed, our previous studies have shown that early-life exposure of *Mecp2*-null mice to the extrasynaptic $GABA_AR$ agonist THIP alleviates several RTT-like symptoms including breathing disorders, motor dysfunction, social behaviors, and lifespan. However, how the chronic THIP affects the *Mecp2*$^{-/Y}$ mice at the cellular level remains elusive. Here, we show that the THIP exposure in early lives markedly alleviated hyperexcitability of two types of brainstem neurons in *Mecp2*$^{-/Y}$ mice. In neurons of the locus coeruleus (LC), known to be involved in breathing regulation, the hyperexcitability showed clear age-dependence, which was associated with age-dependent deterioration of the RTT-like breathing irregularities. Both the neuronal hyperexcitability and the breathing disorders were relieved with early THIP treatment. In neurons of the mesencephalic trigeminal nucleus (Me5), both the neuronal hyperexcitability and the changes in intrinsic membrane properties were alleviated with the THIP treatment in *Mecp2*-null mice. The effects of THIP on both LC and Me5 neuronal excitability remained one week after withdrawal. Persistent alleviation of breathing abnormalities in *Mecp2*$^{-/Y}$ mice was also observed a week after THIP withdrawal. These results suggest that early-life exposure to THIP, a potential therapeutic medicine, appears capable of controlling neuronal hyperexcitability in *Mecp2*$^{-/Y}$ mice, which occurs in the absence of THIP in the recording solution, lasts at least one week after withdrawal, and may contribute to the RTT-like symptom mitigation.

7.2 Introduction

Rett syndrome (RTT) is a neurodevelopmental disorder, caused mostly by mutations of the X-linked *Mecp2* gene, a transcriptional regulator. Patients with RTT, almost exclusively girls, develop various symptoms, such as stereotype behaviors, autism-like social defects, motor dysfunctions and life-threatening breathing abnormalities [194]. As a widely used RTT mouse model, *Mecp2*$^{-/Y}$ mice with *Mecp2* gene turned off in all cells recapitulate most of these RTT-like symptoms and die in early ages [26]. Besides uncovering RTT symptomatic and pathological changes, the mouse model is useful for finding potential therapeutic agents.

The studies in *Mecp2*$^{-/Y}$ mice suggest that imbalanced excitation/inhibition in the central nervous system (CNS) play a major role in the development of RTT. The altered excitation and inhibition have been found in multiple brain regions, including the brainstem [53, 147, 168] and the hippocampus [66]. In *Mecp2*-null mice, excessive excitatory activity was seen in expiratory cranial and spinal nerves [12]. Neurons in the LC, the major NE source in the CNS, are overly excitable in *Mecp2*-null mice, which is attributable to their defective intrinsic membrane properties and the reduced GABAergic inhibition, and may contribute to breathing abnormalities [4, 10, 147]. Neurons in the mesencephalic trigeminal nucleus (Me5) nucleus, located adjacent to the LC, were found hyperexcitable as well [53, 56], which may contribute to the difficulties in chewing and eating in people with RTT [54, 55].

The neuronal hyperexcitability involves the GABA system. Mice with *Mecp2* gene deletion selectively in the GABAergic neurons display RTT-like phenotypes [11]. Restoration of the gene in the *Mecp2*-null GABAergic cells rescued these symptoms, including lifespan, social behaviors and motor functions [73]. Therefore, enhancing GABAergic inhibition may help to

rebalance the excitation/inhibition in mouse models and perhaps human patients with RTT, leading to alleviation of the RTT-like symptoms. Consistent with the idea, treatment with GABA reuptake blocker NO711 and synaptic GABAR agonist benzodiazepine relieves the RTT-like breathing difficulties in *Mecp2*-null mice [12, 13].

In *Mecp2*-null LC neurons, both $GABA_AR$ and $GABA_BR$ are deficient [10]. In contrast to the synaptic $GABA_A$ receptors, the expression level of extrasynaptic $GABA_AR$ is well maintained in *Mecp2*-null LC neurons [67]. They may provide an alternative target to alter the excitation/inhibition balance. Indeed, we have recently shown that early treatment with THIP (also known as Gaboxadol), an extrasynaptic $GABA_AR$ agonist, alleviates the RTT-like motor dysfunction, breathing abnormalities and the defects in social behaviors, expands the lifespan by enhancing the tonic GABAergic inhibition in *Mecp2*-null mice [83]. However, several questions remain: How does the THIP treatment affect the *Mecp2*-null mice at the cellular level? Will the systemic THIP treatment affect other brainstem neurons? Are the THIP effects lost totally after THIP clearance with withdrawal? Does a rebound excitation occur after THIP withdrawal? To address these questions, therefore, we performed the experiments.

7.3 Results

7.3.1 Age-dependent hyperexcitability of LC and Me5 neurons in Mecp2$^{-/Y}$ mice

All experiments were done in male *Mecp2*$^{-/Y}$ mice because the males offer a completely *Mecp2*-null condition that is not always available in *Mecp2*$^{+/-}$ females owing to X-chromosome inactivation.

Previous studies indicate that LC neurons are overly excitable in *Mecp2*-null mice compared to the WT [4, 147]. To show how such hyperexcitability progresses with age, we studied LC neuronal excitability in three age groups of WT and *Mecp2*-null mice. Our results showed that such neuronal hyperexcitability was age-dependent (Fig. 7-1A_{1-2}). When the spontaneous firing rate of LC neurons was plotted against ages, a linear age-dependent increase in the firing rate is seen, in which the regression is significant in *Mecp2*-null but not WT mice (Fig. 7-1A_3; WT: R = 0.14, n = 82, $P = 0.21$; *Mecp2*-null: R = 0.65, n = 79, $P < 0.001$; WT vs. *Mecp2*-null: $P = 0.001$). A significant increase in spontaneous firing activity of LC neurons started at 2-4 weeks, and became more obvious at age 4-6 weeks. The neuronal firing rate doubled that of the WT at 6-8 weeks (Fig. 7-1A_4; 2-4 weeks: n = 45 and n = 38; 4-6 weeks: n = 17 and n = 20; 6-8 weeks: n = 12 and n = 21; WT and *Mecp2*-null, respectively). Both are consistent with the onset time of RTT-like symptoms and the age-dependent symptom deterioration of *Mecp2*-null mice. In contrast, the age-dependent increase in LC neuronal excitability was not observed in WT mice (Fig. 7-1A_4).

Me5 neurons were silent at basal condition without current injection in both WT and *Mecp2*-null mice. In response to depolarizing current injection, the Me5 neurons in *Mecp2*-null mice tended to fire multiple action potentials (APs) in comparison to one or two APs in their WT counterparts (Fig. 7-1B_1-B_2). With comparable levels of current injection, Me5 neurons showed significantly higher firing rate in *Mecp2*-null mice than in the WT, indicating that they also are hyperexcitable. Unlike LC neurons, the Me5 neuronal hyperexcitability did not show significant age dependence (Fig. 7-1A_4; WT: n = 14; *Mecp2*-null 4-6 weeks: n = 17; *Mecp2*-null 6-8 weeks: n = 14; Fig. 7-1B_3).

7.3.2 Relationship of LC neuronal excitability with breathing abnormalities

It is possible that inhibition of LC neuronal hyperexcitability by THIP may affect breathing abnormalities, as LC neurons play a role in breathing regulation, and as the age-dependent deterioration was found the *Mecp2*-null mice in our previous studies [83] , Therefore, we performed electrophysiological recording from in 6-8 week-old mice whose breathing activity was measured on the same day immediately before euthanasia (Fig. 7-2A). When LC neuronal firing rate was plotted against apnea rate (Fig. 7-2B, n = 20) or breathing frequency variation (Fig. 7-2C, n = 20), we found that the LC neuronal firing rate increases proportionally with the severity of these breathing abnormalities. Both can be described with a linear regression (*Mecp2*-null: Fig. 7-2B: R = 0.66, $P < 0.01$; 2C: R = 0.62, $P < 0.01$). Such proportional changes in firing rate with breathing abnormalities were not seen in WT neurons (Fig. 7-2B,C).

7.3.3 THIP alleviates LC neuronal hyperexcitability in Mecp2$^{-/Y}$ mice

One of the common features of RTT in humans and animal models is the defect in the NE system [5, 42, 47]. Previous studies have shown that excitability of LC neurons increases in *Mecp2*-null mice [4, 147]. The LC neurons are the main source of NE in the CNS, and play an important role in breathing regulation, locomotion, arousal, emotion and other behaviors [3, 8, 195]. Therefore, we chose these neurons to find whether THIP treatment may stabilize LC neuronal excitability in *Mecp2*-null mice.

In the brain slice preparation, whole-cell current clamp was performed in LC neurons from mice with and without THIP treatment. Of four groups of mice, only did the LC neurons from *Mecp2*-null mice in vehicle control show an obvious increase in spontaneous firing activity (Fig. 7-3A, B). Detailed analysis of the passive and active membrane properties showed that the THIP

treatment did not significantly change membrane potential, input resistance, action potential overshoot and firing threshold of either groups of neurons (Fig. 7-3C, D, E, F). In *Mecp2*-null neurons, the spontaneous firing rate is significantly higher than that in WT. The THIP treatment, however, abolished the difference (Vehicle: 3.1 ± 0.3 Hz and 5.1 ± 0.3 Hz; THIP: 3.6 ± 0.2 Hz and 3.7 ± 0.3 Hz; WT and *Mecp2*-null, respectively; Fig. 7-3G). Thus, these results suggest that the LC neuronal hyperexcitability in *Mecp2*-null mice is significantly reduced after THIP exposure.

7.3.4 Mitigation of Me5 neuronal hyperexcitability with THIP exposure

To test how the extrasynaptic $GABA_AR$ agonist THIP affects other hyperexcited brainstem neurons, such as Me5 neurons, WT and *Mecp2*-null mice were exposed to THIP in their drinking water as described in the Methods. With continuing THIP treatment for 5~6 weeks starting from birth, brain slices were obtained from the mice without drug withdrawal, in which neuronal activity was studied. Note that no THIP was added to the recording solutions. A similar excitability relief was found in Me5 neurons of *Mecp2*-null mice (Fig. 7-4B). The evoked firing activity with depolarizing current injection was significantly lower in Me5 cells from THIP-treated *Mecp2*-null mice than the vehicle-treated (Fig. 7-4A; vehicle: n = 14; THIP: n = 18). No significant difference in Me5 neuronal firing rates was found between the THIP- and vehicle-treated WT (Fig. 7-4B). With the current injection, some Me5 cells fired repetitive APs. The ratio of cells with multiple APs vs those with one or two APs was significantly higher in *Mecp2*-null mice than in the WT. Such a difference was abolished with the THIP treatment (Fig. 7-4C; vehicle: n = 14 and n = 17; THIP: n = 18 and n = 16; WT and *Mecp2*-null, respectively). Together, these results suggest that early-life THIP exposure significantly suppressed the hyperexcitability of both LC and Me5 neurons in *Mecp2*-null mice.

7.3.5 THIP effects on intrinsic membrane properties of null Me5 neurons

The early-life exposure to THIP may affect these brainstem neurons by changing their intrinsic membrane properties. Thus, we performed detailed studies of subthreshold and suprathreshold properties. Since we had done similar studies in LC neurons before [4, 56], we were focused on Me5 neurons in the present study.

In the Me5 neurons, AP amplitude was measured from its threshold level to the peak. The rise time of AP was measured as the period from the AP threshold to the peak. AP width (D_{50}) measured as the width at half AP amplitude. To measure the resistance, Sag and post-inhibitory rebound (PIR), neurons were injected with a series of hyperpolarizing currents. After the termination of each command, the cell responded with a post-inhibitory depolarization or AP (when the rebound reached AP threshold). The three parameters were calculated based on the trace immediately before the AP was initiated. The input resistance was measured as the ratio of steady-state voltage at the command current. The sag was calculated as the difference between the peak hyperpolarization during the current injection and the steady-state potential. The PIR was defined as the difference between the peak depolarization of the rebound and the resting membrane potential.

Similar to LC neurons, the chronic THIP did not show significant effects on the membrane potential, input resistance, AP properties (amplitude, rise time and D_{50}), Sag and PIR of Me5 neurons (Fig. 7-5), whereas the firing threshold of Me5 neurons in *Mecp2*-null mice was shifted to more depolarizing potentials with THIP treatment, which was significant in comparison to the vehicle control (Fig. 7-5C). Therefore, in *Mecp2*-null mice, early treatment of THIP seems to raise firing threshold without affecting other intrinsic membrane properties of Me5 neurons.

7.3.6 Persistent inhibition of neuronal excitability 1-week after THIP withdrawal

The suppression of brainstem neuronal excitability may be affected by THIP withdrawal, as rebound excitation usually merges with withdrawal of certain neuronal suppressants. Therefore, we studied neuronal activity after THIP withdrawal. To avoid the likelihood that residue THIP may exist in the body, we chose to do the experiments 7 days after withdrawal.

The firing rate of LC neurons in THIP-treated mice remained significantly lower than that of the vehicle control (Fig. 7-6A; WT: 3.6 ± 0.8 Hz and 3.6 ± 1.2 Hz, n = 14 and n = 12; *Mecp2*-null: 6.8 ± 2.2 Hz and 5.0 ± 1.6 Hz, n = 21 and n = 12; vehicle and THIP, respectively). No rebound excitation was found in Me5 neurons either. Instead, the evoked firing rate of Me5 neurons from THIP-treated *Mecp2*-null mice was significantly lower than that of vehicle control a week after THIP withdrawal (Fig. 7-6B_1). Furthermore, the ratio of Me5 cells with vs without multiple APs remained about the same between *Mecp2*-null and WT mice, in comparison to the significant difference in the ratio between vehicle controls (Fig. 7-6B_2). These results suggest that THIP withdrawal does not seem to cause rebound excitation. Instead, the THIP effects seem persistent, as both LC and Me5 neurons of *Mecp2*-null mice retained their excitability similar to their WT counterparts one week after THIP withdrawal (Fig. 7-6B_1-B_2; vehicle: n = 14 and n = 17; THIP: n = 9 and n = 13; WT and *Mecp2*-null, respectively).

7.3.7 Breathing abnormalities remained suppressed one-week after THIP withdrawal

Our previous study has shown that the same THIP treatment significantly suppressed the breathing abnormalities [83] . We thus studied how breathing was affected by THIP withdrawal.

One week after THIP withdrawal, both apnea events and breathing frequency variation in *Mecp2*-null mice remained lower than the vehicle control (Fig. 7-7A_1-A_2). Statistical analysis

showed that in *Mecp2*-null mice, the apnea rate and breathing frequency variation were significantly lower in mice that had been treated with THIP than those treated with vehicle (Fig. 7-7B-C; WT: n = 17 and n = 3; *Mecp2*-null: n = 19 and n = 8; sham and THIP, respectively). These results, consistent with the prolonged neuronal excitability depression, indicate that the effects of THIP treatment seem to persist at least for one week after THIP withdrawal without apparent rebound excitation.

7.3.8 THIP affects the gene expressions in Mecp2$^{-/Y}$ mice

Previous studies have shown that the *Mecp2* disruption leads to reductions in NE content in the CNS and expression levels of the rate-limiting enzymes TH and DBH for NE biosynthesis [6, 42, 50, 147]. Persistent hyperexcitation of LC neurons may interfere with the homeostatic state in NE biosynthesis and release, leading to the reduced expression of TH and DBH in *Mecp2*-null mice [67]. Thus, moderation of LC neuronal hyperexcitability may improve expression of TH and DBH in *Mecp2*-null mice. To test this possibility, we studied the TH and DBH at mRNA and protein levels. The qPCR analysis showed that THIP treatment significantly increased both TH and DBH transcript levels in the pontine extracts of *Mecp2*-null mice (Fig. 7-8A-C). Western blot analysis showed ~2 fold increase in TH protein level and ~1.5 fold increase in DBH protein level (Fig. 7-8D-F).

Early-life exposure to THIP might also reshuffle the GABA receptor subunits. Therefore, quantitative PCR was performed to detect the mRNA levels of δ, α6, β1 and β2 subunits, which were reported as significantly changed in *Mecp2*-null LC area. In comparison with vehicle control, a significant reduction of α6 subunit was detected in *Mecp2*-null mice with THIP treatment, while no significant changes in other subunit expression were found (Fig. 7-9).

7.4 Discussion

This is the first study of the cellular outcome of early-life exposure to THIP. We have found that the THIP exposure markedly alleviates hyperexcitability of two types of brainstem neurons in *Mecp2*$^{-/Y}$ mice. In LC neurons known to be involved in breathing regulation, the hyperexcitability shows clear age-dependence associated with age-dependent deterioration of the RTT-like breathing irregularities, both of which are relieved with early THIP treatment. In Me5 neurons of *Mecp2*-null mice, the hyperexcitability as well as the changes in intrinsic membrane properties are both improved with the THIP treatment. One week after THIP withdrawal, excitability of both LC and Me5 neurons remained depressed. Consistent with the proportional relationship between LC firing rate and breathing irregularities and the persistent effects of THIP on cellular excitability, RTT-like breathing abnormalities of *Mecp2*-null mice remain low in the time period after THIP withdrawal. In addition, early exposure of THIP improved the biosynthesis enzyme gene expression in *Mecp2*-null LC neurons.

Mecp2-null mice start to display a range of RTT-like symptoms, including mobility problems and breathing difficulties around 3 weeks after birth, and most of the animals die within 2 months of age [26]. The symptom development is consistent with the onset and deterioration of the neuronal hyperexcitation, especially LC neurons as shown in the present study. Indeed, our results have shown that LC neuronal excitability increases proportionally with the severity of breathing abnormalities. Thus, the defects in LC neuronal excitability may play a role in the development of the RTT-like symptoms in the mouse model. Consistent with this idea, the chronic THIP stabilizes LC neuronal excitability and breathing abnormalities to a similar degree (Fig. 7-3A). Also consistent with the idea are our recent studies showing that by enhancing the tonic

GABAergic inhibition, early-life exposure of *Mecp2*-null mice to THIP alleviates various RTT-like symptoms and extends lifespan [83].

Although THIP may affect other brain regions by augmenting local extrasynaptic $GABA_A$ receptors, the stabilization of LC neuronal excitability may benefit a range of target regions. The LC is the major NE source in the CNS. The homeostasis of the LC neuronal excitability vs the NE synthesis, ensures the persistent production and release of NE. LC neuronal hyperexcitability may interrupt this balance and lead to impairment of the NE system, including the reduced expression of rate-limiting enzyme, tyrosine hydroxylase (TH) and dopamine beta hydroxylase (DBH), and reduced NE concentration in the CNS [5, 6, 50, 115, 147]. A relief of LC hyperexcitability may reinstall the homeostatic state in the cells and improve NE output, which may benefit the LC-NE projected target regions, including the brainstem, the spinal cord and the prefrontal cortex, brains areas critical for breathing, motor function and social behaviors [59, 164].

The hyperexcitation is not limited to LC neurons. Our results have shown that Me5 neurons are also hyperexcitable [53]. The Me5 neurons are the only group of propriosensory neurons with soma located in the CNS, which provide servo feedback control to the jaw muscles. The increased excitability in these neurons may impair these cranial muscles, consistent with the defects of chewing, drinking, speaking and teeth grinding in people with RTT [53-56]. Suppression of overly excited Me5 neurons may lead to a correction in the proprioception of muscles, leading to the improvement of motor function in RTT. The Me5 neuronal hyperexcitability may be attributable to the impaired intrinsic membrane properties in *Mecp2*-null mice.

Our results show that early-life THIP exposure suppresses the neuronal hyperexcitability without affecting most of the intrinsic membrane properties, which suggests that THIP seems to restore the normal function of *Mecp2*-null neurons via presynaptic inhibition. However, the firing

threshold is shifted to more depolarizing potentials in both LC and Me5 neurons, indicating THIP may also alter postsynaptic mechanisms such as Na^+ channel expressions that have been shown abnormal in *Mecp2*-null mice [4, 53].

In contrast to the neuronal hyperexcitability, hypoexcitability is found in certain forebrain neurons, which may contribute to the impaired sensorimotor gating function in RTT [68]. Interestingly, inhibition of the NMDA receptors with ketamine can reverse the neuronal hypoexcitability and improve associated behaviors in *Mecp2*-null mice, likely by disinhibiting cortical pyramidal cells [68, 120]. Apparently, excessive excitation may also be a problem in the cortical neuronal networks, which responds to NMDA receptor antagonism. Besides ketamine, enhancing the GABAergic inhibition might benefit hypoexcitability of certain forebrain neurons in *Mecp2*-null mice as well.

THIP was previously tested as a potential clinical medicine for insomnia. With a short half-life time around half an hour, the THIP concentration in the plasma diminished within 3 hours [183]. However, continuous oral treatment may allow the THIP to remain at a certain level for a long period in the plasma and CNS, leading to the persistent effects on neurons and the associated phenotypes.

Due to the fast decay of the THIP, the withdrawal for one week may allow a total clearance of THIP from the plasma and the CNS. This time period seems adequate for evaluation of the persistence of its effects. Our results indicate that the THIP effects on relieving neuronal hyperexcitability remain one week after THIP withdrawal, which suggest chronic treatment of THIP may alter the expression of certain proteins involving the rebalance of excitation vs inhibition in the CNS. The results are consistent with the expanded lifespan in the THIP treated *Mecp2*-null mice [83] . Although neuronal activity and breathing abnormalities remained

alleviated with the THIP withdrawal in *Mecp2*-null mice, their absolute levels were higher than the WT, indicating a gradual decline of the THIP effects.

Our results do not support the presence of rebound excitation one week after THIP withdrawal. However, the results cannot rule out the possibility of rebound excitation during the period of 1-6 days after THIP withdrawal. Because of the availability of these *Mecp2*-null mice, we could not perform these follow-up studies. Thus, further studies are needed to reveal the time course 1-6 days after THIP withdrawal.

LC neurons, the major NE source in the CNS, projects broadly to the other brain regions, including the medulla where the respiratory center located, and the prefrontal cortex where the NE system affects cognitive functions, seizure and social behaviors [59, 164]. In *Mecp2*-null mice with THIP treatment, the target regions of LC-NE projection may benefit from the enhanced NE synthesis, leading to the alleviation of the associated abnormal behaviors.

People with RTT and the mouse models show the delayed onset and progressive symptoms. Although the mechanism for the delayed symptom onset remains unclear, some factors may contribute to it, such as dynamic spatiotemporal relationship between MeCP2 and methylated DNA [196] and the altered allopregananallone modulation of the GABA system during perinatal period [14]. Thus, interfere with neuronal hyperexcitability before the symptom onset may be a potential way to prevent or delay the development of the disease. The δ subunit containing extrasynaptic $GABA_A$Rs are expressed dynamically with growth [187]. Since severe defects in the synaptic $GABA_A$R system have been demonstrated mature *Mecp2*-null mice, treatment with THIP in early lives may be beneficial with respect to enforcement of the inhibitory system in the neurodevelopment of *Mecp2*-null mice.

The reduced expression of α6 subunits suggests that early treatment of THIP may lower the GABAR expression and the consequent GABAergic inhibition. The α6 subunit is known to contribute to both the extrasynaptic receptors together with the δ subunit and the synaptic $GABA_ARs$ with β and γ subunits [19]. The reduction in these $GABA_ARs$ might possibly lead to rebound excitation after THIP withdraw. The stabilization of neuronal excitability, however, might affect cellular mechanisms reducing abnormalities, which could result in a long-term reduction in neuronal hyperexcitabiltiy after THIP withdraw, contributing to the outcome of THIP in breathing, motor function, social behaviors and lifespan.

In conclusion, cellular hyperexcitability has been found in multiple neurons of *Mecp2*-null mice, associated with RTT-like symptoms. Early-life treatment with THIP reduces significantly the hyperexcitability of both LC and Me5 neurons in *Mecp2*-null mice without affecting most of the intrinsic membrane properties. The gene expressions, including the genes of biosynthesis enzyme gene and receptor subunits, are affected in *Mecp2*-null LC neurons. The THIP effect persists for at least one week after THIP withdrawal. The results suggest that THIP, a potential therapeutic medicine, seems capable of stabilizing neuronal excitability and improvement of the biosynthesis enzyme expression in *Mecp2*-null mice, which may contribute to the RTT-like symptom mitigation.

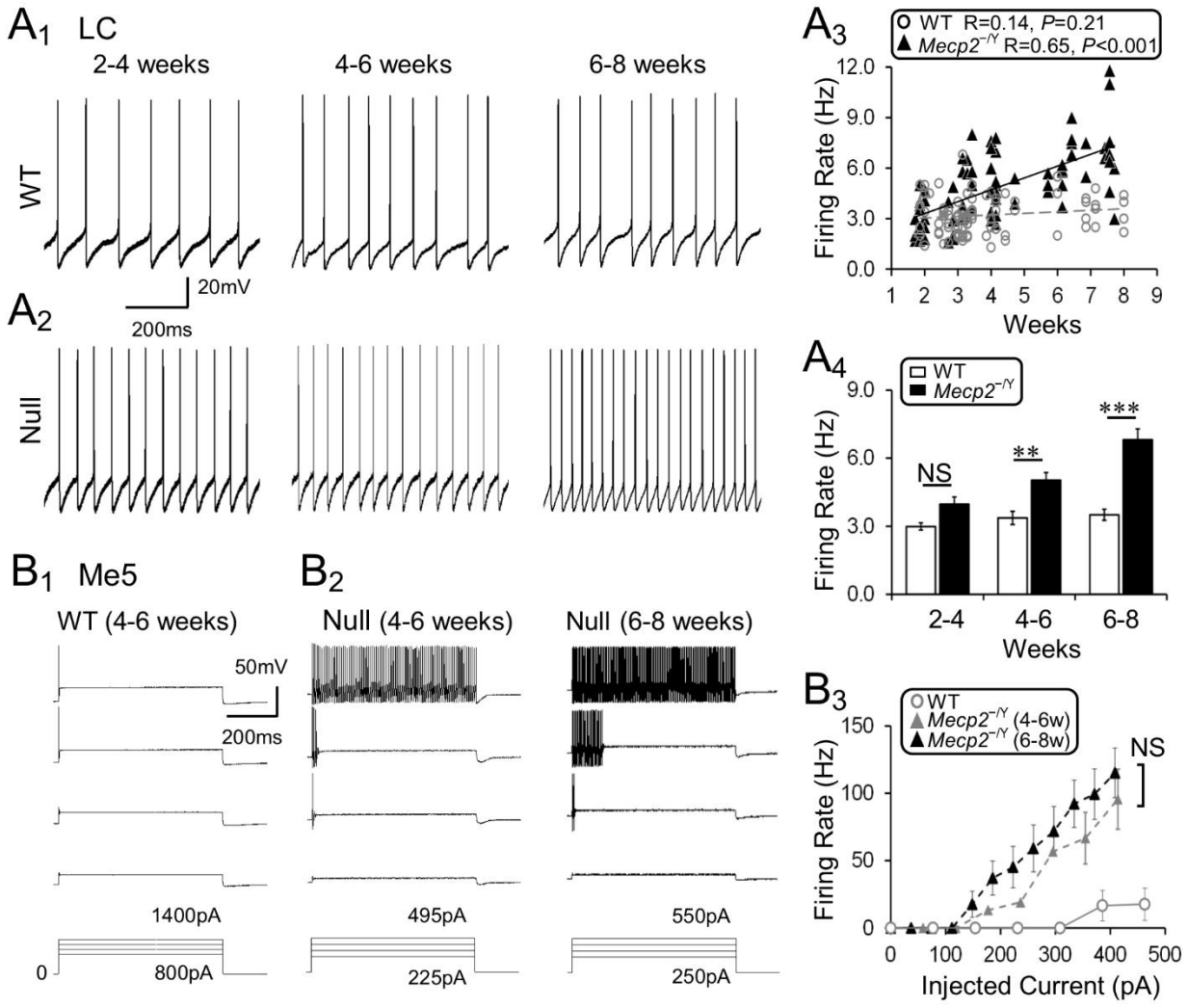

Figure 7- 1. Age-dependent increase in excitability of LC and Me5 neurons in *Mecp2*$^{-/Y}$ mice.

(A_1-A_2) Neuronal activity was studied in whole-cell current clamp, LC neurons in *Mecp2*$^{-/Y}$ mouse showed increased firing frequency in comparison to its WT counterpart. Such hyperexcitability deteriorated with growth. **(A_3-A_4)** Statistically, the increased LC neuronal excitability in *Mecp2*-null mice was significantly different from the WT, and showed age dependence (A_3: Pearson correlation. A_4: Significant differences were found in the main factors of genotype (df = 1, F = 66.14, $P < 0.001$) and age (df = 1, F = 16.53, $P < 0.001$). Significant interaction was found between the two factors as well. ###P < 0.01; Two-way ANOVA and **$P < 0.01$, ***$P < 0.001$; Tukey's

post-hoc). **(B_1-B_2)** With injections of a series of depolarizing currents, most of the Me5 neurons in WT neurons fired single action potential, while the *Mecp2*-null Me5 ones fired multiple action potentials. The excitability of Me5 neurons in *Mecp2*-null did not show the age dependence (NS, not significantly different; Student's t-test).

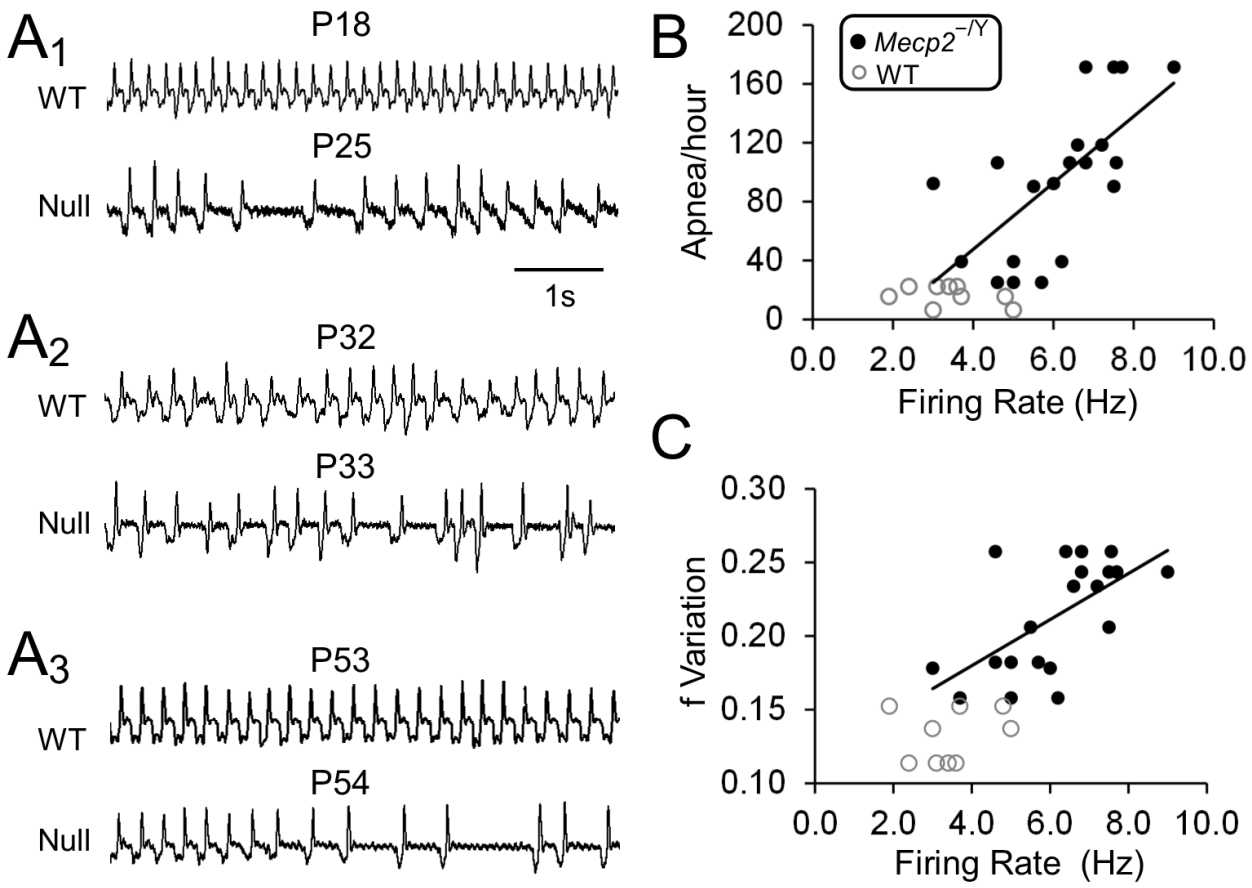

Figure 7- 2. Relationship of LC neuronal excitability with breathing abnormalities.

(A1-A3) Typical records of breathing activity from both WT and *Mecp2*-null mice at different ages and the breathing abnormalities deterioration with the age. **(B-C)** Breathing activity was measured immediately before *Mecp2*-null mice were used for brain slice studies. In the *Mecp2*-null mice older than 6 weeks, LC neuronal firing rate increased proportionally with the severities of apnea rate and breathing frequency variation (Pearson correlation). Such relationship was not found in the WT mice.

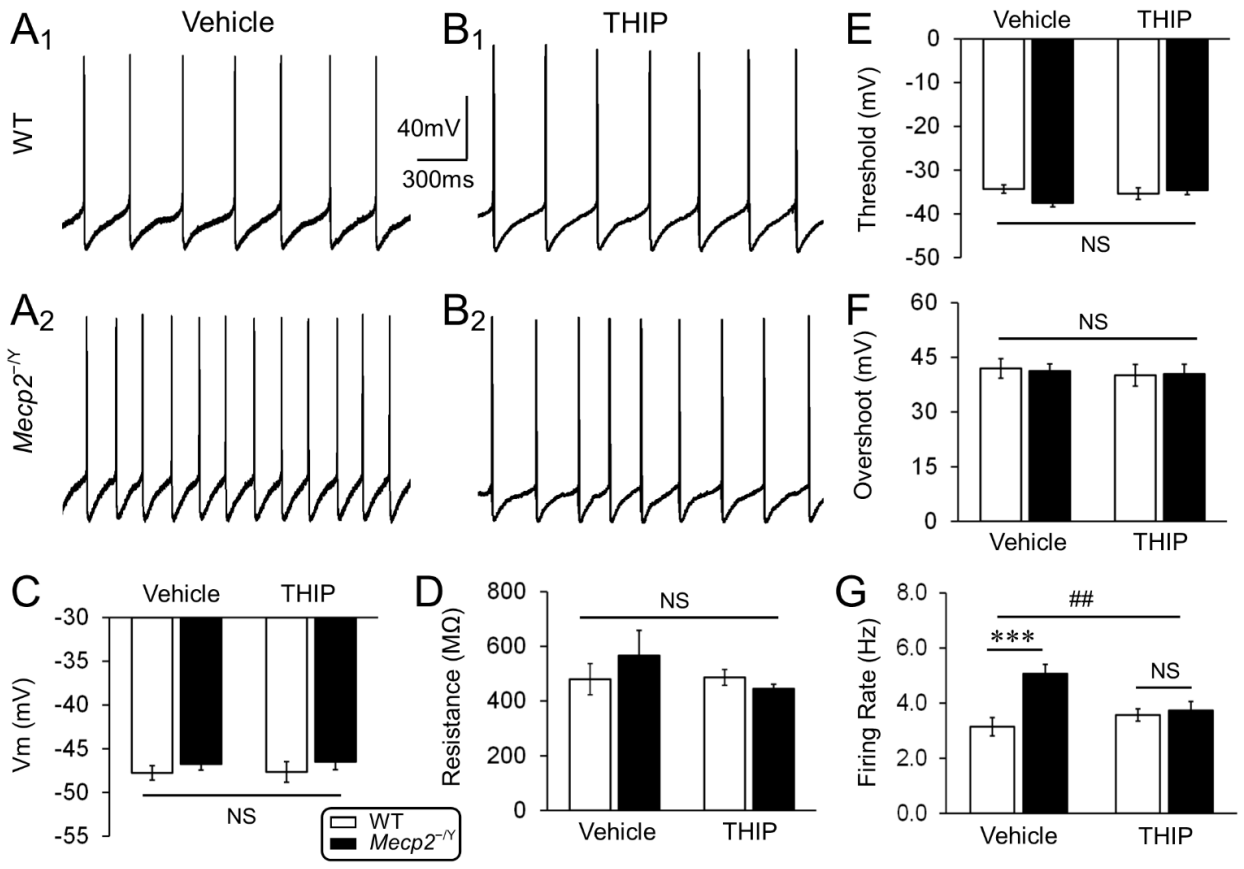

Figure 7- 3. THIP administration suppressed the hyperexcitability of LC neurons in *Mecp2*-null mice.

(A1-A2) Typical recordings of spontaneous firing of LC neurons in WT and *Mecp2*-null mice at one-month of age without THIP treatment. **(B1-B2)** Spontaneous firing of LC neurons in WT and *Mecp2*-null mice of the same age with THIP treatment. (**C-F)** THIP administration did not significantly change membrane potentials, input resistance, action potential overshoot and action potential threshold in both WT and *Mecp2*-null mice. No significant main effect of THIP treatment (F = 0.09, *df* = 1, *P* = 0.765; F = 1.15, *df* = 1, *P* = 0.289; F = 0.27, *df* = 1, *P* = 0.606; F = 0.76, *df* = 1, *P* = 0.387; Fig C, D, E, F, respectively) and genotype (F = 1.45, *df* = 1, *P* = 0.234; F = 0.09, *df* = 1, *P* = 0.765; F = 0.01, *df* = 1, *P* = 0.921; F = 0.99, *df* = 1, *P* = 0.324; Fig C, D, E, F, respectively) were observed, either the interaction (F = 0, *df* = 1, *P* = 1.000; F = 1.46, *df* = 1, *P* =

0.232; F = 0.03, *df* = 1, *P* = 0.863; F = 3.58, *df* = 1, *P* = 0.064; Fig C, D, E, F, respectively). **(G)** The main effect of genotype was significant (F = 10.06, *df* = 1, *P* < 0.01), whereas the main effect of THIP treatment was not (F = 1.72, *df* = 1, *P* = 0.196). The interaction of these two factors was significant (F = 8.6, *df* = 1, *P* < 0.01) as well (## *P* < 0.01; Two-way ANOVA). The firing activity of LC neurons in *Mecp2*-null mice is significantly increased compared to the WT and chronic treatment with THIP abolished the hyperexcitability (Vehicle: n = 14 and n = 13; THIP: n = 13 and n = 16; in WT and *Mecp2*-null, respectively; *** *P* < 0.001; Tukey's post hoc).

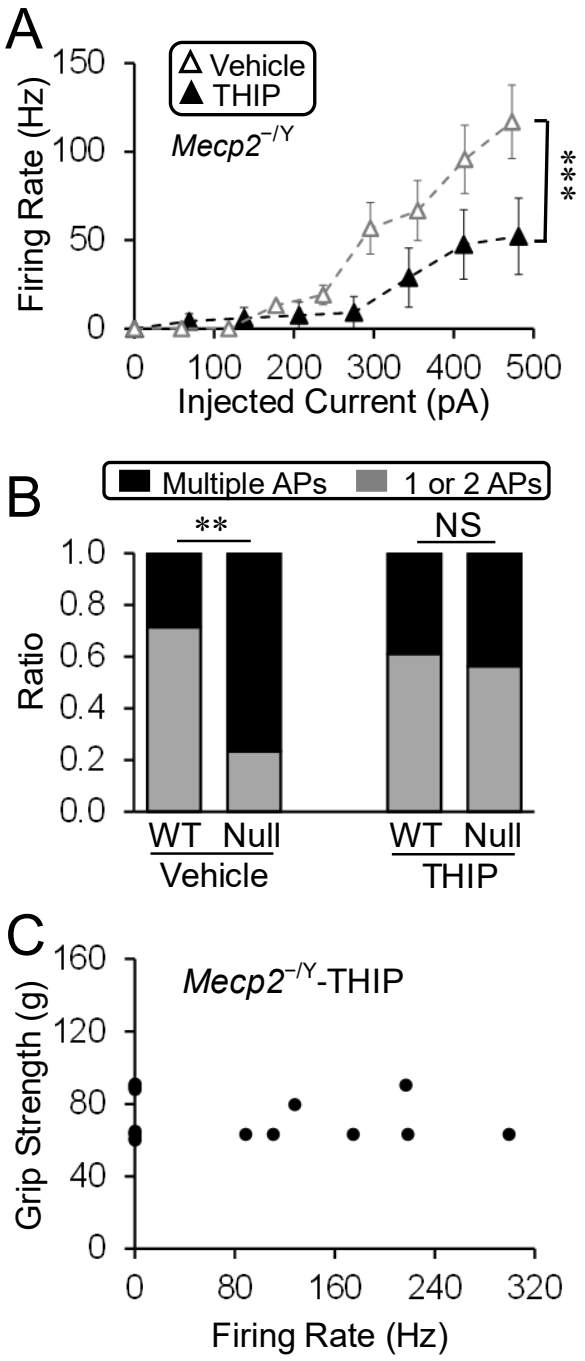

Figure 7- 4. THIP exposure alleviated the Me5 neuronal hyperexcitability.

(A-C) THIP significantly reduced the firing rate of Me5 neurons in *Mecp2*-null mice with comparative amount of current injections (A). Such a relief of Me5 neuronal excitability was not found in the WT mice (B). In comparison to the WT, a significantly larger number of Me5 neurons

in *Mecp2*-null mice fired multiple action potentials, which was also suppressed by THIP treatment (C) (*** $P < 0.001$, ** $P < 0.01$; Student's t-test and $\chi 2$-test).

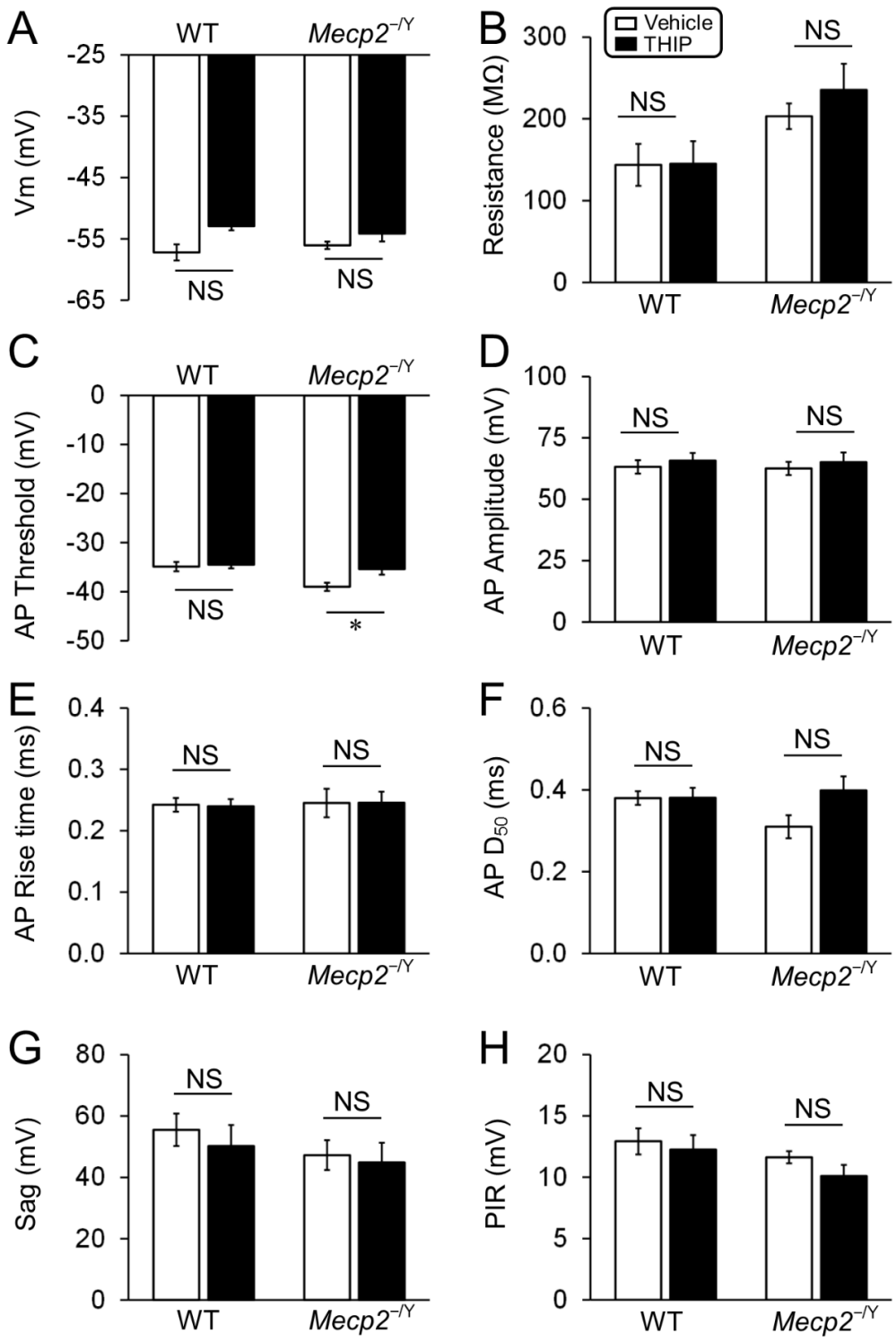

Figure 7- 5. THIP effects on intrinsic membrane properties of *Mecp2*-null Me5 neurons.

(A-B) The membrane potential and input resistance were not altered with THIP treatment in either *Mecp2*-null Me5 cells or WT ones. **(C-F)** THIP significantly shifted the firing threshold of Me5

neurons to more depolarizing potentials in *Mecp2*-null mice, but not in WT (C). THIP did not change the other parameters of AP morphology, including amplitude, rise time and half width (D_{50}, measured at 50% amplitude) in either WT or *Mecp2*-null neurons (D-F). **(G-H)** In Me5 cells, Sag and PIR was not significantly changed with THIP treatment as well (* $P < 0.05$; Student's t-test).

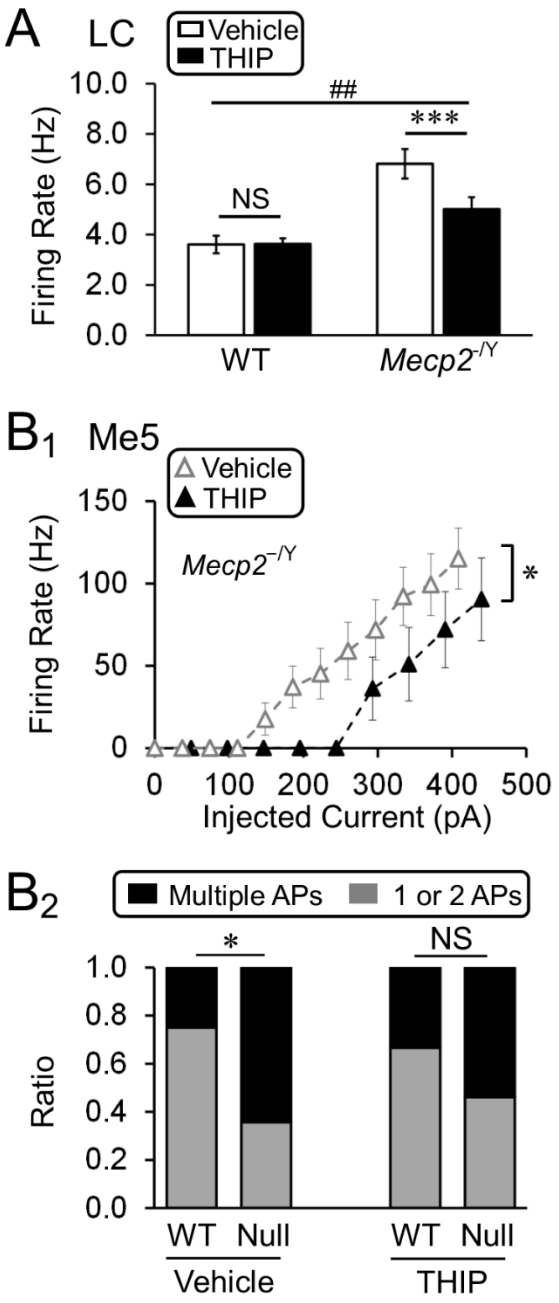

Figure 7- 6. The THIP effects on neuronal excitability one week after withdrawal.

(A) The hyperexcitability of LC neurons was significantly lower in *Mecp2*-null mice with THIP treatment than in those without. Significant differences were found in the main factors of genotype (df = 1, F = 34.27, $P < 0.001$) and treatment (df = 1, F = 7.55, $P = 0.008$). No significant interaction was found between the two factors (##$P < 0.01$, Two-way ANOVA and ***$P < 0.001$, Tukey's

post-hoc). **(B)** In *Mecp2*-null Me5 neurons, the suppression of neuronal excitability by THIP was remained (B_1). The number of cells with repetitive firing activity was significantly reduced with THIP treatment in comparison to those without (B_2) (*$P < 0.05$; Student's t-test and $\chi 2$-test).

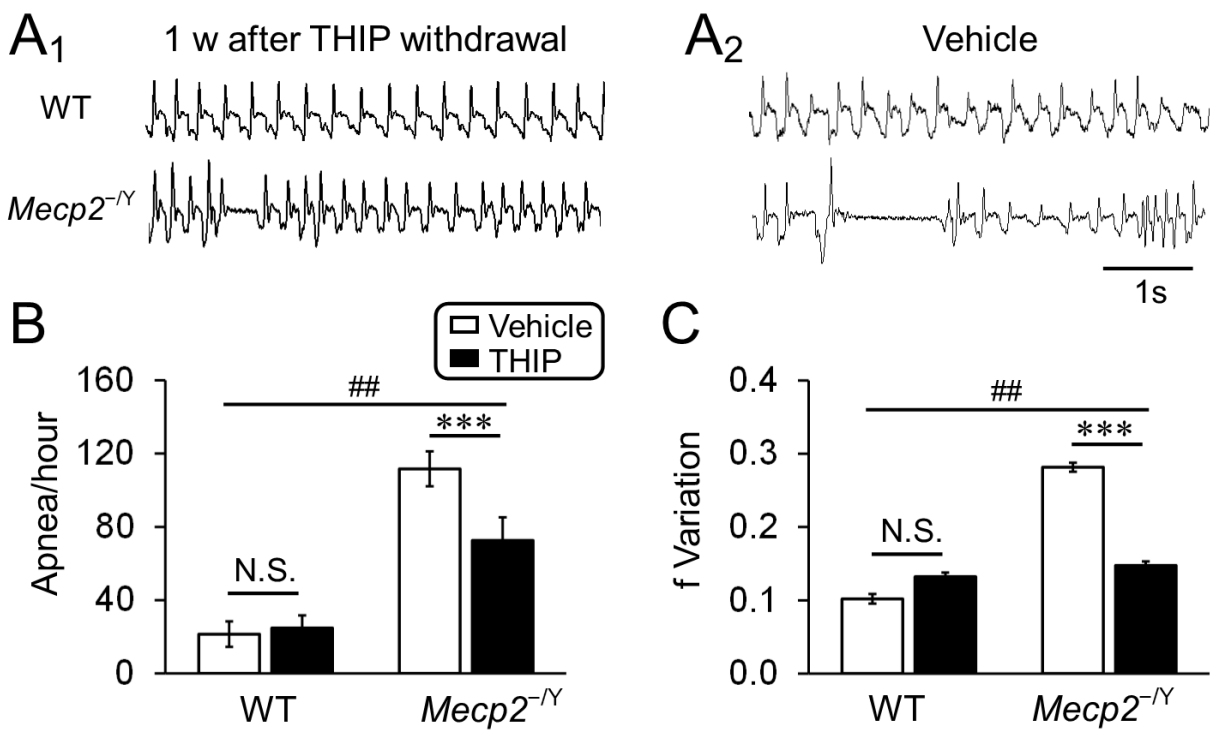

Figure 7- 7. Breathing abnormalities remained suppressed one-week after THIP withdrawal.

(A1-A2) Typical records of breathing activity from both WT and *Mecp2*-null mice at P61. **(B-C)** The apnea rate (B) and breathing frequency variation (C) in *Mecp2*-null mice were significantly reduced in comparison to the vehicle control. Significant differences were found in the main factors of genotype (B: df = 1, F = 57.89, $P < 0.001$; C: df = 1, F = 34.44, $P < 0.001$) and treatment (B: df = 1, F = 8.11, $P = 0.007$; C: df = 1, F = 10.33, $P = 0.003$). Significant interactions were found between the two factors in apnea, but not in breathing frequency variation (##$P < 0.01$, Two-way ANOVA and ***$P < 0.001$, Tukey's post-hoc).

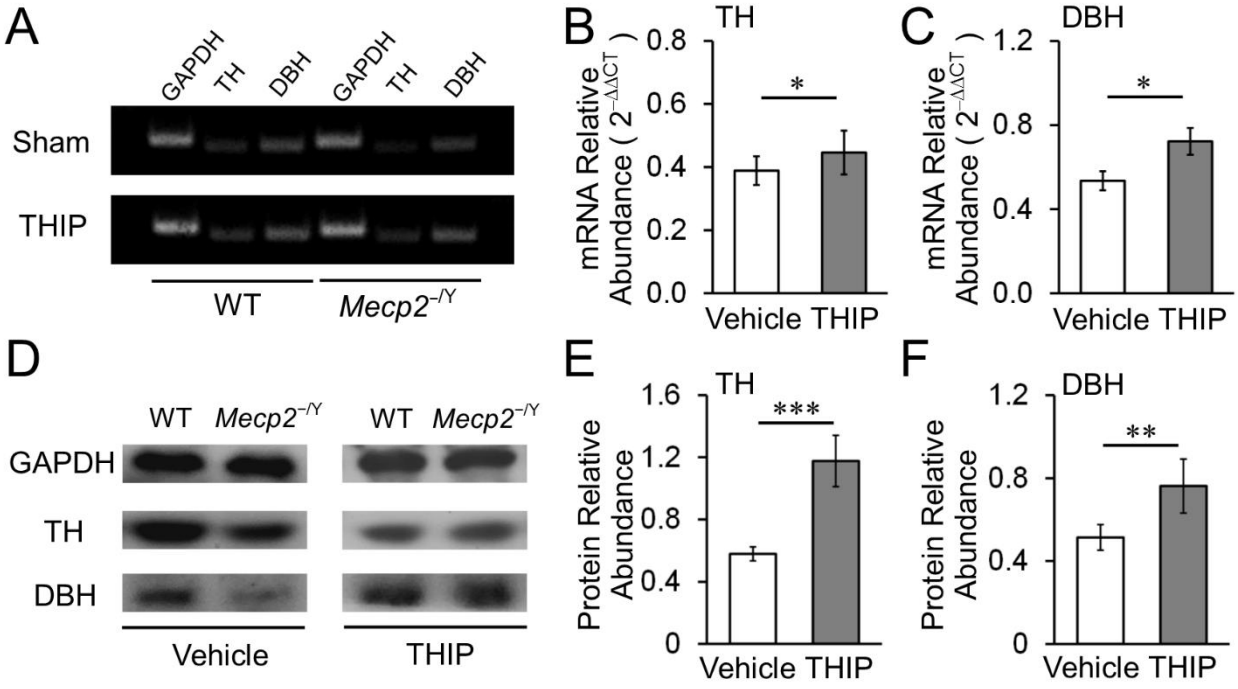

Figure 7- 8. Improvement of TH and DBH expressions with THIP administration in *Mecp2*-null mice.

(A-B) qPCR analysis showed that during THIP treatment (P37), both TH and DBH transcript levels were significantly increased (Vehicle: n = 4 and n = 4 animals; THIP: n = 5 and n = 5 animals; WT and *Mecp2*-null, respectively). **(C-D)** The Western analysis also indicated that THIP treatment significantly increased the protein expressions of both TH and DBH (Vehicle: n = 4 and n = 4 animals; THIP: n = 4 and n = 4 animals; WT and *Mecp2*-null, respectively; * $P < 0.05$, ** $P < 0.01$, *** $P < 0.001$; One-tailed Student's *t*-test).

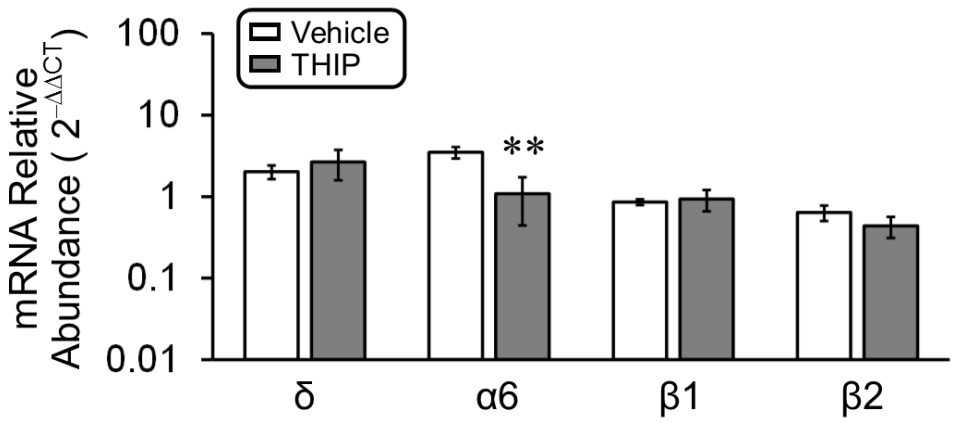

Figure 7- 9. Alteration of $GABA_AR$ subunits in the LC area of *Mecp2*-null mice.

qPCR analysis indicated that the mRNA levels of δ and α6 subunits were 2.0 and 3.5 Times higher than the WT levels, while THIP treatment significantly reduced the expression level of α6 subunit, without alteration of δ, β1 and β2 subunits (Vehicle: n = 4 and n = 4 animals; THIP: n = 5 and n = 5 animals; WT and *Mecp2*-null, respectively; ** $P < 0.01$; Student's *t*-test).

8 CHAPTER4: EFFECTS OF EXTRASYNAPTIC $GABA_AR$ AGONISTS EXPOSURE ON BRAINSTEM NEURONAL EXCITABILITY IN THE FEMALE MOUSE MODEL OF RETT SYNDROME

Publication: **Zhong W,** Johnson CM, Cui N, Xing H, Wu Y and Jiang C. (2016) Effects of chronic exposure to low dose THIP on brainstem neuronal excitability in mouse models of Rett syndrome: Evidence from symptomatic females. Neuropharmacology. Accepted.

Contribution disclosure: Weiwei Zhong and Dr. Chun Jiang designed the research and write the article. Weiwei Zhong performed the experiments and analyzed the data. Christopher M Johnson assisted in symptom identification and the electrophysiology experiments. Ningren Cui assisted in the electrophysiology experiments. Hao Xing and Yang Wu assisted in the ICC experiments.

8.1 Abstract

Rett Syndrome (RTT) is a neurodevelopmental disorder caused by mutations of the *MECP2* gene, affecting predominantly females. One of the characteristic features of the disease is defective brainstem autonomic function. In *Mecp2*$^{-/Y}$ mice, several groups of brainstem neurons are overly excitable, which causes destabilization of neuronal networks for the autonomic control. We have previously shown that the extrasynaptic $GABA_A$ receptor agonist THIP relieves many RTT-like symptoms in *Mecp2*$^{-/Y}$ mice. Although neuronal activity is inhibited by acute THIP exposure, how a chronic treatment affects neuronal excitability remains elusive. Thus, we performed studies to address whether increased excitability occurs in brainstem neurons of female *Mecp2*$^{+/-}$ mice, how the MeCP expression affects the neuronal excitability, and whether chronic THIP exposure improves the neuronal hyperexcitability. Symptomatic *Mecp2*$^{+/-}$ (s*Mecp2*$^{+/-}$) female mice were identified with a two-step screening system. Whole-cell recording was performed in brain slices after a prior exposure of the s*Mecp2*$^{+/-}$ mice to a 5-week low-dose THIP. Neurons in the locus coeruleus (LC) and the mesencephalic trigeminal nucleus (Me5) showed excessive firing activity in the s*Mecp2*$^{+/-}$ mice. THIP pretreatment reduced the hyperexcitability of both LC and Me5 neurons in the s*Mecp2*$^{+/-}$ mice, to a similar level as their counterparts in *Mecp2*$^{-/Y}$ mice. In identified LC neurons, the hyperexcitability appeared to be determined by not only the MeCP2 expression, but also their environmental cues. The alleviation of LC neuronal hyperexcitability seems to benefit brainstem autonomic function as THIP also improved breathing abnormalities of these s*Mecp2*$^{+/-}$ mice.

8.2 Introduction

Rett Syndrome (RTT) is an X chromosome-linked neurodevelopmental disorder, affecting 1/10,000 live-birth females worldwide [1]. The major cause of the disease is mutations in the *MECP2* gene encoding the transcriptional regulator methyl-CpG binding protein 2 (MeCP2). Targeting on the *Mecp2* gene, a variety of rodent models has been developed in the RTT study. Like humans with RTT, the animal models show many RTT-like symptoms, including the motor dysfunction, social behavioral defects and dysfunctions in the autonomic nervous system [3, 107, 173].

Mutations in the *Mecp2* gene cause defects in neurons of the CNS as well. In the *Mecp2*$^{-/Y}$ mice, the locus coeruleus (LC) neurons show increased membrane excitability, which may interfere with their NE biosynthesis, leading to the defects in the autonomic functions including breathing abnormalities [6, 50, 147]. Hyperexcitability also occurs in neurons in the mesencephalic trigeminal nucleus (Me5), which may affect proprioceptive control of several cranial motoneurons [53, 56], consistent with clinical manifestations of RTT such as difficulties in chewing, swallowing and tooth grinding [54, 55].

The neuronal hyperexcitability may be relieved by interventions to neurotransmission and neuromodulation. GABA is the prominent inhibitory neurotransmitter in the brain. In *Mecp2*$^{-/Y}$ mice, neurotransmission mediated by both $GABA_A$-receptors and $GABA_B$-receptors is defective [10]. The insufficient GABAergic inhibition may contribute to the neuronal hyperexcitability and several RTT-like symptoms. Indeed, inhibition of the neuronal hyperexcitability with GABA reuptake blocker NO711 and the $GABA_A$ receptor agonist benzodiazepine improves the breathing activity in *Mecp2*$^{-/Y}$ mice [12, 13]. In addition to these synaptic $GABA_A$ receptors, there is a group of extrasynaptic $GABA_A$ receptors. We have recently found that 4,5,6,7-tetrahydroisoxazolo(5,4-

c)pyridin-3-ol (THIP, also known as Gaboxadol), an extrasynaptic $GABA_A$-receptor agonist, alleviated the breathing abnormalities, motor dysfunctions and defects in social activities in *Mecp2*$^{-/Y}$ mice by enhancing the GABAergic inhibition and stabilizing the neuronal hyperexcitability [67]. Thus, further studies of the effects of THIP on the neuronal hyperexcitability and the consequent RTT-like symptoms in animal models may lead to a potential therapeutic agent for the disease.

Although current studies are mostly performed in the male models that have a clean *Mecp2*-null genetic background, it is necessary to show how these research findings manifest themselves in the heterozygous *Mecp2*$^{+/-}$ females. This is particularly important when potential therapeutics are concerned. Several factors may affect the symptom development in the *Mecp2*$^{+/-}$ mice differently from the males. 1) The X inactivation impacts the phenotypic outcome [105]. Although the random X chromosome inactivation would theoretically render a half of *Mecp2*$^{+/-}$ individuals to carry the mutated gene, our previous study suggests that only ~20% the *Mecp2*$^{+/-}$ mice developed breathing disorders [107]. Indeed, the nonrandom X (or preferred) inactivation has been reported to contribute to clinical symptom variations [106]. 2) Instead of uniform expression, central neurons show mosaic patterns of MeCP2 expression in the *Mecp2*$^{+/-}$ mice, which vary among regions and animal ages [104]. The MeCP2 expression may affect symptom development in human patients and female animal models. 3) A previous study has shown that neurons with defective MeCP2 can affect the development of surrounding cells in *Mecp2*$^{+/-}$ mice [109], a phenomenon that may affect neuronal response to interfering with their membrane excitability in the *Mecp2*$^{+/-}$ mice.

However, it is still unknown what happens to excitability of brainstem neurons in the *Mecp2*$^{+/-}$ mice, how the neuronal excitability is related to MeCP2 expression, and whether the

THIP treatment may lead to different effects on the neuronal excitability in the *Mecp2*$^{+/-}$ mice from *Mecp2*$^{-/Y}$ mice. To address these questions, we performed this study in two groups of brainstem neurons in the *Mecp2*$^{+/-}$ mice, and compared their excitability as well as THIP effects with those in *Mecp2*$^{-/Y}$ mice. A special attention was paid to the cellular outcome of the THIP administration in LC neurons with respect to neuronal firing activity and breathing abnormalities.

8.3 Results

8.3.1 LC neurons in symptomatic Mecp2$^{+/-}$ *mice showed hyperexcitability that was alleviated with THIP exposure in early life*

Owing to random inactivation of the X chromosome, symptoms varied between heterozygous females. To separate these mice, a two-step identification procedure was used. Firstly, we adopted the scoring system proposed previously [51] with modifications to determine potential symptomatic *Mecp2*$^{+/-}$ mice, which consisted of 1) abnormal mobility, 2) abnormal gait, 3) hindlimb clasping, 4) tremor, 5) breathing abnormalities and 6) weak general condition. Score 0 was assigned to a mouse if none of these signs was found; the animal was scored 1 if any one of the 6 signs was shown to be mild (score 6 if the mouse showed all); score 2 if any of the signs was severe (maximum 12). The *Mecp2*$^{+/-}$ mouse was placed in the potential symptomatic group if it received 3 scores or more. Secondly, the mouse was considered to be symptomatic when it also showed breathing abnormality in the plethysmograph test as we reported previously [107]. Only were the symptomatic *Mecp2*$^{+/-}$ (s*Mecp2*$^{+/-}$) mice used in the present study, which were divided into two groups and treated with vehicle or THIP as described in the Methods.

LC neurons were recorded from the s*Mecp2*$^{+/-}$ and WT *Mecp2*$^{+/+}$ mice in whole-cell current clamp. In the vehicle-treated group, the LC neurons showed significantly higher firing activity in the s*Mecp2*$^{+/-}$ mice than in the *Mecp2*$^{+/+}$ mice (Fig. 8-1A). The firing rate of these neurons was 5.7 ± 0.3 Hz in s*Mecp2*$^{+/-}$ mice and 4.0 ± 0.4 Hz in *Mecp2*$^{+/+}$ mice, respectively. They were significantly different from each other (*Mecp2*$^{+/+}$: n = 15; s*Mecp2*$^{+/-}$: n = 27; P = 0.002; Fig. 8-1C).

In the THIP group treated for 5 consecutive weeks, LC neuronal firing activity was similar between s*Mecp2*$^{+/-}$ and *Mecp2*$^{+/+}$ mice (Fig. 8-1B). Statistical analysis indicated that THIP treatment significantly reduced the firing rate to 3.8 ± 0.4 Hz in s*Mecp2*$^{+/-}$ mice (*Mecp2*$^{+/+}$: n = 15 and n = 11; s*Mecp2*$^{+/-}$: n = 27 and n = 22; Vehicle and THIP, respectively; Fig. 1D, Table 1). Note that there was no THIP added to the recording chamber in this and the rest of our studies. Thus, LC neurons in the s*Mecp2*$^{+/-}$ mice showed excessive firing activity like cells in their male *Mecp2*$^{-/Y}$ counterpart, and chronic exposure to THIP reduced the neuronal hyperexcitability.

8.3.2 The THIP exposure affected both MeCP2-positive and MeCP2-negative LC neurons

Because of the mosaic expression of MeCP2 in the female neurons, cells with different genetic backgrounds may contribute unevenly to the overall LC NE-ergic output in s*Mecp2*$^{+/-}$ females, leading to variant responses to the THIP pretreatment. To test this possibility, single-cell PCR (scPCR) was performed to identify the MeCP2 expression in each individual LC cell. In the experiment, a strong negative pressure was applied to the recording pipette for ~10s immediately after the electrophysiological recording. The pipette was then placed in a cold RNAase inhibitor containing buffer solution with the pipette tip carefully broken, followed by PCR test (Fig. 8-2D).

In comparison to the WT cells, both MeCP2-positive and MeCP2-negative LC neurons showed increased firing activity, although the latter appeared slightly higher (Fig. 8-2A-C). Statistically, the firing rate of both was significantly different from WT LC neurons, whereas no significant difference was found between the MeCP2-positive and MeCP2-negative cells (*Mecp2*$^{+/+}$: n = 13; MeCP2-positive: n = 14; MeCP2-negative: n = 11; Fig. 8-2E, Table 2), suggesting that the hyperexcitability of LC neurons may not be determined solely by endogenous MeCP2 expression, and exogenous factors or presynaptic events seem to play a role as well.

To show how the chronic THIP exposure affects hyperexcitability of LC neurons with and without MeCP2 expression, we compared the firing rate of identified LC neurons with respect to MeCP2 expression. The chronic THIP treatment significantly reduced the firing rate of both MeCP2-positive and MeCP2-negative cells in s*Mecp2*$^{+/-}$ mice (*Mecp2*$^{+/+}$: n = 13 and n = 11; MeCP2-positive: n = 14 and n = 11; MeCP2-negative: n = 11 and n = 9; Vehicle and THIP, respectively; Fig. 8-3A, C, Table 2), while in the vehicle control cells from either group remained hyperexcitable (Fig. 8-3B). When the percentage inhibition of LC neuronal firing rate by the THIP exposure was compared, no significant difference was seen between MeCP2-positive cells, MeCP2-negative cells and cells from s*Mecp2*$^{+/-}$ mice without MeCP2 identification (MeCP2-positive: n = 11; MeCP2-negative : n = 9; s*Mecp2*$^{+/-}$: n = 20; Fig. 8-3D). Therefore, the THIP exposure suppressed the excessive firing activity of LC neurons in s*Mecp2*$^{+/-}$ mice to a similar degree in MeCP2-positive and MeCP2-negative cells.

8.3.3 The THIP pretreatment did not change MeCP2 expression in LC neurons of Mecp2$^{+/-}$ mice

To test whether THIP pretreatment alters the MeCP2 expression pattern in LC neurons of *Mecp2*$^{+/-}$ mice, immunocytochemistry was used to visualize the MeCP2 expression. In the LC area, ~70% TH-positive cells showed positive MeCP2 immunoreactivity. The THIP pretreatment for 5 weeks did not change the expression ratio (Vehicle: 4 animals; THIP: 4 animals; Fig. 8-4A,B).

The presence of MeCP2 mRNA was examined with scPCR in individual cells that had undergone electrophysiological studies. The scPCR experiment showed a slightly lower occurrence rate (~60%) of MeCP2-positive cells than immunocytochemistry. This ratio was not enhanced after the 5-week THIP treatment (Vehicle: 2 animals; THIP: 4 animals; Fig. 8-4C). Therefore, the alleviation of the LC neuronal hyperexcitability with THIP pretreatment did not seem to be mediated by increased MeCP2-positive cells in s*Mecp2*$^{+/-}$ mice.

8.3.4 THIP exposure relieved Me5 neuronal hyperexcitability in symptomatic Mecp2$^{+/-}$ mice

It is possible that the THIP exposure improves hyperexcitability in other neurons as well. We have previously found that neurons in the mesencephalic trigeminal nucleus (Me5), located adjacent to the LC nuclei in the brainstem, are hyperexcitable in male *Mecp2*-null mice [53, 56]. Therefore, we chose the Me5 neurons to further examine the THIP effects. Although the Me5 neurons are silent at basal condition in both WT and *Mecp2*-null mice, their excitability can be tested with depolarizing current injections.

With step depolarizing currents the Me5 neurons showed firing activity. When the firing rate was compared, we found that the Me5 neurons in s*Mecp2*$^{+/-}$ mice fired a significantly higher

frequency of action potentials than the cells in WT (*Mecp2*$^{+/+}$) mice (Fig. 8-5A, B). With the comparable current injection, the Me5 neuronal firing rate was significantly higher in s*Mecp2*$^{+/-}$ mice than in WT mice ($P < 0.001$; Fig. 8-5C). The chronic THIP treatment reduced Me5 neuronal hyperexcitability in s*Mecp2*$^{+/-}$ mice ($P < 0.001$, Fig. 8-5D) without affecting the membrane potential and input resistance (Table 1) suggesting that THIP exposure affects excitability of multiple neuronal types in s*Mecp2*$^{+/-}$ mice.

8.3.5 The THIP effect on neuronal excitability was comparable between Mecp2$^{-/Y}$ *and symptomatic Mecp2*$^{+/-}$ *mice*

How do the remaining MeCP2-positive neurons contribute to the THIP effects on neuronal hyperexcitability in the s*Mecp2*$^{+/-}$ mice? To address this question, we compared the THIP effects in the s*Mecp2*$^{+/-}$ mice with those in male *Mecp2*-null mice. Under the *Mecp2*-null condition, spontaneous firing rate of LC neurons was much higher than in the male WT, consistent with previous reports [67, 147]. The neuronal hyperexcitability was significantly reduced with THIP pretreatment compared to the vehicle control (WT: n = 14 and n = 13, *Mecp2*$^{-/Y}$: n = 14 and n = 13; Vehicle and THIP, respectively; Fig. 8-6A). THIP exposure also affected firing activity of Me5 neurons in *Mecp2*-null mice. With comparable current injections, The THIP pretreatment markedly suppressed the evoked firing of Me5 neurons in *Mecp2*-null mice (Vehicle: n = 17, THIP: n = 16; $P < 0.001$; Fig. 8-6B$_2$), whereas there was no significant alteration in WT cells (Vehicle: n = 14, THIP: n = 18; $P > 0.05$; Fig. 8-6B$_1$).

To compare the THIP effects on neuronal excitability between *Mecp2*$^{-/Y}$ and s*Mecp2*$^{+/-}$ mice, the firing rate of these *Mecp2*-defective neurons was normalized to their vehicle control. Chronic THIP exposure reduced the excessive firing of LC neurons by 30% in s*Mecp2*$^{+/-}$ mice,

which was similar to the *Mecp2*$^{-/Y}$ mice (s*Mecp2*$^{+/-}$: n = 22; *Mecp2*$^{-/Y}$: n = 13; $P > 0.05$; Fig. 8-7A$_1$). The reduction in LC neuronal firing activity with the THIP pretreatment made the FR of s*Mecp2*$^{+/-}$ mice similar to that in the WT control, which also resembled *Mecp2*$^{-/Y}$ mice when the data were described as the percentage of the WT levels ($P > 0.05$; Fig. 8-7A$_2$). In Me5 neurons, THIP produced similar levels of reductions in neuronal firing activity in *Mecp2*$^{-/Y}$ and s*Mecp2*$^{+/-}$ mice with 400-500pA injection (s*Mecp2*$^{+/-}$: n = 13; *Mecp2*$^{-/Y}$: n = 17; $P > 0.05$; Fig. 8-7B$_1$). Compared to the WT controls, the degree of the THIP effect was not significantly different between *Mecp2*$^{-/Y}$ and s*Mecp2*$^{+/-}$ mice ($P > 0.05$; Fig. 8-7B$_2$). Therefore, these results suggested that chronic THIP treatment significantly suppressed the neuronal hyperexcitability to the similar degree in *Mecp2*-null and s*Mecp2*$^{+/-}$ mice.

8.3.6 The THIP pretreatment improved breathing in symptomatic Mecp2$^{+/-}$ *mice*

LC neurons are known to play a role in breathing regulation, and the moderation of its hyperexcitation may improve breathing abnormalities. Therefore, we studied breathing activity in plethysmography. In the experiment, 14 s*Mecp2*$^{+/-}$ animals were randomly separated into two groups. One group was pretreated with THIP as described in the Methods and the other was pretreated with regular water as vehicle control. Similarly, 14 *Mecp2*$^{+/+}$ mice were grouped, serving for negative controls. Breathing abnormalities were found in s*Mecp2*$^{+/-}$ mice as significantly higher apnea rate and breathing frequency variation in comparison to their WT counterpart before THIP pretreatment (WT: n = 7 and n = 7, *Mecp2*$^{-/Y}$: n = 7 and n = 7; Vehicle and THIP, respectively; Fig. 8-8). The chronic THIP treatment for 5 weeks abolished the difference between s*Mecp2*$^{+/-}$ and *Mecp2*$^{+/+}$ mice. Such an effect was not seen in the vehicle treated group. Therefore, the THIP pretreatment also alleviated the breathing abnormalities in s*Mecp2*$^{+/-}$ mice.

To compare the 5-week THIP effects on breathing activity between *Mecp2*$^{-/Y}$ and s*Mecp2*$^{+/-}$ mice, the apnea rate and frequency variation were normalized to their vehicle control. THIP reduced the apnea rate by half in s*Mecp2*$^{+/-}$ mice, and 45% in the *Mecp2*$^{-/Y}$ mice. No significant difference was found (s*Mecp2*$^{+/-}$: n = 7; *Mecp2*$^{-/Y}$: n = 8; $P > 0.05$; Fig 8-9A), suggesting THIP pretreatment seems to have similar effects on these two models. Although the relief of in s*Mecp2*$^{+/-}$ mice was significantly lower than the *Mecp2*$^{-/Y}$ ones ($P = 0.016$; Fig 8-9B$_1$), THIP brought the variation to their WT level similarly in both s*Mecp2*$^{+/-}$ and *Mecp2*$^{-/Y}$ mice (s*Mecp2*$^{+/-}$: n = 7; *Mecp2*$^{-/Y}$: n = 8; $P > 0.05$; Fig 8-9B$_2$).

8.4 Discussion

We have shown evidence for increased neuronal excitability in s*Mecp2*$^{+/-}$ mice. In identified LC neurons, the hyperexcitability seems to be determined by not only the MeCP2 expression pattern, but also their environmental cues. The neuronal hyperexcitation is also found in Me5 neurons in the s*Mecp2*$^{+/-}$ mice. Chronic THIP treatment reduced the hyperexcitability of both LC and Me5 neurons in the s*Mecp2*$^{+/-}$ mice, to a similar level as their counterparts in *Mecp2*$^{-/Y}$ mice. The alleviation of LC neuronal hyperexcitability may benefit brainstem autonomic function as THIP also improves breathing abnormalities in s*Mecp2*$^{+/-}$ mice.

8.4.1 Identification of symptomatic females

In comparison to the *Mecp2*-null models, heterozygous *Mecp2*$^{+/-}$ mice recapitulate only some of the RTT-like phenotypes, and show relatively mild symptoms. They usually develop RTT-like symptoms around 6 months of age, which is much later than the *Mecp2*-null mice. The number of mice with clear RTT-like phenotypes is not as high as expected based on the X chromosome

inactivation. According to our previous study, only 15-20% *Mecp2*$^{+/-}$ mice at ages of 1-6 months show breathing abnormalities [107]. These variations in phenotype manifestation, defect severity and symptom onset time complicate the pharmacological intervention to the female models.

A crucial step to approach the female models is to identify the s*Mecp2*$^{+/-}$ mice from the rest. Thus, a scoring system has been used previously [51]. In the present study, we adopted this scoring system with modifications. In addition, we have introduced the second tier of phenotypical identification based on two types of breathing abnormalities. Using this new screening system, we have identified s*Mecp2*$^{+/-}$ mice for our electrophysiological studies in a ratio of approximately one in every three females at age of 6-9 months. Supporting such a phenotype identification procedure are our data showing that LC neurons with negative expression of MeCP2 are hyperexcitable to the same degree as in the s*Mecp2*$^{+/-}$ mice.

8.4.2 Neuronal hyperexcitability in female and male models and the THIP effects

Imbalance in neuronal excitation-inhibition has been found in several brain regions of *Mecp2*-null mice, including the hippocampus, medial prefrontal cortex (mPFC) and brainstem [18, 66, 68, 140, 147, 164, 165, 168, 197, 198]. In the hippocampus, the decreased inhibitory rhythmic activity in hippocampal CA3 circuit makes the cells prone to hyperexcitability [66, 197]. In the cortex, layer 5 pyramidal neurons of the mPFC are hyperexcitable due to the reduced GABAergic input [164]. In the brainstem, neurons in the solitary tract nucleus in the medulla show increased Fos expression associated with increased frequency of spontaneous and miniature EPSCs and increased amplitude of evoked EPSCs in *Mecp2*-null mice [68]. Interestingly, suppression of neuronal hyperexcitability with ketamine, an NMDA receptor antagonist, has been shown to benefit cortical neuronal hypoexcitability [199].

In LC neurons of the *Mecp2*-null mice, we have previously shown that synaptic inhibition mediated by both $GABA_A$-receptors and $GABA_B$-receptors are markedly reduced with inadequate GABA release from presynaptic terminals [10], which may contribute to neuronal hyperexcitability, leading to the consequent defects in the autonomic system. Instability in Me5 neuronal excitability was also reported in *Mecp2*-null mice [53, 56], which may affect proprioception of facial muscles and motor function [200-202], consistent with clinical manifestations of RTT showing defects in chewing, swallowing and teeth grinding [54, 55]. A previous study has shown that selective deletion of *Mecp2* gene in GABAergic neurons recapitulates most of the symptoms as RTT, which indicated the GABA neurotransmission system may be a target to control the neuronal hyperexcitability and consequently alleviate RTT-like symptoms. Indeed, in *Mecp2*-null mice, administration of benzodiazepine or GABA reuptake blocker suppresses breathing defects [12, 13]. In addition, a recent study showed restoration of the *Mecp2* gene in GABAergic neurons rescued some of the RTT-like symptoms substantially not only in *Mecp2*-null, but also *Mecp2*$^{+/-}$ mice [203]. Therefore, GABAergic neurons may be a key to control the excitation/inhibition balance in RTT mouse models. Indeed, we have found that chronic treatment of THIP reduced the LC hyperexcitability and alleviated a series of RTT-like symptoms in *Mecp2*-null mice [83]. With the chronic treatment, the GABAergic inhibition was persistently enhanced, which may result in the alteration of gene expression or functional improvement of the neuronal network, leading to the consequent persistent alleviation of neuronal hyperexcitability and the behavior abnormalities.

8.4.3 MeCP2 expression and potential mechanisms underlying the THIP effects

Although the mechanism is unclear, the X chromosome inactivation has an impact on RTT phenotype development [105]. The large individual variation of RTT symptoms has been

suggested attributable to the nonrandom X inactivation [106]. Another previous study also suggest that the nonrandom X inactivation caused by suppression of mutated paternal allele activation may lead to the milder phenotype clinically [204]. Therefore, altering the X inactivation ratio or the MeCP2 expression pattern in the CNS may be beneficial to the RTT symptoms.

In this study, we have found neuronal hyperexcitability in two types of brainstem neurons in s*Mecp2*$^{+/-}$ mice. The levels of the neuronal hyperexcitability in s*Mecp2*$^{+/-}$ mice in age of 7~10 months are comparable to those in 4~6 week old *Mecp2*-null mice. By grouping cells with or without MeCP2 expression, we have studied both types of LC neurons. Our results indicate that both MeCP2-positive and MeCP2-negative LC neurons show similar levels of hyperexcitability. This finding is a bit surprising as the MeCP2-positive neurons were supposed to be able to manage some of the defects. Although what makes both types of cells hyperexcitable is still unknown, it is reasonable to believe that certain exogenous factors may play a role, including the cellular micro-environments and presynaptic modulation. This suggests that at the cellular level, defects may not be limited to neurons that lack MeCP2 expression in s*Mecp2*$^{+/-}$ mice, while the defects seem to involve both pre- and postsynaptic mechanisms. Supporting the hypothesis is the GABA deficiency found in *Mecp2*-null and *Mecp2*$^{+/-}$ mice [69, 83], which is a significant presynaptic factor to LC neurons [10]. THIP, as the extrasynaptic $GABA_AR$ agonist, may favor the reinstallation of the GABAergic inhibition and lead to the consequent improvement of excitation/inhibition balance in the target cells in RTT mouse models. In addition, consistent with the hypothesis, previous studies have shown that cells expressing mutated *Mecp2* gene in *Mecp2*$^{+/-}$ mice can affect the development of surrounding cells, including those with WT *Mecp2* [109]. Also consistent with the hypothesis are our findings that the high firing rate of both MeCP2-positive and MeCP2-negative cells in s*Mecp2*$^{+/-}$ mice is moderated with THIP pretreatment. The

hypothesis may explain the similar hyperexcitability between MeCP2-negative neurons and unidentified LC cells in s*Mecp2*$^{+/-}$ mice as well, as both MeCP2-positive and MeCP2-negative cells exist in the s*Mecp2*$^{+/-}$ mice, and as both these cells are hyperexcitable.

8.4.4 Therapeutical implications

THIP is currently under clinical trials for Angelman Syndrome, and may be moved to fragile X syndrome soon. As a potential therapeutical drug, THIP in the chronic exposure shows several beneficial effects in RTT models. In addition to counterbalancing neuronal hyperexcitability shown in the present study, we have recently shown that the THIP exposure improves general physical conditions, motor function, social behaviors and lifespan in *Mecp2*-null mice [83]. Although the genetic backgrounds of *Mecp2*-null and *Mecp2*$^{+/-}$ mice are different, their RTT phenotypical manifestations share many similarities. Also similar is the defective GABAergic transmission, which may allow intervention to the GABA system in both models. Indeed, chronic THIP treatment suppressed neuronal hyperexcitability in *Mecp2*$^{+/-}$ mice and alleviated mouse breathing disturbance as in *Mecp2*-null mice. Further studies are needed to evaluate systemically THIP as a potential therapeutic drug, including its effects on motor function, cognition and social behaviors with comparable hormone levels in each individual *Mecp2*$^{+/-}$ mouse as well as pharmacodynamics and pharmacokinetics. In this regard, the understanding of cellular changes in the CNS appears to facilitate the further studies of THIP in animal models of RTT.

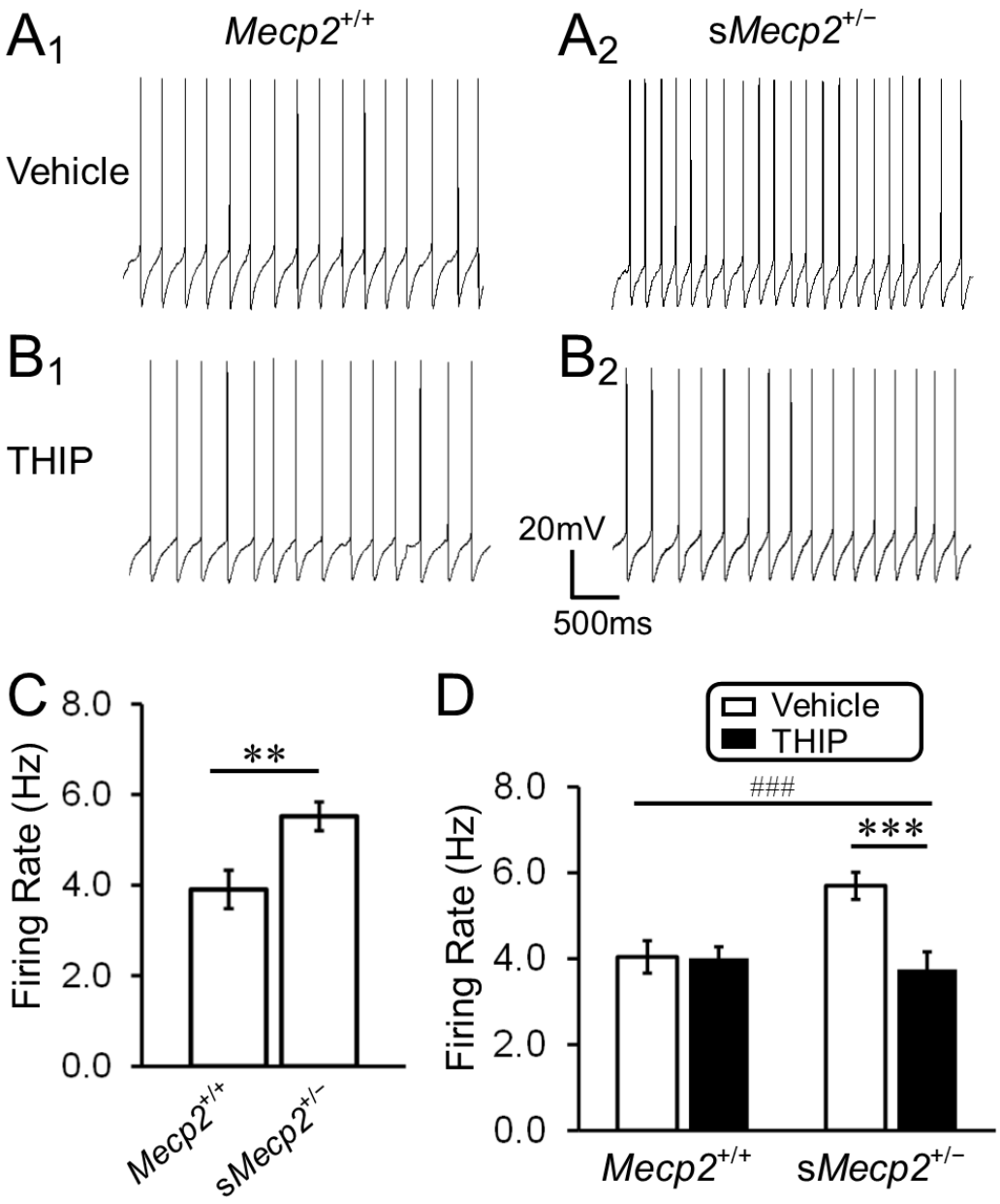

Figure 8- 1. Firing activity of LC neurons in mice after a chronic exposure to THIP or the vehicle.

(A-B) Typical records of spontaneous firing rate in LC neurons from both WT (*Mecp2*$^{+/+}$) and s*Mecp2*$^{+/-}$ mice with and without prior THIP exposure. **(C)** The LC neurons in the s*Mecp2*$^{+/-}$ mice showed significantly higher firing rate than the WT. (*Mecp2*$^{+/+}$: n = 15; s*Mecp2*$^{+/-}$: n = 27; ** $P <$ 0.01; Student's *t*-test) **(D)** The prior THIP exposure significantly reduced the LC neuronal

hyperexcitability in s*Mecp2*$^{+/-}$ mice without any change in the WT. Note that open bars were from Figure 1C. Significant main effect of treatment (F = 11.87, df = 1, $P < 0.001$) and genotype (F = 4.21, df = 1, $P = 0.044$) were observed, as well as the interaction of these two factors (F = 5.92, df = 1, $P = 0.018$). (*Mecp2*$^{+/+}$: n = 15 and n = 11; s*Mecp2*$^{+/-}$: n = 27 and n = 22; Vehicle and THIP, respectively; ### $P < 0.001$; Two-way ANOVA; *** $P < 0.001$; Fisher's LSD post hoc)

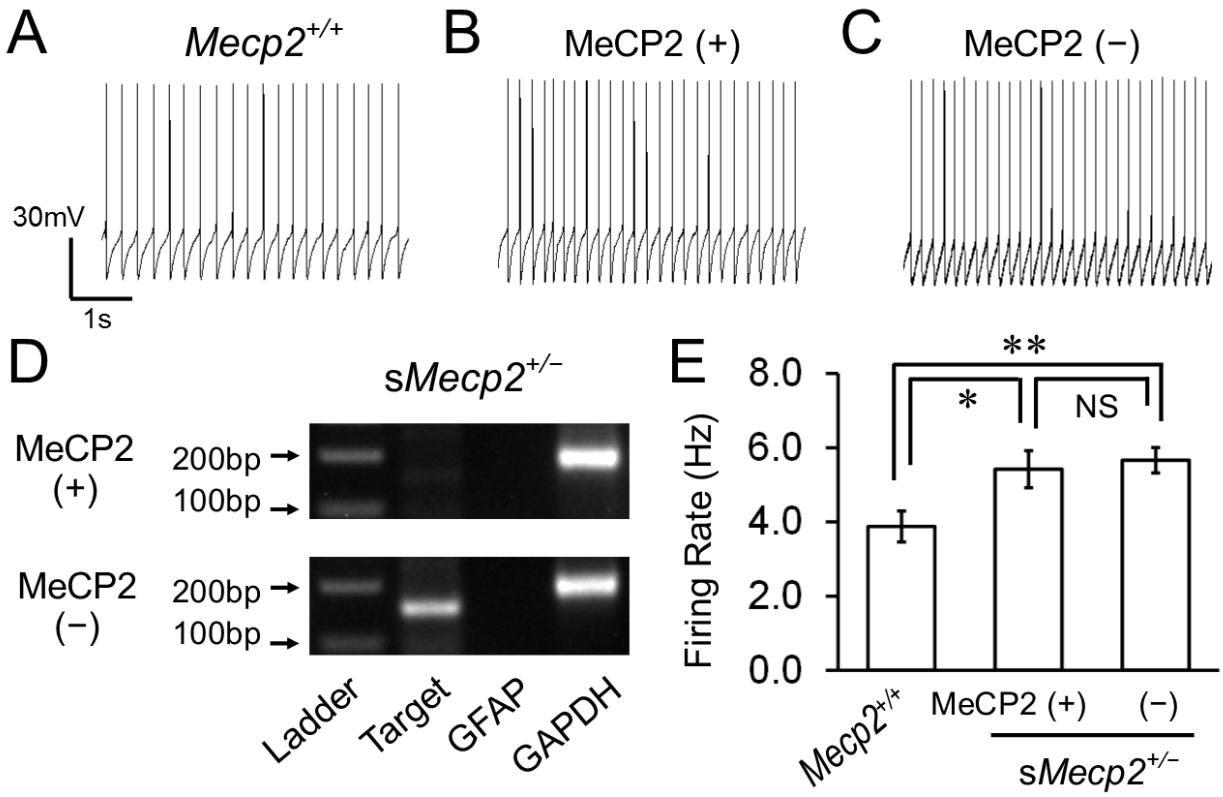

Figure 8- 2. The influence of MeCP2 expression on LC neuronal hyperexcitability in s*Mecp2*$^{+/-}$ mice.

(A-C) Representative records of spontaneous firing rate from WT (*Mecp2*$^{+/+}$), MeCP2 (+) (MeCP2-positve) and MeCP2 (-) (MeCP2-negative) LC neurons. **(D)** The MeCP2 expression pattern in MeCP2-positve and MeCP2-negative LC cells viewed with single cell PCR. **(E)** The firing rate of both MeCP2-positve and MeCP2-negative cells was significantly higher than the WT, whereas no difference was found between these two. (*Mecp2*$^{+/+}$: n = 13; MeCP2+: n = 14; MeCP2-: n = 11; One-way ANOVA; * $P < 0.05$, ** $P < 0.01$; Fisher's LSD post hoc)

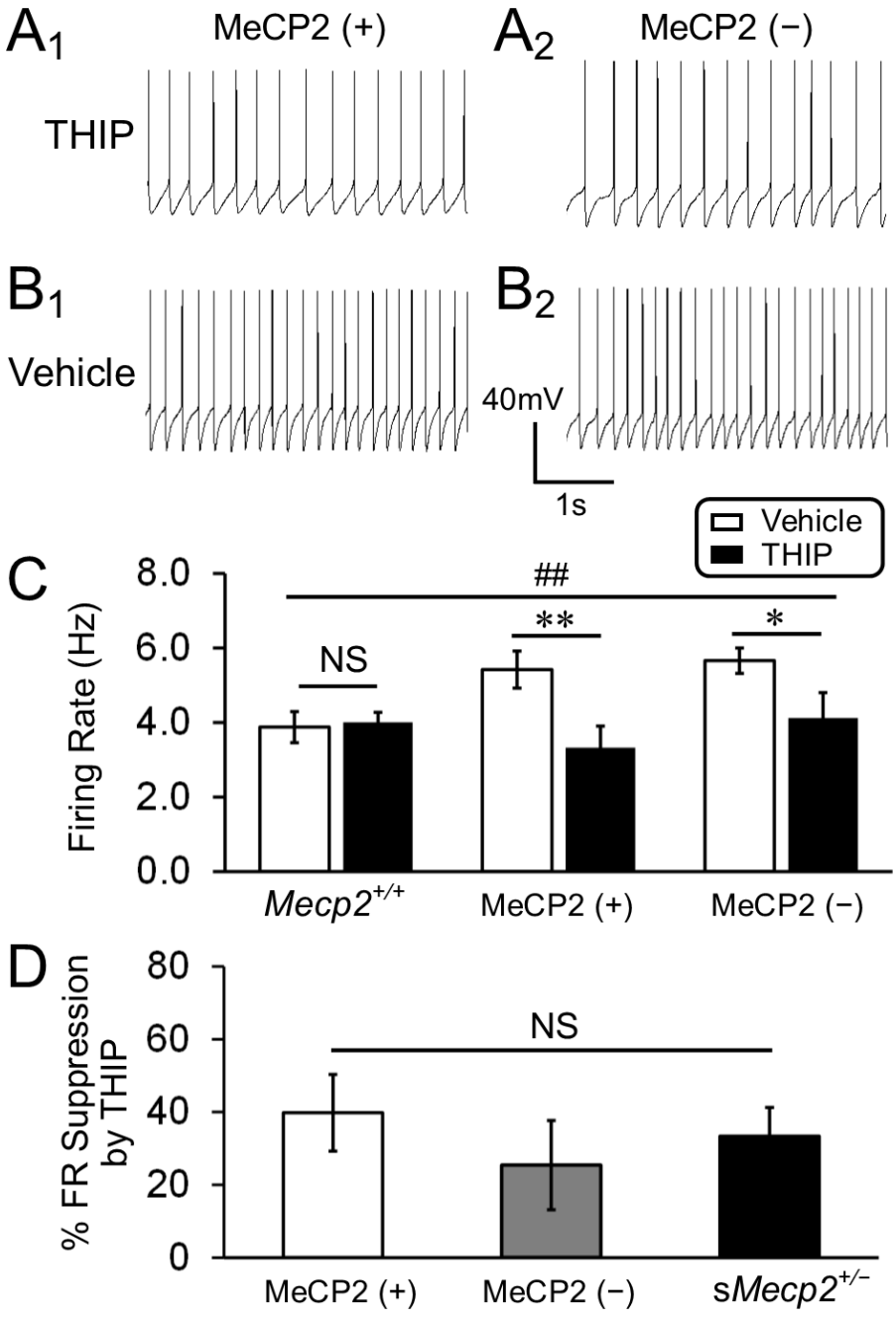

Figure 8- 3. Chronic THIP exposure stabilized hyperexcitability of MeCP2-positve and MeCP2-negative LC cells.

(A-B) Typical records of firing rate from MeCP2-positve and MeCP2-negative LC cells with and without prior THIP exposure. **(C)** The THIP exposure significantly reduced the firing rate of both

MeCP2-positve and MeCP2-negative LC cells without affecting the WT ones. Note that open bars were from Figure 2E. The main effect of treatment was significant (F = 8.81, df = 1, P = 0.004). No significant differences were found in the main effect of genotype (F = 2.27, df = 2, P = 0.112) and the interaction of these two factors was significant (F = 3.10, df = 2, P = 0.052). (*Mecp2*$^{+/+}$: n = 13 and n = 11; MeCP2+: n = 14 and n = 11; MeCP2-: n = 11 and n = 9; Vehicle and THIP, respectively; ## P < 0.01; Two-way ANOVA; * P < 0.05, ** P < 0.01; Fisher's LSD post hoc) **(D)** The THIP effect was compared between LC neurons that were MeCP2-positve, MeCP2-negative and non-identified from s*Mecp2*$^{+/-}$ mice after normalization of their firing rate to that of the vehicle control neuron. No significant difference was seen between these cells. (MeCP2+: n = 11; MeCP2-: n = 9; s*Mecp2*$^{+/-}$: n = 20; P > 0.05; One-way ANOVA)

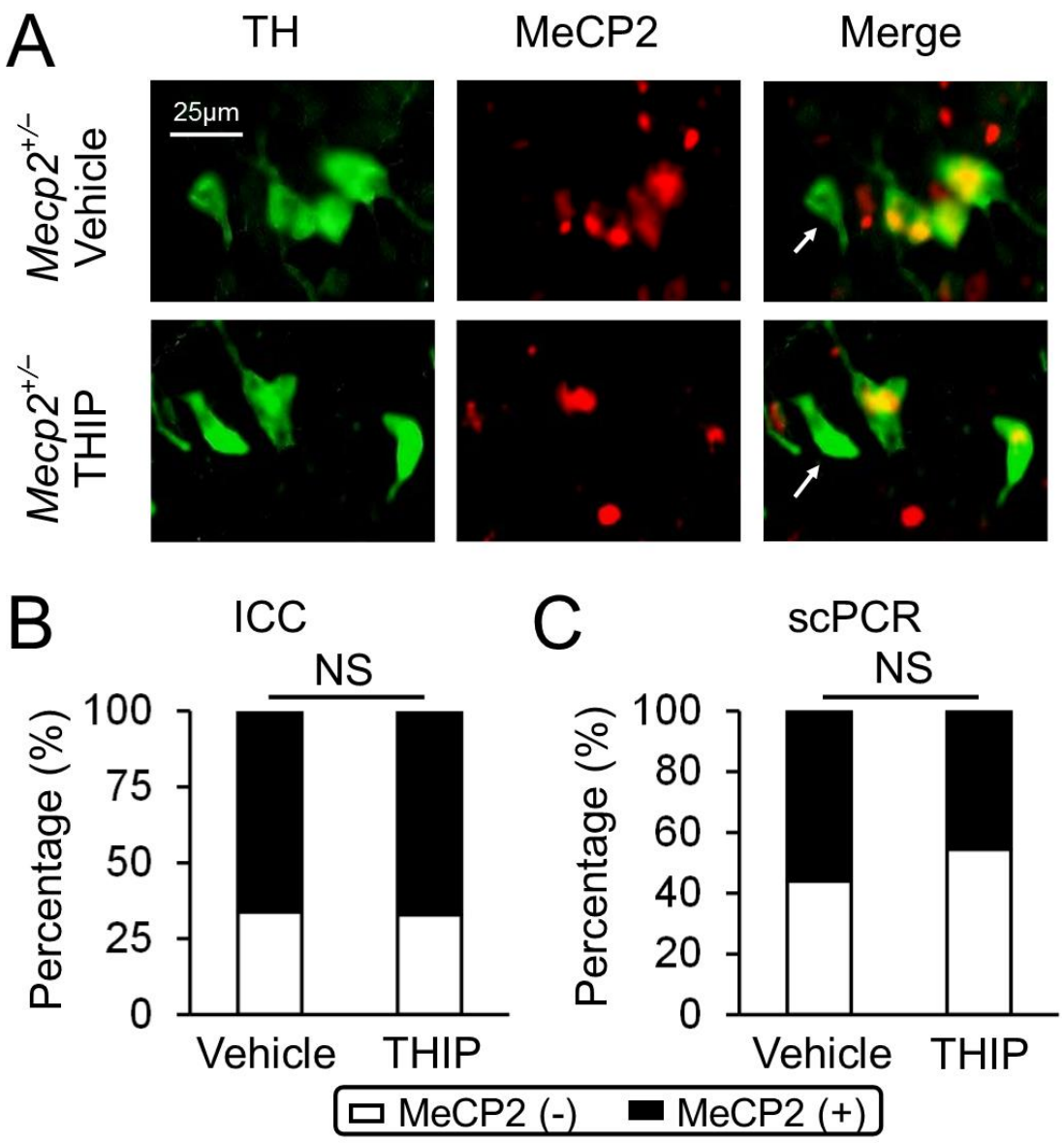

Figure 8- 4. Chronic THIP exposure did not change MeCP2 expression in LC neurons of *Mecp2*$^{+/-}$ mice.

(A) In the immunocytochemistry (ICC) experiment, similar numbers of MeCP2-positve and MeCP2-negative LC cells were seen in s*Mecp2*$^{+/-}$ mice with or without the THIP exposure. **(B)** The ratio of MeCP2-positve vs MeCP2-negative LC cells did not show any statistical significance. (THIP: 4 animals; Vehicle: 4 animals; $P > 0.05$; χ2-test) **(C)** In the single cell PCR (scPCR)

experiment, 14 of 25 cells expressed MeCP2 in *Mecp2*$^{+/-}$ mice and THIP treatment did not significantly change the ratio. (THIP: 4 animals; Vehicle: 2 animals; $P > 0.05$; χ2-test)

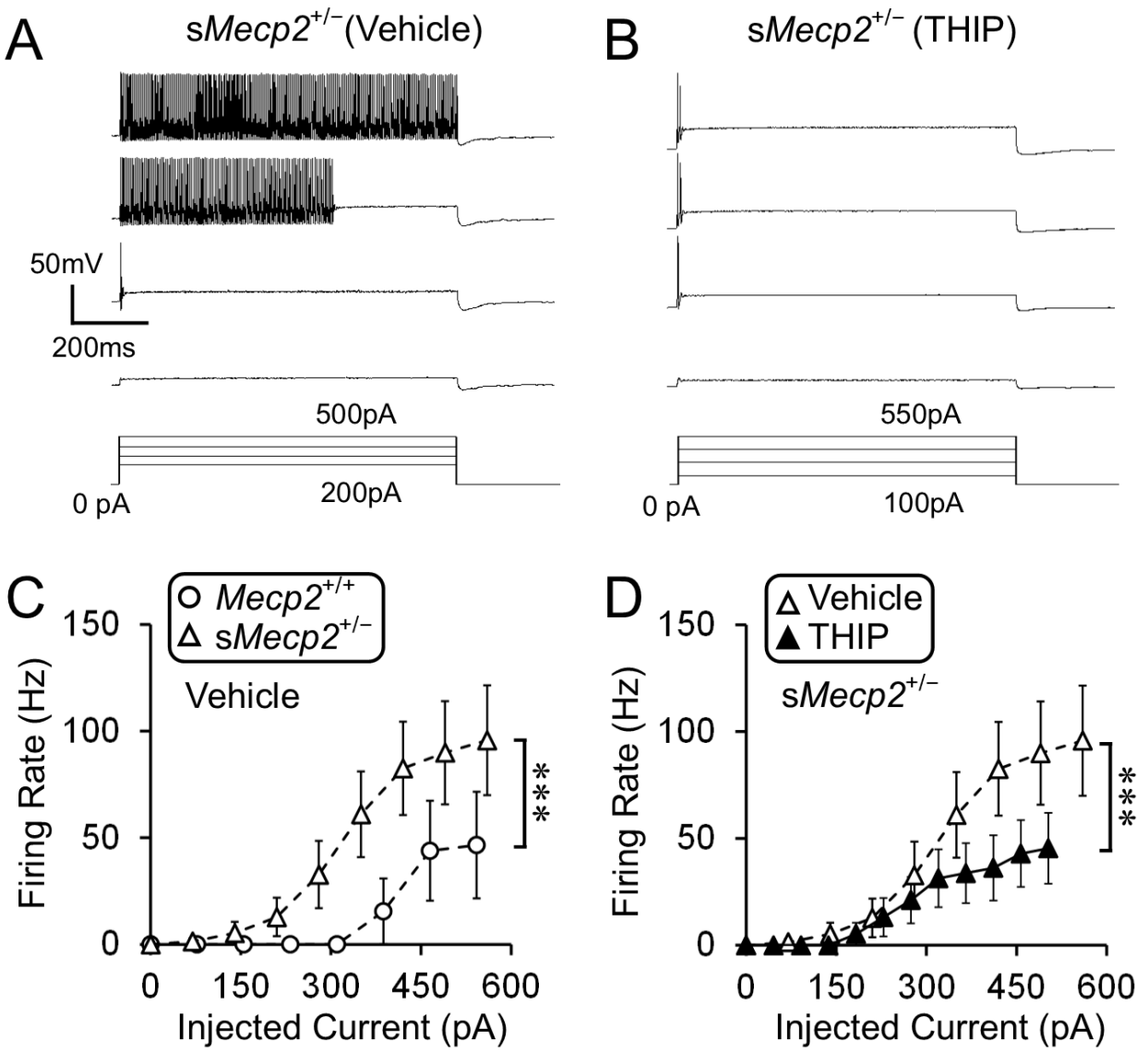

Figure 8- 5. Chronic THIP exposure resumed Me5 neuronal excitability in s*Mecp2*$^{+/-}$ mice.

(A-B) Me5 neurons did not fire action potentials spontaneously. With step depolarizing current injections, most Me5 neurons in s*Mecp2*$^{+/-}$ mice fired multiple action potentials. The THIP exposure diminished the tendency of hyperexcitability. **(C)** With similar amount of current injections, the Me5 neurons in s*Mecp2*$^{+/-}$ mice tended to fire more action potential in comparison to the WT (*Mecp2*$^{+/+}$). **(D)** The THIP administration stabilized the neuronal excitability of Me5 neurons in s*Mecp2*$^{+/-}$ mice compared to the control. (Vehicle: n = 12 and n = 17, THIP: n = 10 and

n = 14, WT and s*Mecp2*$^{+/-}$, respectively; *** $P < 0.001$; Student's *t*-test) **(E-F)** THIP did not affect the resting membrane potential (E) and input resistance (F) of the Me5 cells in both WT and s*Mecp2*$^{+/-}$ mice ($P > 0.05$; Two-way ANOVA)

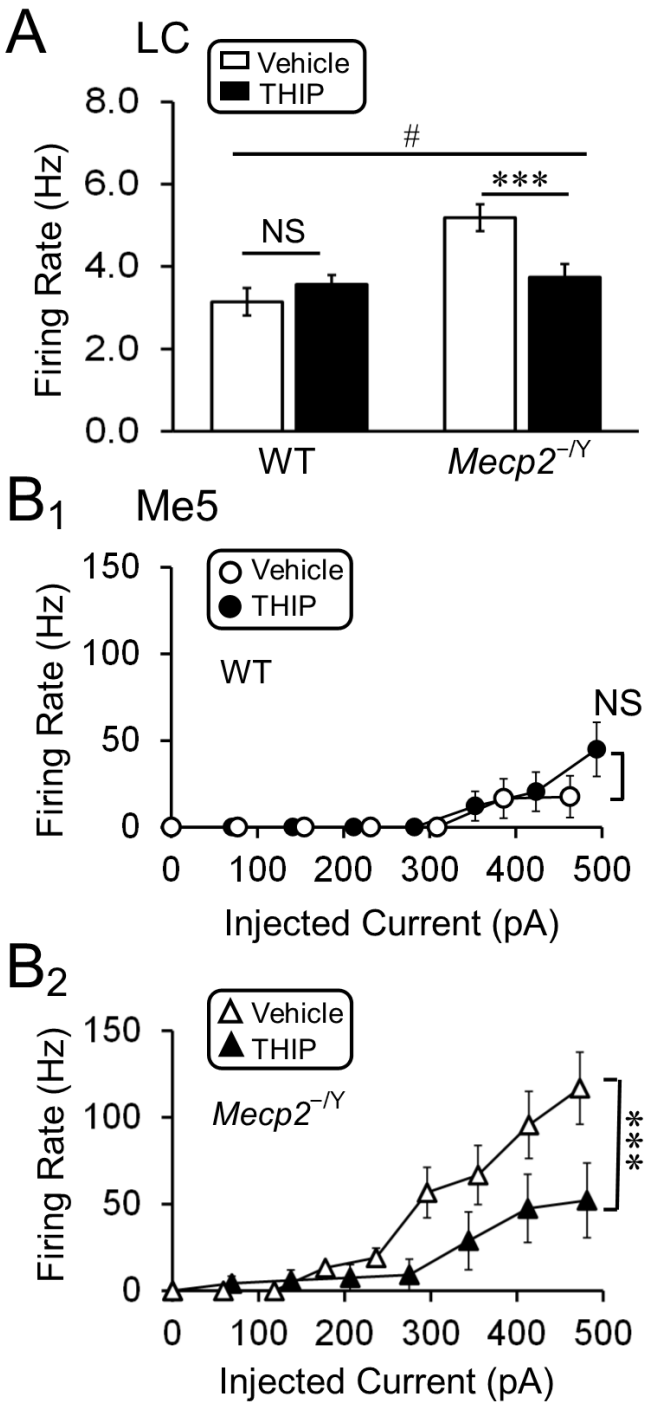

Figure 8- 6. The effect of chronic THIP exposure on neuronal excitability in *Mecp2*$^{-/Y}$ mice.

(A) Chronic THIP exposure significantly diminished the hyperexcitability of LC neurons in *Mecp2*$^{-/Y}$ mice without any significant change in WT ones. Significant differences were found in both main effect of genotype (F = 9.65, df = 1, *P* = 0.003) and treatment (F = 4.44, df = 1, *P* =

0.040). The significant interaction between the two factors (F = 12.27, df = 1, P = 0.001) was shown as well. (WT: n = 14 and n = 13, *Mecp2*$^{-/Y}$: n = 14 and n = 13; Vehicle and THIP, respectively; # $P < 0.05$; Two-way ANOVA; *** $P < 0.001$; Fisher's post hoc) **(B_1-B_2)** In Me5 neurons with comparable current injections, the THIP exposure suppressed the evoked firing in *Mecp2*-null without any significant effect on WT cells. (WT: n = 14 and n = 18; *Mecp2*$^{-/Y}$: n = 17, THIP: n = 16; Vehicle and THIP, respectively; *** $P < 0.001$; Student's *t*-test)

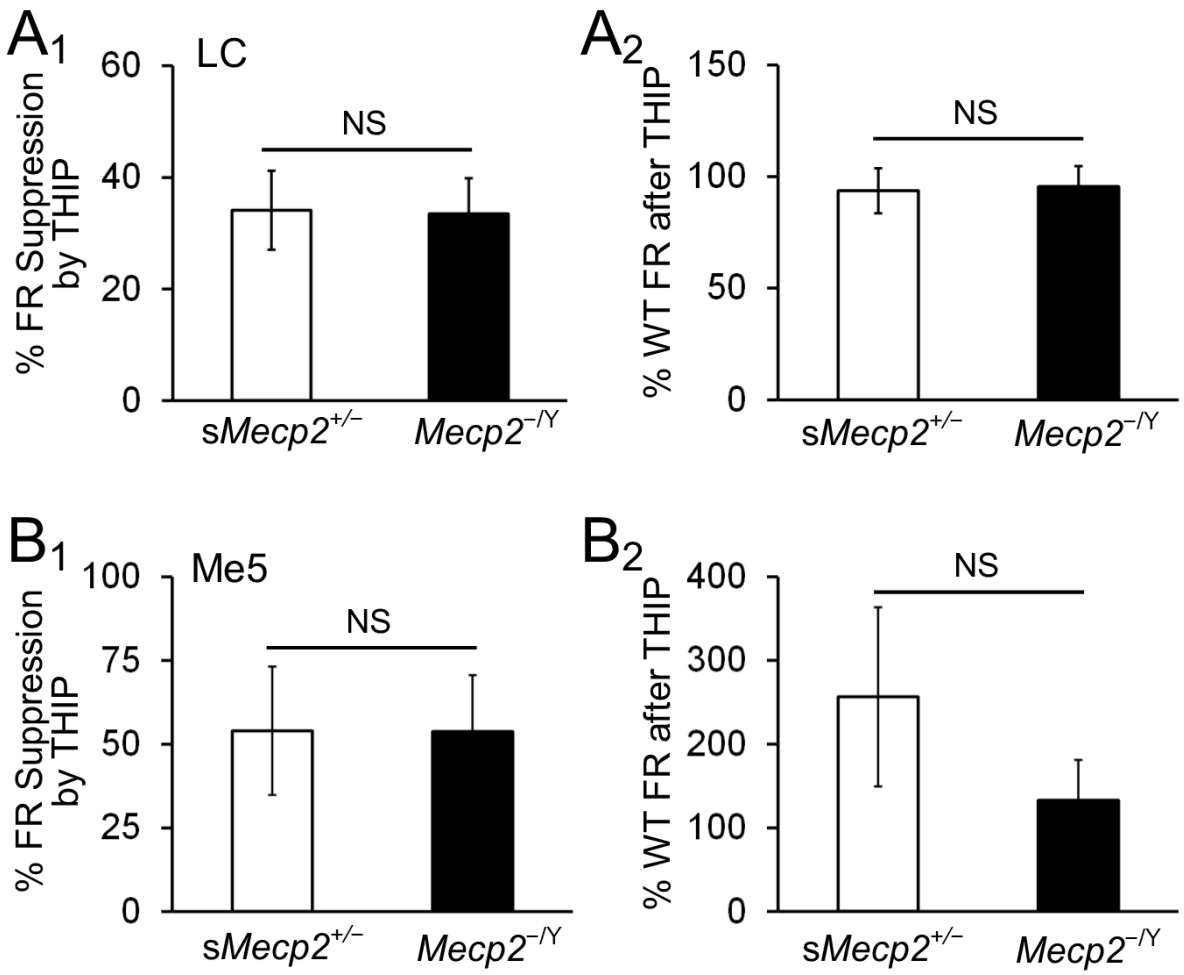

Figure 8- 7. Comparison of THIP effects on neuronal excitability between *Mecp2*$^{-/Y}$ and s*Mecp2*$^{+/-}$ mice.

(A_1-A_2) After normalization to their vehicle control, chronic THIP exposure suppressed the firing rate of LC neurons similarly between *Mecp2*$^{-/Y}$ and s*Mecp2*$^{+/-}$ mice (A_1). Also, THIP brought the firing rate of both *Mecp2*$^{-/Y}$ and s*Mecp2*$^{+/-}$ neurons to their WT level in the mice (A_2) (s*Mecp2*$^{+/-}$: n = 22; *Mecp2*$^{-/Y}$: n = 13). **(B_1-B_2)** With 400~500pA injection, THIP treatment suppressed the firing rate of s*Mecp2*$^{+/-}$ Me5 neurons by 60% after normalizing to the vehicle control, which is similar to the *Mecp2*$^{-/Y}$ ones (B_1). In s*Mecp2*$^{+/-}$ mice, the THIP treatment kept Me5 neurons firing high rate to 256% compared to their WT control with same current injection, but still no difference

was found between the *Mecp2*$^{-/Y}$ and s*Mecp2*$^{+/-}$ mice due to large variations (B_1). (s*Mecp2*$^{+/-}$: n = 13; *Mecp2*$^{-/Y}$: n = 17; $P > 0.05$; Student's *t*-test)

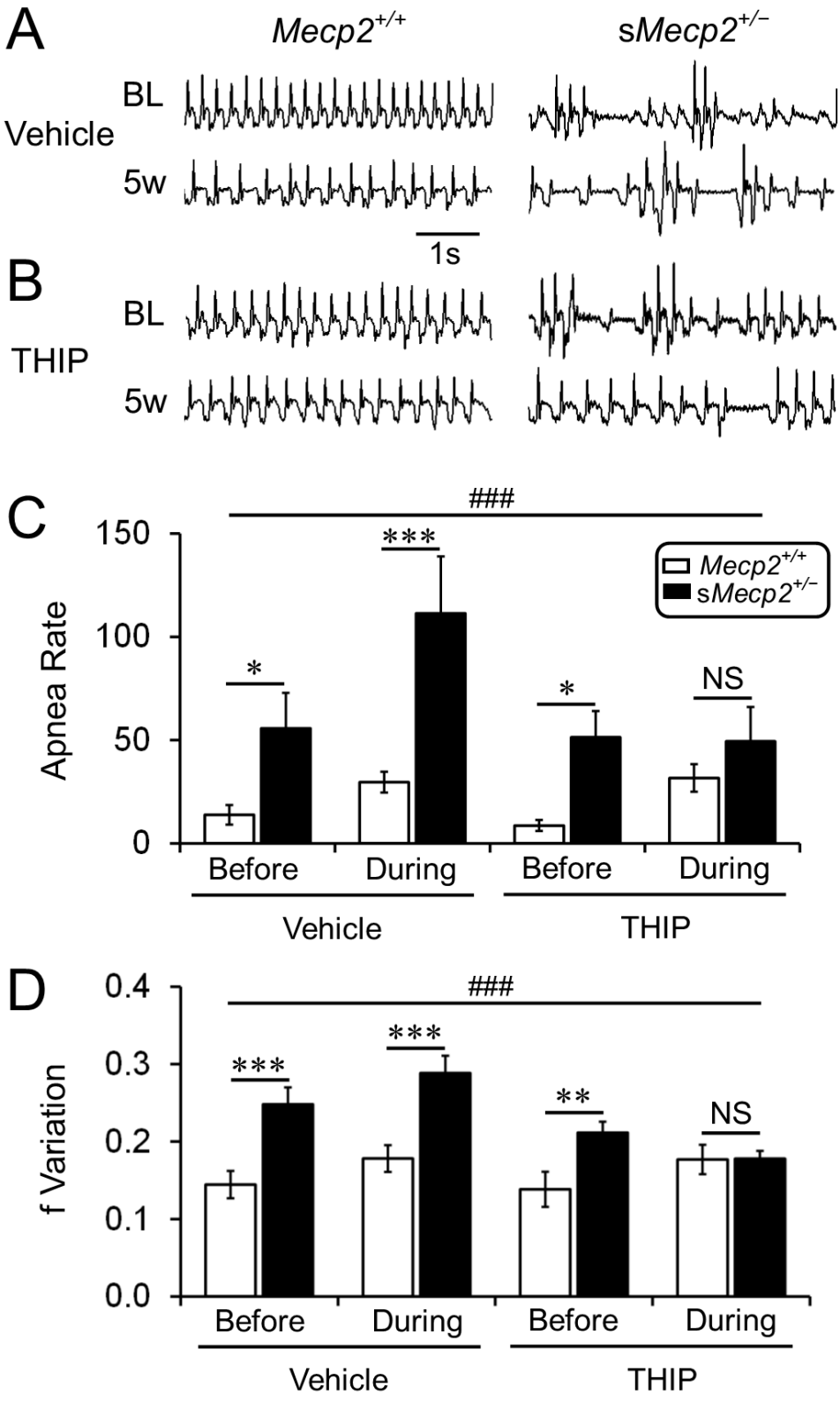

Figure 8- 8. The chronic THIP exposure improved breathing in s*Mecp2*$^{+/-}$ mice.

(A-B) Typical records of breathing activity from both *Mecp2*$^{+/+}$ and s*Mecp2*$^{+/-}$ mice with and without THIP treatment. Inspiration: downdraft. **(C-D)** The s*Mecp2*$^{+/-}$ mice developed severe breathing abnormalities showing high apnea rate (C) and breathing frequency variation (D) compared to their WT (*Mecp2*$^{+/+}$) control. The chronic THIP treatment abolished the difference between s*Mecp2*$^{+/-}$ and WT mice in both apnea rate and f variation. (* $P < 0.05$, ** $P < 0.01$, *** $P < 0.001$; Fisher's LSD post hoc) (C) The main effect of genotype ($F = 21.28$, $df = 1$, $P < 0.001$) and time ($F = 5.37$, $df = 1$, $P = 0.025$) were significant. The main effect of treatment ($F = 3.04$, $df = 1$, $P = 0.088$), interactions of genotype × treatment ($F = 2.51$, $df = 1$, $P = 0.120$), genotype × time ($F = 0.14$, $df = 1$, $P = 0.712$), treatment × time ($F = 1.60$, $df = 1$, $P = 0.212$) or genotype × treatment × time ($F = 2.65$, $df = 1$, $P = 0.110$) were not significant. (### $P < 0.001$; Three-way ANOVA) (D) The main effect of genotype ($F = 30.13$, $df = 1$, $P < 0.001$), treatment ($F = 8.67$, $df = 1$, $P = 0.005$) and interactions of genotype × treatment ($F = 7.11$, $df = 1$, $P = 0.010$) were significant. The main effect of time ($F = 2.25$, $df = 1$, $P = 0.140$), interaction of genotype × time ($F = 1.55$, $df = 1$, $P = 0.219$), treatment × time ($F = 1.73$, $df = 1$, $P = 0.195$) or genotype × treatment × time ($F = 2.25$, $df = 1$, $P = 0.140$) were not significant. (WT: n = 7 and n = 7, *Mecp2*$^{-/Y}$: n = 7 and n = 7; Vehicle and THIP, respectively; ### $P < 0.001$; Three-way ANOVA)

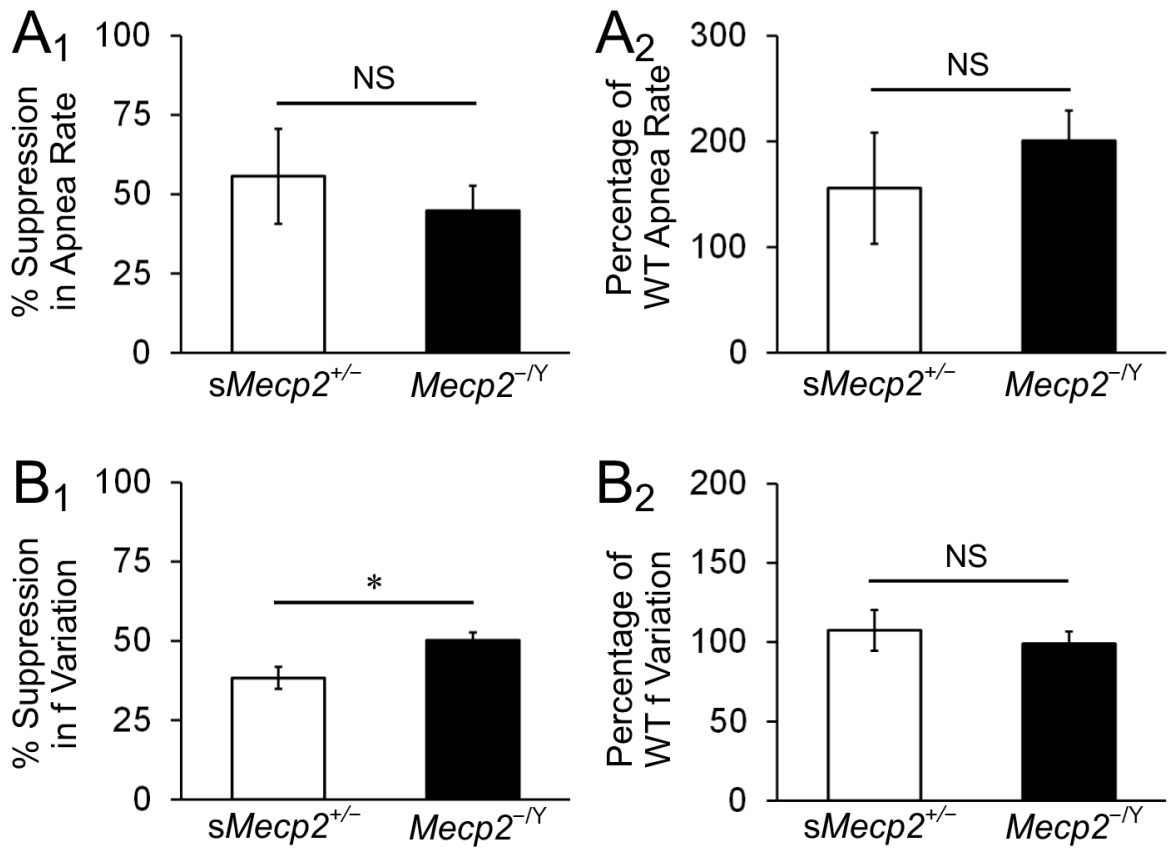

Figure 8- 9. Comparison of THIP effects on breathing activity between *sMecp2*$^{+/-}$ and *Mecp2*$^{-/Y}$ mice.

(A$_1$-A$_2$) THIP reduced the apnea rate of s*Mecp2*$^{+/-}$ mice to ~56% after normalization to their vehicle control, which is not different from the *Mecp2*$^{-/Y}$ (A$_1$). After normalization to their WT control, the THIP effects were similar between s*Mecp2*$^{+/-}$ and *Mecp2*$^{-/Y}$ mice, though it appeared higher in the latter (A$_2$) (s*Mecp2*$^{+/-}$: n = 7; *Mecp2*$^{-/Y}$: n = 8). **(B$_1$-B$_2$)** After normalizing to the vehicle control, the effect of THIP in the f variation of s*Mecp2*$^{+/-}$ mice was reduced by 38%, which is significantly lower than the *Mecp2*$^{-/Y}$ (50%) (B$_1$). THIP treatment made the f variation of s*Mecp2*$^{+/-}$ mice very close to their WT control, which is similar to the *Mecp2*$^{-/Y}$ ones (B$_2$) (s*Mecp2*$^{+/-}$: n = 7; *Mecp2*$^{-/Y}$: n = 8; * $P < 0.05$; Student's *t*-test).

Table 8.1. Effects of chronic THIP treatment on LC and Me5 neurons in *Mecp2*$^{+/+}$ and s*Mecp2*$^{+/-}$ mice.

		Mecp2$^{+/+}$		s*Mecp2*$^{+/-}$	
		Vehicle	THIP	Vehicle	THIP
LC	V_m (mV)	-43.3 ± 0.5 (n = 15)	-43.6 ± 1.7 (n = 11)	-41.9 ± 1.4 (n = 27)	-42.0 ± 0.9 (n = 22)
	R_m (MΩ)	548.4 ± 43.0 (n = 15)	571.2 ± 44.1 (n = 11)	655.9 ± 41.6 (n = 27)	637.7 ± 58.2 (n = 22)
	FR (Hz)	4.0 ± 0.4 (n = 15)	4.0 ± 0.3 (n = 11)	5.7 ± 0.3 (n = 27)	3.8 ± 0.4*** (n = 22)
Me5	V_m (mV)	-51.0 ± 1.2 (n = 12)	-52.8 ± 1.6 (n = 10)	-54.2 ± 1.2 (n = 16)	-51.6 ± 4.1 (n = 14)
	R_m (MΩ)	141.5 ± 37.6 (n = 12)	187.6 ± 54.4 (n = 10)	220.4 ± 34.3 (n = 16)	286.5 ± 47.5 (n = 14)

LC, locus coeruleus; Me5, mesencephalic trigeminal V; V_m, membrane potential; R_m, input resistance; FR, firing rate. Data are shown as means ± SE; n, number of cells; *** $P < 0.001$ compared between treatment.

Table 8.2 THIP effects on LC neurons with and without MeCP2 expression

LC	*Mecp2*$^{+/+}$		MeCP2-positive		MeCP2-negative	
	Vehicle	THIP	Vehicle	THIP	Vehicle	THIP
V_m (mV)	-43.4 ± 0.5 (n = 13)	-43.6 ± 1.7 (n = 11)	-41.8 ± 2.1 (n = 14)	-41.7 ± 1.1 (n = 11)	-41.6 ± 2.4 (n = 11)	-42.5 ± 1.6 (n = 9)
R_m (MΩ)	563.9 ± 46.4 (n = 13)	571.2 ± 44.1 (n = 11)	678.0 ± 56.3 (n = 14)	632.4 ± 99.5 (n = 11)	637.5 ± 75.1 (n = 11)	653.1 ± 80.4 (n = 9)
FR (Hz)	3.9 ± 0.4 (n = 13)	4.0 ± 0.3 (n = 11)	5.4 ± 0.5 (n = 14)	3.3 ± 0.6** (n = 11)	5.7 ± 0.3 (n = 11)	4.1 ± 0.7* (n = 9)

V_m, membrane potential; R_m, input resistance; FR, firing rate. ** $P < 0.01$, * $P < 0.05$ compared between treatment.

9 General discussions

9.1 THIP administration

9.1.1 Administration protocols

RTT patients and mouse models start to develop symptoms a period after birth. In *Mecp2*$^{-/Y}$ mice, breathing disorders start at 2-3 weeks after birth, and defects in motor and social behaviors begin at 4-6 weeks. Pharmacological intervention before symptom manifestation in these RTT animals may prevent further development of the symptoms. To achieve such a goal, appropriate targets need to be found. The existence of extrasynaptic GABARs in the CNS enables such early intervention with respect to their spatial and temporal variations in subunit expressions, especially the δ subunit [80]. Thus, we chose to deliver THIP to the test animals starting from the date when they were born and continued the treatment till P53 in this study. With such treatment, our results show beneficial effects of THIP on RTT-like behaviors which might come from the early intervention by preventing the development of the neuronal defects. Indeed, the LC biosynthesis function was reinstalled and the THIP effects persisted one week after withdrawal, which indicated early treatment of THIP might innervate the gene expressions in the CNS of RTT mice, leading to the beneficial effects.

In this study, THIP was also delivered to the animals after RTT-like breathing difficulties appearance, and the symptom was alleviated as well. This is consistent with the idea that THIP directly benefits neuronal excitability. Besides, in *Mecp2*$^{+/-}$ mice, most of the RTT-like symptoms show up after 6 months of age, and the symptoms vary between individuals, which makes the treatment in female RTT models quite complicated. Therefore, the identification of symptomatic *Mecp2*$^{+/-}$ animals becomes necessary. In our results, five weeks continuous THIP

treatment after symptoms were identified alleviated the breathing activities in s*Mecp2*$^{+/-}$ animals by suppressing the neuronal hyperexcitability, regardless of *Mecp2* mosaic expression pattern [205]. Therefore, chronic treatment of THIP seems to be able to correct neuronal abnormalities, leading to the alleviation of symptoms. Meanwhile, early intervention may reinstall the normal neuronal activity, which benefits the RTT animals as well.

9.1.2 Pharmacokinetics

THIP is a structural analog of GABA, which enables activation of extrasynaptic $GABA_A$ receptors, specific for those containing the δ subunit. As an investigational drug, THIP was originally developed as an analgesic and anxiolytic, and put in the clinical trials to treat insomnia. Tested as a potential clinical medicine, the pharmacokinetics of THIP has been well studied in multiple species, including mouse, rat, dogs and human [181-184]. In rats, subcutaneously injection of 2.5, 5 and 10 mg/kg THIP rapidly entered the CNS with a peak in the range of 0.7 to 3 μM. A preclinical study in mice, rats, and humans using ^{14}C-labelled THIP showed a rapid absorption of THIP with the highest concentration in the kidney, and the peak concentration reached within 0.5 h in several organs including the brain. Three different metabolites were detected, of which glucuronic acid conjugated THIP seems to be the main one [184]. Although THIP has a characteristic short half-life, chronic treatment of THIP may allow it to be accumulated in the plasma and CNS to keep a constant and effective therapeutical concentration. Another clinic report on postural sway treatment indicated that THIP reached the maximum plasma concentration ~140ng/ml in 2.0 h in elderly humans with a daily dose of 10 mg, and the half-life is 1.7 h [181]. Our preliminary studies suggested that 20 mg/kg THIP orally reached plasma concentration around 3 nM in mice. THIP started to have effects within 0.5 h

after i.p. delivery, while chronic treatment remained a reasonable level in the plasma in test animals.

9.1.3 Potential side effects

THIP was withdrawal in the clinical trials of insomnia treatment, due to the less efficacy and potential adverse effects. Indeed, THIP has been tested in over 3,000 patients with various dosages, (such as 10~120mg/day), among which some cases were reported with side effects at high doses of THIP, including sedation, confusion, dizziness and even hallucination [135]. However, high dosage treatment with synaptic GABAR agonists, such as barbiturate and benzodiazepine, may lead to the severer adverse effects, including breathing suppression, coma and death. THIP thus provides a relatively safer alternative, although further studies are still needed. The unsatisfactory efficacy for insomnia might be good for THIP application to RTT as the unnecessary sedative effects may be avoided. A report indicated THIP appeared to be more effective on women than man (44), which seems to be good for RTT treatment when considering the female dominance of the disease.

In our study, the calculated dosage used in mice is 6.3 ± 0.4 mg/kg/day, which is similar to that in several previous studies of Fragile X syndrome and Angelman Syndrome in mice. No obvious side effects were reported before. Our test of spontaneous locomotion supports the non-sedative effects of the dosage. THIP has been under clinical trials for Angelman Syndrome by Ovid Therapeutics and preclinical study for Fragile X syndrome since 2015. RTT shares multiple similarities with these rare diseases, such as impaired GABA system, neuronal hyperexcitability, and autism-like behaviors. Therefore, the information obtained in the present study seems likely to favor moving the drug for clinical trials.

9.2 Homeostasis between neuronal excitability and metabolic synthesis

In LC neurons, NE is synthesized from tyrosine by a series of enzymes, including TH and DBH, and released with from vesicles into the synaptic cleft. The homeostasis between the LC neuronal excitability and the NE synthesis ensures the constant production and release of NE. Although increased firing rate of LC neurons may augment the NE level in the synaptic cleft by increasing the NE releasing frequency, persistent LC neuronal hyperexcitability may interrupt this balance between NE synthesis and release, and lead to impairment of the NE system. Such an idea was confirmed by a recent report in our lab that further stimulation of LC terminals failed to improve the modulation of hypoglossal neurons in the *Mecp2*$^{-/Y}$ brainstem [115]. Also, previous studies suggest that the TH and DBH expression levels are drastically reduced in *Mecp2*$^{-/Y}$ LC neurons [6, 50], consistent with the breathing disorders onset and development in our study. Meanwhile, our results also showed that in *Mecp2*$^{-/Y}$ mice, LC neuronal excitability increased with age and proportionally with the severity of breathing abnormalities. Thus, the defects in LC neuronal excitability may play a role in the deterioration of NE synthesis and the consequent development of the RTT-like symptoms in the mouse models. A moderation of neuronal hyperexcitability by THIP, or other GABAR agonists, may enable LC cells to correct or reinstall the homeostasis of NE synthesis/release, beneficial for the NE modulation of a variety of systems and functions in the CNS, in consideration of the broadcast LC-NE projections, such as to cortex, cerebellum and medulla [12, 27, 50, 83]. The enhanced TH and DBH expression with THIP treatment in our results supports the homeostasis-rebuilt idea.

9.3 Potential compensation in GABAR system of LC area

Previous studies have shown that selective knockout of *Mecp2* gene in GABAergic neurons leads to a series of RTT-like phenotypes [11], suggesting the necessity and importance of GABA systems in the development of the disease. In patients with RTT and mouse models, the GABAergic inhibition was significantly suppressed showing global reductions in GABA level and GABARs expressions. In *Mecp2*$^{-/Y}$ LC, the subunit combinations of GABA receptors were altered. Both synaptic $GABA_AR$s and $GABA_B$ receptors were significantly reduced in *Mecp2*$^{-/Y}$ mice, whereas the extrasynaptic $GABA_AR$s level were increased as shown in this study. The enhanced extrasynaptic $GABA_AR$ mediated tonic inhibition might work as a neuroadaptive process to compensate the insufficient GABA synaptic input. Indeed, such compensation has been reported in other regions of CNS. In *Mecp2*$^{-/Y}$ Me5 nuclei, the alteration of the subunits leads to the changes in the fast Na^+ voltage-gated current and the consequent neuronal hyperexcitability. The reduced hyperpolarization-activated h current, resulting in smaller sag and PIR, may compensate the neuronal hyperexcitability [53]. Therefore, the compensatory mechanism may make the animals or patients with RTT viable with milder phenotypes despite the *Mecp2* deficiency. In addition, our results suggest that the hyperexcitability of LC neurons leads to the reduced NE biosynthesis, although we cannot exclude the possibility that the excessive firing of the neurons was the compensatory results from the reduced metabolic function of the LC neurons.

9.4 Impact of global enhancing the GABAergic inhibition

Imbalanced inhibition/excitation ration was considered one of the mechanism leading to the development of a series psychiatry disease, such as schizophrenia and fragile X syndrome. The imbalanced inhibition/excitation ration might be one of the mechanism in the development

of RTT. The *Mecp2* disruption causes the global deficiency of GABA and the consequent imbalance of excitation/inhibition, leading to the hyperexcitation or hyperactivity in central neurons. However, Kron et al. have shown that neuronal hypoexcitation occurs in the forebrain and midbrain, including PFC, somatosensory, auditory and motor cortices, which may affect stereotyped and repetitive behaviors consistent with the current observations of several RTT-like symptoms [206]. Meanwhile, neurons in the brainstem are mostly hyperexcited, especially the neurons in the respiratory centers, including LC and nTS [68]. Although accumulating evidence supports the beneficial effects of enhancing the GABAergic inhibition, its effect on the neuronal hypoexcitability needs to be considered. Would the global GABAergic augmentation cause adverse outcomes on some regions of the CNS? Available evidence suggests that enhancing the GABAergic inhibition ameliorated the hypoexcitability in forebrain as well. A previous study found that ketamine, the NMDA receptors antagonist, reversed the neuronal hypoactivity caused by *Mecp2* deficiency via NMDA receptors, and improved the associated behaviors [68, 120]. This may be produced by disinhibition in the local network involving cortical pyramidal cells, so that reducing the glutamatergic excitation may restore this disinhibitory circuit function [125]. In this regard, it is possible that a global enhancement of the GABAergic inhibition may benefit the hypoexcitability of certain forebrain neurons and associated motor function and social behaviors similarly as ketamine does in *Mecp2*-null mice on. Furthermore, the glutamatergic excitation is elevated in *Mecp2*-null mice, which shifts the ratio to the excitatory side as well, leading to the region specific neuronal abnormality or disturbed network activity in the CNS of RTT. The global enhanced GABAergic inhibition may compensate the upregulation of excitatory glutamatergic regulation, leading to the amelioration of RTT-like symptoms.

9.5 Conclusion

In *Mecp2*$^{-/Y}$ mice, extrasynaptic $GABA_AR$-ergic tonic inhibition is retained in LC neurons and increased significantly, likely to be due to the overexpression of the $GABA_AR$ species containing the δ subunit. The presence of these δ containing extrasynaptic $GABA_ARs$ in *Mecp2*$^{-/Y}$ mice allows a control of neuronal excitability with specific agonists. Early-life exposure to THIP, an agonist specific to δ containing extrasynaptic $GABA_ARs$, extends the lifespan of *Mecp2*$^{-/Y}$ mice, reduces breathing disorders and motor dysfunction, and improves social behaviors. Such effects persist for at least one week after THIP withdrawal. The beneficial effects are likely to be due to the stabilization of neuronal hyperexcitability of both LC and Me5 neurons by THIP in mouse models of RTT without major effects on the neuronal intrinsic membrane properties. The expression of NE biosynthesis enzymes was also improved in *Mecp2*$^{-/Y}$ LC neurons. In identified LC neurons regarding their MeCP2 expression in s*Mecp2*$^{+/-}$ mice, the hyperexcitability seems to be determined by not only the MeCP2 expression but also their environmental cues. Chronic treatment of THIP suppressed hyperexcitability of both neurons with and without the MeCP2 expression. Such a phenomenon seems to contribute to the relief of breathing disorders.

Therefore, the extrasynaptic $GABA_AR$ agonist THIP in low dose with chronic exposure appears beneficial for symptom relief in RTT models, and seems to be a promising candidate for potential therapeutical intervention to RTT.

REFERENCES

1. Chahrour, M. and H.Y. Zoghbi, *The story of Rett syndrome: from clinic to neurobiology.* Neuron, 2007. **56**(3): p. 422-37.
2. Robinson, L., et al., *Morphological and functional reversal of phenotypes in a mouse model of Rett syndrome.* Brain, 2012. **135**(Pt 9): p. 2699-710.
3. Lioy, D.T., W.W. Wu, and J.M. Bissonnette, *Autonomic dysfunction with mutations in the gene that encodes methyl-CpG-binding protein 2: insights into Rett syndrome.* Auton Neurosci, 2011. **161**(1-2): p. 55-62.
4. Zhang, X., et al., *Intrinsic membrane properties of locus coeruleus neurons in Mecp2-null mice.* Am J Physiol Cell Physiol, 2010. **298**(3): p. C635-46.
5. Zoghbi, H.Y., et al., *Reduction of biogenic amine levels in the Rett syndrome.* N Engl J Med, 1985. **313**(15): p. 921-4.
6. Zhang, X., et al., *Pontine norepinephrine defects in Mecp2-null mice involve deficient expression of dopamine beta-hydroxylase but not a loss of catecholaminergic neurons.* Biochem Biophys Res Commun, 2010. **394**(2): p. 285-90.
7. Ide, S., M. Itoh, and Y. Goto, *Defect in normal developmental increase of the brain biogenic amine concentrations in the mecp2-null mouse.* Neurosci Lett, 2005. **386**(1): p. 14-7.
8. Zhang, X., et al., *The disruption of central CO2 chemosensitivity in a mouse model of Rett syndrome.* Am J Physiol Cell Physiol, 2011. **301**(3): p. C729-38.
9. Viemari, J.C., et al., *Ret deficiency in mice impairs the development of A5 and A6 neurons and the functional maturation of the respiratory rhythm.* Eur J Neurosci, 2005. **22**(10): p. 2403-12.
10. Jin, X., et al., *GABAergic synaptic inputs of locus coeruleus neurons in wild-type and Mecp2-null mice.* Am J Physiol Cell Physiol, 2013. **304**(9): p. C844-57.
11. Chao, H.T., et al., *Dysfunction in GABA signalling mediates autism-like stereotypies and Rett syndrome phenotypes.* Nature, 2010. **468**(7321): p. 263-9.
12. Abdala, A.P., et al., *Correction of respiratory disorders in a mouse model of Rett syndrome.* Proc Natl Acad Sci U S A, 2010. **107**(42): p. 18208-13.
13. Voituron, N. and G. Hilaire, *The benzodiazepine Midazolam mitigates the breathing defects of Mecp2-deficient mice.* Respir Physiol Neurobiol, 2011. **177**(1): p. 56-60.
14. Jin, X., W. Zhong, and C. Jiang, *Time-dependent modulation of GABA(A)-ergic synaptic transmission by allopregnanolone in locus coeruleus neurons of Mecp2-null mice.* Am J Physiol Cell Physiol, 2013. **305**(11): p. C1151-60.
15. Calfa, G., et al., *Excitation/inhibition imbalance and impaired synaptic inhibition in hippocampal area CA3 of Mecp2 knockout mice.* Hippocampus, 2014.

16. Dani, V.S., et al., *Reduced cortical activity due to a shift in the balance between excitation and inhibition in a mouse model of Rett syndrome.* Proc Natl Acad Sci U S A, 2005. **102**(35): p. 12560-5.

17. El-Khoury, R., et al., *GABA and glutamate pathways are spatially and developmentally affected in the brain of Mecp2-deficient mice.* PLoS One, 2014. **9**(3): p. e92169.

18. Medrihan, L., et al., *Early defects of GABAergic synapses in the brain stem of a MeCP2 mouse model of Rett syndrome.* J Neurophysiol, 2008. **99**(1): p. 112-21.

19. Sigel, E. and M.E. Steinmann, *Structure, function, and modulation of GABA(A) receptors.* J Biol Chem, 2012. **287**(48): p. 40224-31.

20. Brickley, S.G. and I. Mody, *Extrasynaptic GABA(A) receptors: their function in the CNS and implications for disease.* Neuron, 2012. **73**(1): p. 23-34.

21. Amir, R.E., et al., *Rett syndrome is caused by mutations in X-linked MECP2, encoding methyl-CpG-binding protein 2.* Nat Genet, 1999. **23**(2): p. 185-8.

22. Percy, A.K., et al., *Rett syndrome: North American database.* J Child Neurol, 2007. **22**(12): p. 1338-41.

23. Neul, J.L., et al., *Rett syndrome: revised diagnostic criteria and nomenclature.* Ann Neurol, 2010. **68**(6): p. 944-50.

24. Chahrour, M., et al., *MeCP2, a key contributor to neurological disease, activates and represses transcription.* Science, 2008. **320**(5880): p. 1224-9.

25. Young, J.I., et al., *Regulation of RNA splicing by the methylation-dependent transcriptional repressor methyl-CpG binding protein 2.* Proc Natl Acad Sci U S A, 2005. **102**(49): p. 17551-8.

26. Guy, J., et al., *A mouse Mecp2-null mutation causes neurological symptoms that mimic Rett syndrome.* Nat Genet, 2001. **27**(3): p. 322-6.

27. Zhong, W., et al., *Effects of early-life exposure to THIP on brainstem neuronal excitability in the Mecp2-null mouse model of Rett syndrome before and after drug withdrawal.* Physiol Rep, 2017. **5**(2).

28. Bienvenu, T., et al., *Spectrum of MECP2 mutations in Rett syndrome.* Genet Test, 2002. **6**(1): p. 1-6.

29. Johnson, C.M., et al., *Defects in brainstem neurons associated with breathing and motor function in the Mecp2R168X/Y mouse model of Rett syndrome.* Am J Physiol Cell Physiol, 2016. **311**(6): p. C895-C909.

30. Chao, H.T., H.Y. Zoghbi, and C. Rosenmund, *MeCP2 controls excitatory synaptic strength by regulating glutamatergic synapse number.* Neuron, 2007. **56**(1): p. 58-65.

31. Wu, Y., et al., *Characterization of Rett Syndrome-like phenotypes in Mecp2-knockout rats.* J Neurodev Disord, 2016. **8**: p. 23.

32. Veeraragavan, S., et al., *Loss of MeCP2 in the rat models regression, impaired sociability and transcriptional deficits of Rett syndrome.* Hum Mol Genet, 2016. **25**(15): p. 3284-3302.

33. Patterson, K.C., et al., *MeCP2 deficiency results in robust Rett-like behavioural and motor deficits in male and female rats.* Hum Mol Genet, 2016. **25**(15): p. 3303-3320.

34. Samaco, R.C., et al., *Female Mecp2(+/-) mice display robust behavioral deficits on two different genetic backgrounds providing a framework for pre-clinical studies.* Hum Mol Genet, 2013. **22**(1): p. 96-109.

35. *Specialized medical education in the European Region. EURO Reports and Studies 112.* EURO Rep Stud, 1989(112): p. 1-256.

36. Jiang, C., et al., *Breathing abnormalities in animal models of Rett syndrome a female neurogenetic disorder.* Respir Physiol Neurobiol, 2016.

37. Naidu, S., et al., *Clinical variability in Rett syndrome.* J Child Neurol, 2003. **18**(10): p. 662-8.

38. Herrera, J.A., et al., *Methyl-CpG binding-protein 2 function in cholinergic neurons mediates cardiac arrhythmogenesis.* Hum Mol Genet, 2016.

39. Kerr, A.M., et al., *Rett syndrome: analysis of deaths in the British survey.* Eur Child Adolesc Psychiatry, 1997. **6 Suppl 1**: p. 71-4.

40. Ogier, M. and D.M. Katz, *Breathing dysfunction in Rett syndrome: understanding epigenetic regulation of the respiratory network.* Respir Physiol Neurobiol, 2008. **164**(1-2): p. 55-63.

41. Glaze, D.G., *Neurophysiology of Rett syndrome.* J Child Neurol, 2005. **20**(9): p. 740-6.

42. Viemari, J.C., et al., *Mecp2 deficiency disrupts norepinephrine and respiratory systems in mice.* J Neurosci, 2005. **25**(50): p. 11521-30.

43. Roux, J.C. and L. Villard, *[Pharmacological treatment of Rett syndrome improves breathing and survival in a mouse model].* Med Sci (Paris), 2007. **23**(10): p. 805-7.

44. Zanella, S., et al., *Oral treatment with desipramine improves breathing and life span in Rett syndrome mouse model.* Respir Physiol Neurobiol, 2008. **160**(1): p. 116-21.

45. Meng, X., et al., *Manipulations of MeCP2 in glutamatergic neurons highlight their contributions to Rett and other neurological disorders.* Elife, 2016. **5**.

46. Panayotis, N., et al., *Biogenic amines and their metabolites are differentially affected in the Mecp2-deficient mouse brain.* BMC Neurosci, 2011. **12**: p. 47.

47. Roux, J.C., et al., *Treatment with desipramine improves breathing and survival in a mouse model for Rett syndrome.* Eur J Neurosci, 2007. **25**(7): p. 1915-22.

48. Zhang, Y., et al., *Loss of MeCP2 in cholinergic neurons causes part of RTT-like phenotypes via alpha7 receptor in hippocampus.* Cell Res, 2016. **26**(6): p. 728-42.

49. Oginsky, M.F., et al., *Alterations in the cholinergic system of brain stem neurons in a mouse model of Rett syndrome.* Am J Physiol Cell Physiol, 2014. **307**(6): p. C508-20.

50. Roux, J.C., et al., *Progressive noradrenergic deficits in the locus coeruleus of Mecp2 deficient mice.* J Neurosci Res, 2010. **88**(7): p. 1500-9.

51. Guy, J., et al., *Reversal of neurological defects in a mouse model of Rett syndrome.* Science, 2007. **315**(5815): p. 1143-7.

52. Gold, W.A., et al., *Mitochondrial dysfunction in the skeletal muscle of a mouse model of Rett syndrome (RTT): implications for the disease phenotype.* Mitochondrion, 2014. **15**: p. 10-7.

53. Oginsky, M.F., et al., *Hyperexcitability of Mesencephalic Trigeminal Neurons and Reorganization of Ion Channel Expression in a Rett Syndrome Model.* J Cell Physiol, 2016.

54. Motil, K.J., et al., *Gastrointestinal and nutritional problems occur frequently throughout life in girls and women with Rett syndrome.* J Pediatr Gastroenterol Nutr, 2012. **55**(3): p. 292-8.

55. Isaacs, J.S., et al., *Eating difficulties in girls with Rett syndrome compared with other developmental disabilities.* J Am Diet Assoc, 2003. **103**(2): p. 224-30.

56. Johnson, C.M., et al., *Defects in brainstem neurons associated with breathing and motor function in the Mecp2R168X/Y mouse model of Rett syndrome.* Am J Physiol Cell Physiol, 2016: p. ajpcell 00132 2016.

57. Paine, T.A., N. Swedlow, and L. Swetschinski, *Decreasing GABA function within the medial prefrontal cortex or basolateral amygdala decreases sociability.* Behav Brain Res, 2017. **317**: p. 542-552.

58. Weng, S.J., et al., *Alterations of resting state functional connectivity in the default network in adolescents with autism spectrum disorders.* Brain Res, 2010. **1313**: p. 202-14.

59. Schwarz, L.A., et al., *Viral-genetic tracing of the input-output organization of a central noradrenaline circuit.* Nature, 2015. **524**(7563): p. 88-92.

60. Achterberg, E.J., et al., *Contrasting Roles of Dopamine and Noradrenaline in the Motivational Properties of Social Play Behavior in Rats.* Neuropsychopharmacology, 2016. **41**(3): p. 858-68.

61. Gogolla, N., et al., *Common circuit defect of excitatory-inhibitory balance in mouse models of autism.* J Neurodev Disord, 2009. **1**(2): p. 172-81.

62. Yizhar, O., et al., *Neocortical excitation/inhibition balance in information processing and social dysfunction.* Nature, 2011. **477**(7363): p. 171-8.

63. Gibson, J.R., et al., *Imbalance of neocortical excitation and inhibition and altered UP states reflect network hyperexcitability in the mouse model of fragile X syndrome.* J Neurophysiol, 2008. **100**(5): p. 2615-26.

64. Souchet, B., et al., *Pharmacological correction of excitation/inhibition imbalance in Down syndrome mouse models.* Front Behav Neurosci, 2015. **9**: p. 267.

65. Nelson, S.B. and V. Valakh, *Excitatory/Inhibitory Balance and Circuit Homeostasis in Autism Spectrum Disorders.* Neuron, 2015. **87**(4): p. 684-98.

66. Calfa, G., et al., *Excitation/inhibition imbalance and impaired synaptic inhibition in hippocampal area CA3 of Mecp2 knockout mice.* Hippocampus, 2015. **25**(2): p. 159-68.

67. Zhong, W., et al., *Methyl CpG Binding Protein 2 Gene Disruption Augments Tonic Currents of gamma-Aminobutyric Acid Receptors in Locus Coeruleus Neurons: IMPACT ON NEURONAL EXCITABILITY AND BREATHING.* J Biol Chem, 2015. **290**(30): p. 18400-11.

68. Kron, M., et al., *Brain activity mapping in Mecp2 mutant mice reveals functional deficits in forebrain circuits, including key nodes in the default mode network, that are reversed with ketamine treatment.* J Neurosci, 2012. **32**(40): p. 13860-72.

69. Abdala, A.P., et al., *Deficiency of GABAergic synaptic inhibition in the Kolliker-Fuse area underlies respiratory dysrhythmia in a mouse model of Rett syndrome.* J Physiol, 2016. **594**(1): p. 223-37.

70. Kline, D.D., et al., *Exogenous brain-derived neurotrophic factor rescues synaptic dysfunction in Mecp2-null mice.* J Neurosci, 2010. **30**(15): p. 5303-10.

71. Blue, M.E., S. Naidu, and M.V. Johnston, *Development of amino acid receptors in frontal cortex from girls with Rett syndrome.* Ann Neurol, 1999. **45**(4): p. 541-5.

72. Patrizi, A., et al., *Chronic Administration of the N-Methyl-D-Aspartate Receptor Antagonist Ketamine Improves Rett Syndrome Phenotype.* Biol Psychiatry, 2016. **79**(9): p. 755-64.

73. Ure, K., et al., *Restoration of Mecp2 expression in GABAergic neurons is sufficient to rescue multiple disease features in a mouse model of Rett syndrome.* Elife, 2016. **5**.

74. Belelli, D., et al., *Extrasynaptic GABAA receptors: form, pharmacology, and function.* J Neurosci, 2009. **29**(41): p. 12757-63.

75. Yamashita, Y., et al., *Decrease in benzodiazepine receptor binding in the brains of adult patients with Rett syndrome.* J Neurol Sci, 1998. **154**(2): p. 146-50.

76. Blatt, G.J., et al., *Density and distribution of hippocampal neurotransmitter receptors in autism: an autoradiographic study.* J Autism Dev Disord, 2001. **31**(6): p. 537-43.

77. Kang, S.K., et al., *Temporal- and Location-Specific Alterations of the GABA Recycling System in Mecp2 KO Mouse Brains.* J Cent Nerv Syst Dis, 2014. **6**: p. 21-8.

78. Fatemi, S.H., et al., *GABA(A) receptor downregulation in brains of subjects with autism.* J Autism Dev Disord, 2009. **39**(2): p. 223-30.

79. Samaco, R.C., A. Hogart, and J.M. LaSalle, *Epigenetic overlap in autism-spectrum neurodevelopmental disorders: MECP2 deficiency causes reduced expression of UBE3A and GABRB3.* Hum Mol Genet, 2005. **14**(4): p. 483-92.

80. Whissell, P.D., et al., *Altered expression of deltaGABAA receptors in health and disease.* Neuropharmacology, 2015. **88**: p. 24-35.

81. Olmos-Serrano, J.L., et al., *Defective GABAergic neurotransmission and pharmacological rescue of neuronal hyperexcitability in the amygdala in a mouse model of fragile X syndrome.* J Neurosci, 2010. **30**(29): p. 9929-38.

82. Egawa, K., et al., *Decreased tonic inhibition in cerebellar granule cells causes motor dysfunction in a mouse model of Angelman syndrome.* Sci Transl Med, 2012. **4**(163): p. 163ra157.

83. Zhong, W., et al., *Effects of early-life exposure to THIP on phenotype development in a mouse model of Rett syndrome.* J Neurodev Disord, 2016. **8**: p. 37.

84. Tuchman, R. and I. Rapin, *Epilepsy in autism.* Lancet Neurol, 2002. **1**(6): p. 352-8.

85. Dolen, G., et al., *Mechanism-based approaches to treating fragile X.* Pharmacol Ther, 2010. **127**(1): p. 78-93.

86. Blue, M.E., et al., *Temporal and regional alterations in NMDA receptor expression in Mecp2-null mice.* Anat Rec (Hoboken), 2011. **294**(10): p. 1624-34.

87. Li, W., X. Xu, and L. Pozzo-Miller, *Excitatory synapses are stronger in the hippocampus of Rett syndrome mice due to altered synaptic trafficking of AMPA-type glutamate receptors.* Proc Natl Acad Sci U S A, 2016. **113**(11): p. E1575-84.

88. Johnston, M., M.E. Blue, and S. Naidu, *Recent advances in understanding synaptic abnormalities in Rett syndrome.* F1000Res, 2015. **4**.

89. Banerjee, A., J. Castro, and M. Sur, *Rett syndrome: genes, synapses, circuits, and therapeutics.* Front Psychiatry, 2012. **3**: p. 34.

90. Chang, Q., et al., *The disease progression of Mecp2 mutant mice is affected by the level of BDNF expression.* Neuron, 2006. **49**(3): p. 341-8.

91. Ogier, M., et al., *Brain-derived neurotrophic factor expression and respiratory function improve after ampakine treatment in a mouse model of Rett syndrome.* J Neurosci, 2007. **27**(40): p. 10912-7.

92. Kron, M., W. Zhang, and M. Dutschmann, *Developmental changes in the BDNF-induced modulation of inhibitory synaptic transmission in the Kolliker-Fuse nucleus of rat.* Eur J Neurosci, 2007. **26**(12): p. 3449-57.

93. Thoby-Brisson, M., et al., *Expression of functional tyrosine kinase B receptors by rhythmically active respiratory neurons in the pre-Botzinger complex of neonatal mice.* J Neurosci, 2003. **23**(20): p. 7685-9.

94. Balkowiec, A., D.L. Kunze, and D.M. Katz, *Brain-derived neurotrophic factor acutely inhibits AMPA-mediated currents in developing sensory relay neurons.* J Neurosci, 2000. **20**(5): p. 1904-11.

95. Zheng, W.H. and R. Quirion, *Comparative signaling pathways of insulin-like growth factor-1 and brain-derived neurotrophic factor in hippocampal neurons and the role of the PI3 kinase pathway in cell survival.* J Neurochem, 2004. **89**(4): p. 844-52.

96. Tropea, D., et al., *Partial reversal of Rett Syndrome-like symptoms in MeCP2 mutant mice.* Proc Natl Acad Sci U S A, 2009. **106**(6): p. 2029-34.

97. Mellen, M., et al., *MeCP2 binds to 5hmC enriched within active genes and accessible chromatin in the nervous system.* Cell, 2012. **151**(7): p. 1417-30.

98. Guo, J.U., et al., *Distribution, recognition and regulation of non-CpG methylation in the adult mammalian brain.* Nat Neurosci, 2014. **17**(2): p. 215-22.

99. Pohodich, A.E. and H.Y. Zoghbi, *Rett syndrome: disruption of epigenetic control of postnatal neurological functions.* Hum Mol Genet, 2015. **24**(R1): p. R10-6.

100. Baker, S.A., et al., *An AT-hook domain in MeCP2 determines the clinical course of Rett syndrome and related disorders.* Cell, 2013. **152**(5): p. 984-96.

101. Schluth, C., et al., *Phenotype in X chromosome rearrangements: pitfalls of X inactivation study.* Pathol Biol (Paris), 2007. **55**(1): p. 29-36.

102. Young, J.I. and H.Y. Zoghbi, *X-chromosome inactivation patterns are unbalanced and affect the phenotypic outcome in a mouse model of rett syndrome.* Am J Hum Genet, 2004. **74**(3): p. 511-20.

103. Renault, N.K., et al., *Human X-chromosome inactivation pattern distributions fit a model of genetically influenced choice better than models of completely random choice.* Eur J Hum Genet, 2013. **21**(12): p. 1396-402.

104. Wither, R.G., et al., *Regional MeCP2 expression levels in the female MeCP2-deficient mouse brain correlate with specific behavioral impairments.* Exp Neurol, 2013. **239**: p. 49-59.

105. Weaving, L.S., et al., *Effects of MECP2 mutation type, location and X-inactivation in modulating Rett syndrome phenotype.* Am J Med Genet A, 2003. **118A**(2): p. 103-14.

106. Hoffbuhr, K.C., et al., *Associations between MeCP2 mutations, X-chromosome inactivation, and phenotype.* Ment Retard Dev Disabil Res Rev, 2002. **8**(2): p. 99-105.

107. Johnson, C.M., et al., *Breathing abnormalities in a female mouse model of Rett syndrome.* J Physiol Sci, 2015. **65**(5): p. 451-9.

108. Rietveld, L., et al., *Genotype-specific effects of Mecp2 loss-of-function on morphology of Layer V pyramidal neurons in heterozygous female Rett syndrome model mice.* Front Cell Neurosci, 2015. **9**: p. 145.

109. Braunschweig, D., et al., *X-Chromosome inactivation ratios affect wild-type MeCP2 expression within mosaic Rett syndrome and Mecp2-/+ mouse brain.* Hum Mol Genet, 2004. **13**(12): p. 1275-86.

110. Meunier, J.C. and J.P. Changeux, *Comparison between the affinities for reversible cholinergic ligands of a purified and membrane bound state of the acetylcholine-receptor protein from Electrophorus electricus.* FEBS Lett, 1973. **32**(1): p. 143-8.

111. Larionov, A.I., V.P. Gavrik, and V.N. Lukach, *[A device for conducting artificial ventilation of the lungs using an injection method during bronchoscopy].* Vestn Khir Im I I Grek, 1988. **141**(12): p. 87.

112. *[Respiration and the environment. Congress on Pneumology in the Upper Rhine. 8th meeting of the Southern German Society of Pneumology jointly with the College of Respiratory Pathology, Strasbourg. Freiburg i.Br., 17-20 June 1987].* Prax Klin Pneumol, 1988. **42 Suppl 1**: p. 195-414.

113. Langeland, N., et al., *Interaction of polylysine with the cellular receptor for herpes simplex virus type 1.* J Gen Virol, 1988. **69 (Pt 6)**: p. 1137-45.

114. Bruce-Chwatt, L.J., *Letter: No provocation without foundation.* Lancet, 1974. **1**(7862): p. 875.

115. Zhang, S., et al., *An optogenetic mouse model of rett syndrome targeting on catecholaminergic neurons.* J Neurosci Res, 2016. **94**(10): p. 896-906.

116. Takahashi, K., et al., *Locus coeruleus neuronal activity during the sleep-waking cycle in mice.* Neuroscience, 2010. **169**(3): p. 1115-26.

117. Aston-Jones, G. and J.D. Cohen, *An integrative theory of locus coeruleus-norepinephrine function: adaptive gain and optimal performance.* Annu Rev Neurosci, 2005. **28**: p. 403-50.

118. Nestler, E.J., M. Alreja, and G.K. Aghajanian, *Molecular control of locus coeruleus neurotransmission.* Biol Psychiatry, 1999. **46**(9): p. 1131-9.

119. Jin, X., et al., *Identification of a Group of GABAergic Neurons in the Dorsomedial Area of the Locus Coeruleus.* PLoS One, 2016. **11**(1): p. e0146470.

120. Patrizi, A., et al., *Chronic Administration of the N-Methyl-D-Aspartate Receptor Antagonist Ketamine Improves Rett Syndrome Phenotype.* Biol Psychiatry, 2015.

121. Chapleau, C.A., et al., *Recent Progress in Rett Syndrome and MeCP2 Dysfunction: Assessment of Potential Treatment Options.* Future Neurol, 2013. **8**(1).

122. Levitt, E.S., et al., *A selective 5-HT1a receptor agonist improves respiration in a mouse model of Rett syndrome.* J Appl Physiol (1985), 2013. **115**(11): p. 1626-33.

123. Ohno, K., et al., *Effect of Serotonin 1A Agonists and Selective Serotonin Reuptake Inhibitors on Behavioral and Nighttime Respiratory Symptoms in Rett Syndrome.* Pediatr Neurol, 2016. **60**: p. 54-59 e1.

124. Nikiforuk, A., *Targeting the Serotonin 5-HT7 Receptor in the Search for Treatments for CNS Disorders: Rationale and Progress to Date.* CNS Drugs, 2015. **29**(4): p. 265-75.

125. Abdala, A.P., et al., *Effect of Sarizotan, a 5-HT1a and D2-like receptor agonist, on respiration in three mouse models of Rett syndrome.* Am J Respir Cell Mol Biol, 2014. **50**(6): p. 1031-9.

126. Lonetti, G., et al., *Early environmental enrichment moderates the behavioral and synaptic phenotype of MeCP2 null mice.* Biol Psychiatry, 2010. **67**(7): p. 657-65.

127. Johnson, R.A., et al., *7,8-dihydroxyflavone exhibits therapeutic efficacy in a mouse model of Rett syndrome.* J Appl Physiol (1985), 2012. **112**(5): p. 704-10.

128. Lang, M., et al., *Rescue of behavioral and EEG deficits in male and female Mecp2-deficient mice by delayed Mecp2 gene reactivation.* Hum Mol Genet, 2014. **23**(2): p. 303-18.

129. Lotan, M. and S. Hanks, *Physical therapy intervention for individuals with Rett syndrome.* ScientificWorldJournal, 2006. **6**: p. 1314-38.

130. Townend, G.S., et al., *Eye Gaze Technology as a Form of Augmentative and Alternative Communication for Individuals with Rett Syndrome: Experiences of Families in The Netherlands.* J Dev Phys Disabil, 2016. **28**: p. 101-112.

131. Qvarfordt, I., I.W. Engerstrom, and A.C. Eliasson, *Guided eating or feeding: three girls with Rett syndrome.* Scand J Occup Ther, 2009. **16**(1): p. 33-9.

132. Armstrong, D.D., *Neuropathology of Rett syndrome.* J Child Neurol, 2005. **20**(9): p. 747-53.

133. Vardya, I., et al., *Cell type-specific GABA A receptor-mediated tonic inhibition in mouse neocortex.* J Neurophysiol, 2008. **100**(1): p. 526-32.

134. Wojtowicz, A.M., et al., *Reduced tonic inhibition in striatal output neurons from Huntington mice due to loss of astrocytic GABA release through GAT-3.* Front Neural Circuits, 2013. **7**: p. 188.

135. Roth, T., et al., *Effect of gaboxadol on patient-reported measures of sleep and waking function in patients with Primary Insomnia: results from two randomized, controlled, 3-month studies.* J Clin Sleep Med, 2010. **6**(1): p. 30-9.

136. Kjaer, M. and H. Nielsen, *The analgesic effect of the GABA-agonist THIP in patients with chronic pain of malignant origin. A phase-1-2 study.* Br J Clin Pharmacol, 1983. **16**(5): p. 477-85.

137. Maguire, J., et al., *Excitability changes related to GABAA receptor plasticity during pregnancy.* J Neurosci, 2009. **29**(30): p. 9592-601.

138. Samaco, R.C., et al., *Crh and Oprm1 mediate anxiety-related behavior and social approach in a mouse model of MECP2 duplication syndrome.* Nat Genet, 2012. **44**(2): p. 206-11.

139. Faul, F., et al., *G*Power 3: a flexible statistical power analysis program for the social, behavioral, and biomedical sciences.* Behav Res Methods, 2007. **39**(2): p. 175-91.

140. Boggio, E.M., et al., *Synaptic determinants of rett syndrome.* Front Synaptic Neurosci, 2010. **2**: p. 28.

141. Farrant, M. and Z. Nusser, *Variations on an inhibitory theme: phasic and tonic activation of GABA(A) receptors.* Nat Rev Neurosci, 2005. **6**(3): p. 215-29.

142. Mortensen, M., et al., *Distinct activities of GABA agonists at synaptic- and extrasynaptic-type GABAA receptors.* J Physiol, 2010. **588**(Pt 8): p. 1251-68.

143. Fleming, R.L., W.A. Wilson, and H.S. Swartzwelder, *Magnitude and ethanol sensitivity of tonic GABAA receptor-mediated inhibition in dentate gyrus changes from adolescence to adulthood.* J Neurophysiol, 2007. **97**(5): p. 3806-11.

144. Prenosil, G.A., et al., *Specific subtypes of GABAA receptors mediate phasic and tonic forms of inhibition in hippocampal pyramidal neurons.* J Neurophysiol, 2006. **96**(2): p. 846-57.

145. Glykys, J. and I. Mody, *Hippocampal network hyperactivity after selective reduction of tonic inhibition in GABA A receptor alpha5 subunit-deficient mice.* J Neurophysiol, 2006. **95**(5): p. 2796-807.

146. Smith, S.S., et al., *Neurosteroid regulation of GABA(A) receptors: Focus on the alpha4 and delta subunits.* Pharmacol Ther, 2007. **116**(1): p. 58-76.

147. Taneja, P., et al., *Pathophysiology of locus ceruleus neurons in a mouse model of Rett syndrome.* J Neurosci, 2009. **29**(39): p. 12187-95.

148. Shivers, B.D., et al., *Two novel GABAA receptor subunits exist in distinct neuronal subpopulations.* Neuron, 1989. **3**(3): p. 327-37.

149. Hamann, M., D.J. Rossi, and D. Attwell, *Tonic and spillover inhibition of granule cells control information flow through cerebellar cortex.* Neuron, 2002. **33**(4): p. 625-33.

150. Bright, D.P., M.I. Aller, and S.G. Brickley, *Synaptic release generates a tonic GABA(A) receptor-mediated conductance that modulates burst precision in thalamic relay neurons.* J Neurosci, 2007. **27**(10): p. 2560-9.

151. Drasbek, K.R., K. Hoestgaard-Jensen, and K. Jensen, *Modulation of extrasynaptic THIP conductances by GABAA-receptor modulators in mouse neocortex.* J Neurophysiol, 2007. **97**(3): p. 2293-300.

152. Song, I.S., L. Savtchenko, and A. Semyanov, *Tonic excitation or inhibition is set by GABA(A) conductance in hippocampal interneurons.* Nature Communications, 2011. **2**.

153. Porcello, D.M., et al., *Intact synaptic GABAergic inhibition and altered neurosteroid modulation of thalamic relay neurons in mice lacking delta subunit.* J Neurophysiol, 2003. **89**(3): p. 1378-86.

154. Ye, Z., et al., *The contribution of delta subunit-containing GABAA receptors to phasic and tonic conductance changes in cerebellum, thalamus and neocortex.* Front Neural Circuits, 2013. **7**: p. 203.

155. Carver, C.M., et al., *Perimenstrual-Like Hormonal Regulation of Extrasynaptic delta-Containing GABAA Receptors Mediating Tonic Inhibition and Neurosteroid Sensitivity.* J Neurosci, 2014. **34**(43): p. 14181-97.

156. Maguire, E.P., et al., *Tonic inhibition of accumbal spiny neurons by extrasynaptic alpha4betadelta GABAA receptors modulates the actions of psychostimulants.* J Neurosci, 2014. **34**(3): p. 823-38.

157. Hanchar, H.J., et al., *Alcohol-induced motor impairment caused by increased extrasynaptic GABA(A) receptor activity.* Nat Neurosci, 2005. **8**(3): p. 339-45.

158. Ferando, I. and I. Mody, *GABAA receptor modulation by neurosteroids in models of temporal lobe epilepsies.* Epilepsia, 2012. **53 Suppl 9**: p. 89-101.

159. Clarkson, A.N., et al., *Reducing excessive GABA-mediated tonic inhibition promotes functional recovery after stroke.* Nature, 2010. **468**(7321): p. 305-9.

160. Brown, N., et al., *Pharmacological characterization of a novel cell line expressing human alpha(4)beta(3)delta GABA(A) receptors.* Br J Pharmacol, 2002. **136**(7): p. 965-74.

161. Brickley, S.G., et al., *Adaptive regulation of neuronal excitability by a voltage-independent potassium conductance.* Nature, 2001. **409**(6816): p. 88-92.

162. Patel, B., M. Mortensen, and T.G. Smart, *Stoichiometry of delta subunit containing GABA(A) receptors.* Br J Pharmacol, 2014. **171**(4): p. 985-94.

163. Moretti, P., et al., *Learning and memory and synaptic plasticity are impaired in a mouse model of Rett syndrome.* J Neurosci, 2006. **26**(1): p. 319-27.

164. Zhang, W., et al., *Loss of MeCP2 from forebrain excitatory neurons leads to cortical hyperexcitation and seizures.* J Neurosci, 2014. **34**(7): p. 2754-63.

165. Calfa, G., J.J. Hablitz, and L. Pozzo-Miller, *Network hyperexcitability in hippocampal slices from Mecp2 mutant mice revealed by voltage-sensitive dye imaging.* J Neurophysiol, 2011. **105**(4): p. 1768-84.

166. Blue, M.E., S. Naidu, and M.V. Johnston, *Altered development of glutamate and GABA receptors in the basal ganglia of girls with Rett syndrome.* Exp Neurol, 1999. **156**(2): p. 345-52.

167. Na, E.S. and L.M. Monteggia, *The role of MeCP2 in CNS development and function.* Horm Behav, 2011. **59**(3): p. 364-8.

168. Jin, X.T., et al., *Pre- and postsynaptic modulations of hypoglossal motoneurons by alpha-adrenoceptor activation in wild-type and Mecp2(-/Y) mice.* Am J Physiol Cell Physiol, 2013. **305**(10): p. C1080-90.

169. White, S.R., S.J. Fung, and C.D. Barnes, *Norepinephrine effects on spinal motoneurons.* Prog Brain Res, 1991. **88**: p. 343-50.

170. Caro, A.A. and A.I. Cederbaum, *Role of calcium and calcium-activated proteases in CYP2E1-dependent toxicity in HEPG2 cells.* J Biol Chem, 2002. **277**(1): p. 104-13.

171. Barry, M.A. and A. Eastman, *Endonuclease activation during apoptosis: the role of cytosolic Ca2+ and pH.* Biochem Biophys Res Commun, 1992. **186**(2): p. 782-9.

172. Evers, D.M., et al., *Plk2 attachment to NSF induces homeostatic removal of GluA2 during chronic overexcitation.* Nat Neurosci, 2010. **13**(10): p. 1199-207.

173. Ramirez, J.M., C.S. Ward, and J.L. Neul, *Breathing challenges in Rett syndrome: lessons learned from humans and animal models.* Respir Physiol Neurobiol, 2013. **189**(2): p. 280-7.

174. Kerr, B., et al., *Defective body-weight regulation, motor control and abnormal social interactions in Mecp2 hypomorphic mice.* Hum Mol Genet, 2008. **17**(12): p. 1707-17.

175. Maguire, J. and I. Mody, *GABA(A)R plasticity during pregnancy: relevance to postpartum depression.* Neuron, 2008. **59**(2): p. 207-13.

176. Wesson, D.R., et al., *Diazepam and desmethyldiazepam in breast milk.* J Psychoactive Drugs, 1985. **17**(1): p. 55-6.

177. Dusci, L.J., et al., *Excretion of diazepam and its metabolites in human milk during withdrawal from combination high dose diazepam and oxazepam.* Br J Clin Pharmacol, 1990. **29**(1): p. 123-6.

178. Borgatta, L., et al., *Clinical significance of methohexital, meperidine, and diazepam in breast milk.* J Clin Pharmacol, 1997. **37**(3): p. 186-92.

179. DATABASE, C.T. *Gaboxadol hydrobromide*. Available from: http://chem.sis.nlm.nih.gov/chemidplus/rn/65202-63-3.

180. Olmos-Serrano, J.L., J.G. Corbin, and M.P. Burns, *The GABA(A) receptor agonist THIP ameliorates specific behavioral deficits in the mouse model of fragile X syndrome.* Dev Neurosci, 2011. **33**(5): p. 395-403.

181. Boyle, J., et al., *Tolerability, pharmacokinetics and night-time effects on postural sway and critical flicker fusion of gaboxadol and zolpidem in elderly subjects.* Br J Clin Pharmacol, 2009. **67**(2): p. 180-90.

182. Kesisoglou, F., A. Balakrishnan, and K. Manser, *Utility of PBPK Absorption Modeling to Guide Modified Release Formulation Development of Gaboxadol, a Highly Soluble Compound with Region-Dependent Absorption.* J Pharm Sci, 2015.

183. Cremers, T. and B. Ebert, *Plasma and CNS concentrations of Gaboxadol in rats following subcutaneous administration.* Eur J Pharmacol, 2007. **562**(1-2): p. 47-52.

184. Schultz, B., et al., *Preliminary studies on the absorption, distribution, metabolism, and excretion of THIP in animal and man using 14C-labelled compound.* Acta Pharmacol Toxicol (Copenh), 1981. **49**(2): p. 116-24.

185. Katz, D.M., et al., *Breathing disorders in Rett syndrome: progressive neurochemical dysfunction in the respiratory network after birth.* Respir Physiol Neurobiol, 2009. **168**(1-2): p. 101-8.

186. Kow, L.M. and D.W. Pfaff, *Responses of ventromedial hypothalamic neurons in vitro to norepinephrine: dependence on dose and receptor type.* Brain Res, 1987. **413**(2): p. 220-8.

187. Lee, C.Y. and H.H. Liou, *GABAergic tonic inhibition is regulated by developmental age and epilepsy in the dentate gyrus.* Neuroreport, 2013. **24**(10): p. 515-9.

188. Korsgaard, S., et al., *The effect of tetrahydroisoxazolopyridinol (THIP) in tardive dyskinesia: a new gamma-aminobutyric acid agonist.* Arch Gen Psychiatry, 1982. **39**(9): p. 1017-21.

189. Braat, S. and R.F. Kooy, *Insights into GABAAergic system deficits in fragile X syndrome lead to clinical trials.* Neuropharmacology, 2015. **88**: p. 48-54.

190. Lee, V. and J. Maguire, *The impact of tonic GABAA receptor-mediated inhibition on neuronal excitability varies across brain region and cell type.* Front Neural Circuits, 2014. **8**: p. 3.

191. Smrt, R.D., R.L. Pfeiffer, and X. Zhao, *Age-dependent expression of MeCP2 in a heterozygous mosaic mouse model.* Hum Mol Genet, 2011. **20**(9): p. 1834-43.

192. Meziane, H., et al., *Estrous cycle effects on behavior of C57BL/6J and BALB/cByJ female mice: implications for phenotyping strategies.* Genes Brain Behav, 2007. **6**(2): p. 192-200.

193. Bangasser, D.A., et al., *Sexual dimorphism in locus coeruleus dendritic morphology: a structural basis for sex differences in emotional arousal.* Physiol Behav, 2011. **103**(3-4): p. 342-51.

194. Zoghbi, H.Y., *MeCP2 dysfunction in humans and mice.* J Child Neurol, 2005. **20**(9): p. 736-40.

195. Chandler, D.J., *Evidence for a specialized role of the locus coeruleus noradrenergic system in cortical circuitries and behavioral operations.* Brain Res, 2016. **1641**(Pt B): p. 197-206.

196. Chen, L., et al., *MeCP2 binds to non-CG methylated DNA as neurons mature, influencing transcription and the timing of onset for Rett syndrome.* Proc Natl Acad Sci U S A, 2015. **112**(17): p. 5509-14.

197. Zhang, L., et al., *The MeCP2-null mouse hippocampus displays altered basal inhibitory rhythms and is prone to hyperexcitability.* Hippocampus, 2008. **18**(3): p. 294-309.

198. Ho, E.C., et al., *Network models predict that reduced excitatory fluctuations can give rise to hippocampal network hyper-excitability in MeCP2-null mice.* PLoS One, 2014. **9**(3): p. e91148.

199. Patrizi, A., et al., *Chronic Administration of the N-Methyl-D-Aspartate Receptor Antagonist Ketamine Improves Rett Syndrome Phenotype*. Biol Psychiatry, 2015: p. 79(9):755-64.

200. Zakir, H.M., et al., *Modulation of spindle discharge from jaw-closing muscles during chewing foods of different hardness in awake rabbits.* Brain Res Bull, 2010. **83**(6): p. 380-6.

201. Hidaka, O., et al., *Behavior of jaw muscle spindle afferents during cortically induced rhythmic jaw movements in the anesthetized rabbit.* J Neurophysiol, 1999. **82**(5): p. 2633-40.

202. Kolta, A., J.P. Lund, and S. Rossignol, *Modulation of activity of spindle afferents recorded in trigeminal mesencephalic nucleus of rabbit during fictive mastication.* J Neurophysiol, 1990. **64**(4): p. 1067-76.

203. Ure, K., et al., *Restoration of Mecp2 expression in GABAergic neurons is sufficient to rescue multiple disease features in a mouse model of Rett syndrome.* Elife, 2016. **5**: p. e14198.

204. Ishii, T., et al., *The role of different X-inactivation pattern on the variable clinical phenotype with Rett syndrome.* Brain Dev, 2001. **23 Suppl 1**: p. S161-4.

205. Zhong, W., et al., *Effects of chronic exposure to low dose THIP on brainstem neuronal excitability in mouse models of Rett syndrome: Evidence from symptomatic females.* Neuropharmacology, 2017. **116**: p. 288-299.

206. Jann, K., et al., *Altered resting perfusion and functional connectivity of default mode network in youth with autism spectrum disorder.* Brain Behav, 2015. **5**(9): p. e00358.

APPENDICES: PUBLICATIONS

1. **Zhong W,** Johnson CM, Cui N, Xing H, Wu Y and Jiang C. (2017) Effects of chronic exposure to low dose THIP on brainstem neuronal excitability in mouse models of Rett syndrome: Evidence from symptomatic females. *Neuropharmacology*. 2017 Jan 6. pii: S0028-3908(17)30002-3.
2. **Zhong W,** Johnson CM, Cui N, Oginsky MF, Wu Y and Jiang C. (2017) Effects of early-life exposure to THIP on brainstem neuronal excitability in the *Mecp2*-null mouse model of Rett syndrome before and after drug withdrawal. *Physiological Reports.* 2017 Jan;5(2). pii: e13110.
3. **Zhong W,** Johnson CM, Cui N, Wu Y, Xing H, Zhang S and Jiang C. (2016) Effects of early exposure to gaboxadol on phenotype development in a mouse model of Rett syndrome. *J Neurodev Disord.* 2016 Oct 19;8:37
4. Wu Y*, **Zhong W*,** Cui N, Johnson CM, Xing H, Zhang S, Jiang C. (2016) Characterization of Rett Syndrome-like phenotypes in *Mecp2*-knockout rats. *J Neurodev Disord.* 2016 Jun 16;8:23. doi: 10.1186/s11689-016-9156-7.
5. **Zhong W,** Cui N, Jin X, Oginsky MF, Wu Y, Zhang S, Bondy B, Johnson CM and Jiang C. (2015) Methyl CpG binding protein-2 gene disruption augments tonic currents of γ-aminobutyric acid receptors in locus coeruleus neurons: Impact on neuronal excitability and breathing. *Journal of Biological Chemistry*, 290(30):18400-11.
6. Jiang C, Cui N, **Zhong W**, Johnson CM, Wu Y. (2016) Breathing abnormalities in animal models of Rett syndrome a female neurogenetic disorder. *Respir Physiol Neurobiol*, pii: S1569-9048(16)30257-9. doi: 10.1016/j.resp.2016.11.011.

7. Johnson CM, **Zhong W,** Cui N, Wu Y, Xing H, Zhang S, Jiang C. (2016) Defects in the brainstem neurons associated with breathing and motor function in the *Mecp2* R168X/Y mouse model of Rett Syndrome. *Am J Physiol Cell Physiol*, 311(6):C895-C909.
8. Oginsky MF*, Cui N*, **Zhong W**, Johnson CM, Jiang C. Hyperexcitability of Mesencephalic Trigeminal Neurons and Reorganization of Ion Channel Expression in a Rett Syndrome Model. *J Cell Physiol.* 2016 Sep 27. doi: 10.1002/jcp.25589.
9. Zhang S*, Johnson CM*, Cui N, Xing H, **Zhong W**, Wu Y, Jiang C. (2016) An optogenetic mouse model of rett syndrome targeting on catecholaminergic neurons. *J Neurosci Res.* 2016 Jun 18. doi: 10.1002/jnr.23760.
10. Jin X, Li S, Bondy B, **Zhong W**, Oginsky MF, Wu Y, Johnson CM, Zhang S, Cui N, Jiang C. Identification of a Group of GABAergic Neurons in the Dorsomedial Area of the Locus Coeruleus. *PLoS One.* 2016 Jan 19;11(1):e0146470. doi: 10.1371/journal.pone.0146470.
11. Qu L, Yu L, Wang Y, Jin X, Zhang Q, Lu P, Yu X, **Zhong W**, Zheng X, Cui N, Jiang C, Zhu D. (2015) nward Rectifier K+ Currents Are Regulated by CaMKII in Endothelial Cells of Primarily Cultured Bovine Pulmonary Arteries *PLoS One*. 2015 Dec 23;10(12)
12. Zhang S, Cui N, Wu Y, **Zhong W,** Johnson C, Cui N and Jiang C. (2015) Optogenetic Intervention to the Vascular Endothelium. *Vascular Pharmacology.* In press.
13. Johnson C, Cui N, **Zhong W** and Jiang C. (2015) Breathing abnormalities in a female mouse model of Rett syndrome. Journal of Physiological Sciences, 65(5):451-459.
14. Oginsky MF, Cui N, **Zhong W,** Johnson C and Jiang C. (2014) Alterations in the cholinergic system of brainstem neurons in a mouse model of Rett Syndrome. *Am J PhysiolCell Physiol*. 307(6):C508-20.

15. Jin XT, Cui N, **Zhong W**, Jin X, Wu Z and Jiang C. (2013) Pre- and postsynaptic modulations of hypoglossal neurons by α-adrenoceptor activator in wild-type and *Mecp2*-null mice. Am J Physiol Cell Physiol. 305(10):C 1080-90.
16. Jin X, **Zhong W** and Jiang C. (2013) Effects of allopregnanolone on GABAA-ergic inputs of locus coeruleus neurons in wild-type and *Mecp2*-null mice. Am J Physiol Cell Physiol. 305(11):C 1151-60.
17. Jin X, Cui N, **Zhong W,** Jin XT and Jiang C. (2013) GABA-ergic synaptic inputs of locus coeruleus neurons in wild-type and *Mecp2*-null mice. Am J Physiol Cell Physiol. 304(9):C 844-57.

*** Equal Contributors**